UNIVERSITY OF CALIFORNIA, SAN DIEGO

The Postsynaptic Adhesion Molecule FLRT3 Regulates Synapse Development by Trans-Synaptic Interaction with the Latrophilin Family of Orphan Presynaptic GPCRs

A dissertation submitted in partial satisfaction of the requirements

for the degree Doctor of Philosophy

in

Neurosciences

by

Matthew Liam O'Sullivan

Committee in charge:

Professor Yishi Jin, chair
Professor Edward Callaway
Professor Anirvan Ghosh
Professor Jeffry Isaacson
Professor Terunaga Nakagawa
Professor Massimo Scanziani

The Dissertation of Matthew Liam O'Sullivan is approved, and it is acceptable in quality and form for publication on microfilm and electronically:

_____

_____

_____

_____

_____

_____

Chair

University of California, San Diego

2011

TABLE OF CONTENTS

LIST OF FIGURES

LIST OF ABBREVIATIONS

ADHD – attention deficit hyperactivity disorder

AMPAR – α-amino-3-hydroxy-5-methyl-4-isoxazolepropionic acid receptor

DG – dentate gyrus

EPSC – excitatory postsynaptic current

FLRT – fibronectin and leucine-rich repeat transmembrane protein

FN3 – fibronectin type 3

GPCR – G protein-coupled receptor

LPHN – latrophilin

LRR – leucine-rich repeat

LRRTM – leucine rich repeat transmembrane neuronal protein

mEPSC – miniature excitatory postsynaptic current

NGL – netrin-G ligand

NL – neuroligin

NMDAR – *N*-methyl *D*-aspartate receptor

NRXN – neurexin

SALM – synaptic adhesion-like molecule

ACKNOWLEDGEMENTS

I would like to thank Anirvan Ghosh for his intellectual and practical leadership and support, and my doctoral committee for the time and scientific guidance they have provided. This project has been highly collaborative, and I would like to thank everyone who contributed, but especially Joris de Wit and Jeff Savas. Without their substantial contributions this work would not have been possible.

The work presented in this dissertation has been submitted for publication or is published with the following citations:

Matthew L. O'Sullivan, Joris de Wit, Jeffrey N. Savas, Stefanie Otto, Davide Comoletti, John R. Yates III, and Anirvan Ghosh. Postsynaptic FLRT proteins are endogenous ligands for the black widow spider venom receptor Latrophilin and regulate excitatory synapse development. *Submitted for publication*.

de Wit, J., Sylwestrak, E., O'Sullivan, M.L., Otto, S., Tiglio, K., Savas, J.N., Yates, J.R. 3rd, Comoletti, D., Taylor, P., and Ghosh, A. (2009). LRRTM2 interacts with Neurexin1 and regulates excitatory synapse function. *Neuron 64(6)*, 799-806.

VITA

2006 Bachelor of Arts, Psychology, Reed College

2011 Doctor of Philosophy, Neurosciences, University of California, San Diego

PUBLICATIONS

de Wit, J., Sylwestrak, E., O'Sullivan, M.L., Otto, S., Tiglio, K., Savas, J.N., Yates, J.R. 3rd, Comoletti, D., Taylor, P., and Ghosh, A. (2009). LRRTM2 interacts with Neurexin1 and regulates excitatory synapse function. *Neuron 64(6)*, 799-806.

Kim, J.E., O'Sullivan, M.L., Sanchez, C.A., Hwang, M., Israel, M.A., Brennand, K., Deerinck, T.J., Goldstein, L.S., Gage, F.H., Ellisman, M.H., and Ghosh, A. (2011). Investigating synapse formation and function using human pluripotent stem cell-derived neurons. *Proceedings of the National Academy of Sciences 108(7)*, 3005-10.

O'Sullivan, M.L., de Wit, J., Savas, J.N., Otto, S., Comoletti, D., Yates, J.R. 3rd, and Ghosh, A. (2011). Postsynaptic FLRT proteins are endogenous ligands for the black widow spider venom receptor Latrophilin and regulate excitatory synapse development. *Submitted for publication.*

ABSTRACT OF THE DISSERTATION

The Postsynaptic Adhesion Molecule FLRT3 Regulates Synapse Development by Trans-Synaptic Interaction with the Latrophilin Family of Orphan Presynaptic GPCRs

by

Matthew Liam O'Sullivan

Doctor of Philosophy in Neurosciences

University of California, San Diego, 2011

Professor Yishi Jin, Chair

Latrophilins (LPHNs) are a small family of orphan G-protein coupled receptors (GPCRs) known to mediate the massive synaptic exocytosis caused by the black widow spider venom α-latrotoxin, but their endogenous ligands and function remain unclear. Here we identify the FLRT (Fibronectin and Leucine-rich Repeat Transmembrane) family of transmembrane proteins as novel endogenous ligands for latrophilins using affinity chromatography and mass spectrometry. We demonstrate that FLRT3 and LPHN3 ectodomains interact with high affinity in *trans*. We show that FLRT3 is expressed by specific subpopulations of hippocampal neurons and localizes to postsynaptic sites. Interference with endogenous LPHN complexes using soluble recombinant LPHN3 reduces the density of excitatory synapses in cultured neurons and loss of FLRT3 reduces afferent input strength and synapse number in dentate granule cells *in vivo*. Our results identify a novel function for

the ADHD (Attention Deficit Hyperactivity Disorder)-linked LPHN3 protein in mediating trans-synaptic adhesion with FLRTs and demonstrate that FLRT3 is required for normal synapse development.

Chapter 1:

Introduction

The mature nervous system is comprised of a great diversity of cellular and molecular components arrayed in a precise and highly ordered manner integral to its function. Neurons of different types must form synapses in the proper number and kind with diverse synaptic partners, and these synapses rely upon the coordination of pre- and post-synaptic molecules to achieve transmission of information from neuron to neuron. Glutamatergic synapses, which represent the major population of excitatory synapses in the brain, can be defined by the apposition of cellular synaptic specializations: a presynaptic active zone replete with synaptic vesicles and a postsynaptic density. These specializations are fundamentally constituted by a relatively small set of core synaptic molecules: presynaptic voltage-sensitive calcium channels coupled to exocytosis machinery, and postsynaptic neurotransmitter receptors. How the recruitment and organization of these proteins is orchestrated is a basic and important question in neuroscience, and remains incompletely understood. It is becoming evident that trans-synaptic interactions between other pre- and post-synaptic transmembrane proteins can be instrumental in synaptic development. Identification of synaptic organizing molecules and elucidation of their roles promises to be an important step in understanding the development of neural circuits in health and disease. To this end, we have identified a novel trans-synaptic complex between presynaptic Latrophilins and postsynaptic FLRT proteins, and shown that these proteins are involved in the development of glutamatergic synapses.

1.1: Neurexins and Latrophilins are Synaptic Proteins and Receptors for α-Latrotoxin

Many organisms employ toxins to further their survival, generally employed in predation or defense. Common extant toxins have proven evolutionarily successful as indicated by their conservation across generations and across species. For the same reasons that likely make them evolutionarily favored, many neurotoxins have been deemed useful in scientific investigation of nervous system function; they potently disrupt neuronal function by selectively interacting with neuronal proteins in a manner that can cause disorientation, paralysis, or death *in vivo*. For example, the predatory marine snails of the genus *Conus* produce ω-conotoxins that paralyze prey by potently antagonizing presynaptic voltage-sensitive calcium channels and preventing action potential-induced neurotransmitter release, and have aided in identifying particular calcium channels and their roles in synaptic transmission (Olivera et al., 1994). *Latrodectus* spiders such as the black widow also produce a potent neurotoxin; α-latrotoxin causes tetanic paralysis through massive exocytosis of synaptic vesicles. The prevalence of α-latrotoxin as an experimental tool to induce neurotransmitter release (Scheer et al., 1984; Silva et al., 2009b) led to the identification of 2 new classes presynaptic proteins.

α-Latrotoxin affinity chromatography was used to identify two main classes of neuronal latrotoxin receptors, named neurexins and latrophilins

(Sudhof, 2001). Neurexin-1, now known to be a large family of single-pass transmembrane proteins encoded by 3 genes (*Nrxn1-3*), was the first to be identified by affinity for α-latrotoxin (Ushkaryov et al., 1992). Now, decades later, investigation into the physiological function of neurexins has yielded important insights into synaptic development. The second principal α-latrotoxin receptor, latrophilin, was discovered soon after, and bears no evident structural similarity to neurexin (Krasnoperov et al., 1997; Lelianova et al., 1997). Latrophilin is a presynaptic type 2 GPCR with an unusually large extracellular N-terminal domain and is a member of a protein family encoded by 3 genes, *Lphn1-3* (Ichtchenko et al., 1999; Stacey et al., 2000; Sugita et al., 1998).

The mechanisms of α-latrotoxin's exocytotic effects have proved both multifarious and elaborate, and remain incompletely understood (Silva et al., 2009b). For a toxin, it is a large and structurally complicated protein, and seems capable of inducing neurotransmitter release by two separate modes of action depending on whether it binds to neurexin or latrophilin (Sudhof, 2001; Ushkaryov et al., 2008). In neurons, α-latrotoxin is capable of inducing vesicle secretion either in the presence of absence of extracellular Ca^{2+}, with Ca^{2+}-dependent release mediated by binding to neurexin and Ca^{2+}-independent release mediated by binding to latrophilin (Bittner et al., 1998; Deak et al., 2009; Geppert et al., 1998). The Ca^{2+}-dependent release can be explained by the neurexin-mediated, Ca^{2+}-dependent insertion of α-latrotoxin into the plasma membrane, and ensuing presynaptic influx of extracellular Ca^{2+}

through a pore formed by α-latrotoxin itself (Deak et al., 2009; Geppert et al., 1998; Sugita et al., 1999). The neurexin intracellular domain is not required Neurexin for α-latrotoxin-induced exocytosis (Sugita et al., 1999; Volynski et al., 2000), suggesting that α-latrotoxin binding to neurexin serves to anchor it to synapses, but that neurexin is not directly involved in stimulating exocytosis.

How α-latrotoxin causes exocytosis through latrophilin-binding is less clear; some reports suggest that an a α-latrotoxin Ca^{2+} conductance is formed as in the neurexin case (Bittner, 2000; Bittner et al., 1998; Van Renterghem et al., 2000), but evidence to the contrary also has been published. Latrophilin-mediated exocytosis can be stimulated in the absence of extracellular Ca^{2+} (Deak et al., 2009; Krasnoperov et al., 1997; Tobaben et al., 2002), indicating that influx of extracellular Ca^{2+} cannot in all cases mediate release. Binding of α-latrotoxin to Latrophilin increases phospholipase-C (PLC) activity and generation of IP3, but stimulation of Ca^{2+} release from intracellular stores by IP3 may or may not explain the effect of α-latrotoxin (Davletov et al., 1998; Ichtchenko et al., 1998). Furthermore, the GPCR domain of latrophilin seems to be dispensable for exocytosis (Volynski et al., 2000), indicating that G-protein signaling is not required.

While study of α-latrotoxin led to the identification of two classes of new presynaptic proteins, the neurexins and latrophilins, investigation into how it stimulates synaptic vesicle release has given fewer definitive results and may not be helpful in the pursuit of understanding the normal physiology of synapses. That is, synaptic exocytosis may not be directly downstream of

physiological latrophilin or neurexin signaling pathways, with the endogenous functions of both neurexins and latrophilins not reflected in their roles as receptors for α-latrotoxin. Neurexins have now been shown to serve important functions in regulating synapse development by interactions with several different endogenous ligands.

1.2: Neurexins regulate synapse development by trans-synaptic interaction with neuroligins and LRRTMs

The neurexin protein family is large, diverse, and highly regulated at translational and post-translational levels. The three neurexin genes, *Nrxn1-3*, each have two promoters, which leads to transcription of both an α and shorter, N-terminally truncated, β isoform from each gene (Ullrich et al., 1995). Both α- and β-neurexin transcripts are also extensively alternatively spliced at multiple sites, generating the potential for thousands of distinct isoforms (Ullrich et al., 1995; Ushkaryov et al., 1992), a number of which have demonstrably different spatial expression patterns (Ullrich et al., 1995). The intracellular domain of NRXN1 was found to interact with both the abundant synaptic vesicle protein synaptotagmin 1 (Hata et al., 1993) and the presynaptic cytoplasmic scaffolding protein CASK (Hata et al., 1996), confirming that it is firmly entrenched in the presynaptic active zone and positioned to influence presynaptic function. This hypothesis was substantiated by studies that demonstrated that clustering of presynaptic

neurexin is sufficient for the recruitment of synaptic vesicles (Dean et al., 2003), and that that loss of all 3 α-NRXNs impairs recruitment of voltage gated Ca^{2+} channels to presynaptic sites and almost completely abolishes action potential evoked neurotransmission (Missler et al., 2003). Moreover, β-neurexin is sufficient to induce postsynaptic clustering of PSD95 and NMDARs, but not AMPARs, indicating that neurexins can trans-synaptically induce postsynaptic specializations.

The identification of postsynaptic endogenous ligands for neurexins substantially increased understanding of how they influence synaptic development. The first neurexin ligand identified, neuroligin 1 (NL1), is a postsynaptic transmembrane protein and interacts specifically with β-NRXNs and certain splice variants α-NRXNs (Boucard et al., 2005; Ichtchenko et al., 1995). Neuroligin 1 (NL1) is a member of a family of 4 alternatively spliced genes, *Nlgn1-4*, of which NL1-3 are highly conserved between mice and humans and bind β-neurexins (Ichtchenko et al., 1996), while NL4 is quite evolutionarily divergent (Bolliger et al., 2001; Bolliger et al., 2008; Ichtchenko et al., 1996). Another level of specificity is manifested in that NL2 interacts strongly with all β-neurexins, whereas NL1 and NL3 do not bind well to β-neurexin-2 (Ichtchenko et al., 1996). Neuroligins interact with PSD95 (Irie et al., 1997) and NL1 localizes to glutamatergic and not GABAergic postsynaptic sites and is part of the postsynaptic density (Song et al., 1999). Complementarily to the trans-synaptic effect of the neuroligin-binding β-

NRXNs, NLs are sufficient to induce presynaptic differentiation with functional release sites (Dean et al., 2003; Fu et al., 2003; Scheiffele et al., 2000).

Building on this data about the interactions and localization of neuroligins, it was demonstrated that manipulating the levels of neuroligins in dissociated neurons affected the number of synapses formed onto postsynaptic neurons (Chih et al., 2005). Overexpressing any NL isoform greatly increases the density of glutamatergic and GABAergic synapses, while perturbing NL levels with shRNA or expression of dominant negative mutant NLs decreases synapse density. Additionally, NL2 seems to have stronger effects on GABAergic synapses than on GABAergic synapses, unlike NL1 and NL3 (Chih et al., 2005; Varoqueaux et al., 2006). Given these large synapse density phenotypes in dissociated cortical and hippocampal cultures, it was surprising that genetic knockout of all three NLs was reported not to affect synapse density or structure in the mouse cortex and hippocampus (Varoqueaux et al., 2006). The triple knockout mice do, however, show lethal defects in respiratory rhythms, with reduced numbers of synapses in brainstem respiratory nuclei (Varoqueaux et al., 2006). Further analysis of the NL1 single knockout mice revealed a decrease in the NMDAR/AMPAR ratio at Schaffer collateral-CA1 pyramidal neuron synapse in the hippocampus, indicating that while synapse number and basic function are not impaired, the composition of glutamate receptors is affected by NL1 (Chubykin et al., 2007). Knockout of NL2, but not NL1, selectively impairs GABAergic transmission in the hippocampus, substantiating the preferential role of NL2 at inhibitory

synapses (Chubykin et al., 2007). The results of *in vitro* and *in vivo* manipulations of neuroligins on synapses remain quite discrepant, however, particularly in the case of NL1; *in vitro* NL1 exerts a powerful synapse inducing effect which positively regulates the number of glutamatergic synapses formed on a postsynaptic hippocampal or cortical neuron, whereas *in vivo* NL1 more subtly reduces the relative number of NMDARs at synapses without affecting synapse number. This suggests that perhaps in the intact brain additional mechanisms support synapse formation and basic synaptic function.

The identification of a new class of postsynaptic neurexin ligands, the Leucine-Rich Repeat Transmembrane (LRRTM) proteins, added another piece to the known molecular composition of trans-synaptic regulation and may help explain the robustness of synapses to loss of neuroligin *in vivo* (de Wit et al., 2009; Ko et al., 2009). LRRTMs were found to be synapse regulating molecules by their sufficiency for inducing presynaptic differentiation *in vitro* similarly to neuroligins (de Wit et al., 2009; Linhoff et al., 2009), and this synapse inducing ability depends on their interaction with presynaptic neurexins (de Wit et al., 2009; Ko et al., 2009). Correspondingly, the level of postsynaptic LRRTM2 regulates the number of glutamatergic synapses *in vitro* (de Wit et al., 2009; Ko et al., 2009) and the strength of synaptic transmission *in vivo* (Appendix 1; (de Wit et al., 2009), which may be explained by their ability to bind to PSD95 and AMPARs (de Wit et al., 2009). Like neuroligins, LRRTMs selectively interact with particular neurexin isoforms; unlike NLs, they bind to both α- and β-NRXNs and are sensitive to the presence of a splice

insert at splice site 4 (SS4) (Ko et al., 2009; Siddiqui et al., 2010). For SS4-negative β-neurexins that can bind both neuroligins and LRRTMs with affinity, these interactions are competitive, suggesting an overlapping binding domain in neurexin (Ko et al., 2009; Siddiqui et al., 2010). Thus NRXNs participate in multiple distinct trans-synaptic adhesion complexes with different ligands in an isoform-specific manner to support synapse development and function. These complexes seem to exert different effects on synapses (e.g. NL1 recruits NMDARs and LRRTM2 recruits AMPARs) *in vivo*, but manifest similar phenotypes *in vitro*. The degree to which their functions are redundant or discrete therefore remains somewhat uncertain, and how they interact with one another has not been well explored. It is also not known whether single synapses have both neuroligins and LRRTMs, or whether their presence is regulated by development, synaptic activity, or synapse type.

1.3: The superfamily of synaptic leucine-rich repeat transmembrane proteins

LRRTMs are members of a larger family of over a hundred neuronal transmembrane proteins characterized by extracellular leucine-rich repeat motifs (LRRs) (Chen et al., 2006; Dolan et al., 2007). The LRR is a common conserved domain that mediates protein-protein interactions, with specific sequence differences conferring great binding specificity through subtle structural changes (Kobe and Deisenhofer, 1994; Kobe and Kajava, 2001).

Structurally, LRRs form a curved, toroidal domain with a hydrophobic concave face formed by parallel β-strands and a hydrophilic convex aspect composed of linking α-helices (Bella et al., 2008). The LRR domain seems to be a very general binding motif, as the LRRs of different proteins are known to interact with highly dissimilar ligands.

Several neuronal LRR-containing proteins, in addition to LRRTMs, have been demonstrated to function at synapses (Chen et al., 2006; Ko and Kim, 2007). The SALMs (Synaptic Adhesion-Like Molecules), SALM1-5, are single-pass transmembrane proteins with extracellular LRR, Ig, and FN3 domains, and, for SALM1-3, a C-terminus PDZ domain that binds PSD95 (Nam et al., 2011; Wang et al., 2006). SALMs have been shown to be capable of inducing presynaptic differentiation (SALMs 3 and 5) and involved in regulating synapses in neuronal cultures (SALMs 1, 2, 3, and 5) (Ko et al., 2006; Mah et al., 2010; Wang et al., 2006). SALMs 1-3 strongly bind to PSD95 intracellular and specifically localize to and act on glutamatergic and not GABAergic synapses, whereas SALM5 interacts with PSD95 only weakly and influences both classes of synapse (Ko et al., 2006; Mah et al., 2010). SALMs can form homomeric or heteromeric postsynaptic *cis* complexes, and SALMs 4 and 5 can interact homophilically in *trans* and are found pre- and postsynaptically (Seabold et al., 2008). Presynaptic receptors for SALMs 1-3 have not been found, though the synapse inducing effect of SALM3 in *trans* necessitates some trans-synaptic influence, directly or indirectly, and whether a trans-

synaptic homophilic SALM5 interaction mediates synapse induction is also not known.

The Netrin-G Ligand (NGL) protein subfamily is another exemplar within broader class of LRR-containing synaptic organizers (Woo et al., 2009b). Much like LRRTMs and SALMs, NGLs 1-3 are postsynaptic, PSD95-interacting molecules that promote excitatory synapse formation and are sufficient to induce presynaptic differentiation *in vitro* (Kim et al., 2006; Woo et al., 2009a). NGLs 1 and 2 bind to axonal GPI-anchored Netrin-G1 and Netrin-G2 respectively (Kim et al., 2006; Lin et al., 2003), but it is not clear if this interaction mediates synapse induction since Netrin-Gs are not transmembrane proteins and lack cytoplasmic domains. Thus NGL1 and NGL2 retrograde signaling requires an unknown presynaptic co-receptor to transduce the presynaptic inductive signal intracellularly. NGL3 binds to an unrelated presynaptic receptor: the receptor tyrosine phosphatase leukocyte common antigen-related (LAR), protein tyrosine phosphatase δ (PTPδ), and PTPσ (Kwon et al., 2010; Woo et al., 2009a). Manipulations of NGL3 *in vitro* show the same few phenotypes common to many synaptic regulatory proteins; induction of pre- and postsynaptic differentiation and regulation of synapse density (Kwon et al., 2010; Woo et al., 2009a).

The Netrin-Gs and NGLs may be allocated to distinct populations of synapses in an isoform-specific manner, providing evidence that LRR-containing synaptic molecules could regulate specific neural circuits. Netrin-G1 and Netrin-G2 expression is tightly regulated by cell type, which each

isoform expressed by non-overlapping populations of neurons, leading to distinct Netrin-G1- and Netrin-G2-containing axonal projections (Nakashiba et al., 2002; Niimi et al., 2007). NGL1 and NGL2 expression, in contrast, is broader and overlapping, such that single cells and cell populations express both isoforms (Kim et al., 2006; Nishimura-Akiyoshi et al., 2007). This gives rise to a situation in which a single cell type that expresses both NGL1 and NGL2 receives synapses from both Netrin-G1- and Netrin-G2-positive axons. In many brain regions, including the hippocampus, different afferent pathways are laminarly segregated and NGL1 and NGL2 can be seen to localize to different dendritic lamina that correspond to the terminal zones of Netrin-G1 and Netrin-G2 axons, respectively (Nishimura-Akiyoshi et al., 2007). Subcellular targeting of NGL proteins is receptor dependent, as in Netrin-G1 and Netrin-G2 knockout mice the matching NGL becomes diffusely dispersed across the entire dendritic arbor (Nishimura-Akiyoshi et al., 2007).

The LRRTMs, SALMs, and NGLs set precedents for several features of synaptic LRR-containing molecules that are becoming increasingly well established and relevant to the function of other LRR proteins. First, postsynaptic LRR-containing molecules can interact with extreme specificity with presynaptic receptors of diverse and unrelated structures. Prediction of interactions at the level of conserved protein domains or motifs are not useful. While these trans-synaptic interactions are very selective, they are in every case exclusive; postsynaptic ligands may interact with multiple isoforms of a class of presynaptic receptor, presynaptic receptors may interact with multiple

isoforms of a class of postsynaptic ligands, and presynaptic receptors may interact with multiple distinct classes of postsynaptic ligands. Second, postsynaptic LRR proteins are generally not ubiquitous, but are rather expressed by select populations of neurons and/or localized to subsets of synapses. Lastly, manipulations of different postsynaptic LRR proteins often lead to common phenotypes *in vitro*: induction of presynaptic differentiation and regulation of synapse number. These phenotypes may not accurately represent the proteins' functions *in vivo*, however. While these features are shared by many members of the LRR class, not every individual family member instantiates each property, suggesting that the differences may be important in understanding the relative functions of different trans-synaptic complexes.

1.4: Fibronectin leucine-rich repeat transmembrane (FLRT) proteins

The fibronectin leucine-rich repeat transmembrane (FLRT) subfamily consists of 3 genes, *Flrt1-3*, coding for single-pass transmembrane proteins in single exons (Lacy et al., 1999). FLRTs have domain organizations very similar to the LRRTMs, SALMs, and NGLs, with an extracellular N-terminal bearing 10 LRRs bracketed by characteristic LRR N- and C-terminus flanking sequences, a juxtamembrane FN3 domain, and a short intracellular C-terminal with no evident conserved motifs (Lacy et al., 1999). All 3 *Flrt* genes are

highly expressed in brain, and have differential isoform-specific expression patterns in other tissues including kidney, heart, and pancreas (Lacy et al., 1999). FLRTs are necessary for early embryonic tissue differentiation and morphogenesis (Egea et al., 2008; Maretto et al., 2008; Muller et al., 2011). In the nervous system, *Flrt3* is expressed in dorsal root ganglion cells, is upregulated following peripheral nerve injury, and promotes neurite growth *in vitro* (Robinson et al., 2004; Tsuji et al., 2004).

FLRT3 has been implicated in regulating fibroblast growth factor (FGF) signaling in several contexts. In *Xenopus*, the FLRT3 homolog (xFLRT3) forms a complex with FGF receptors (FGFRs) in *cis*, modulation of xFLRT3 levels affects FGF-induced kinase signaling, and FGF signaling upregulates xFLRT3 in a proposed positive feedback loop (Bottcher et al., 2004). A similar role for FLRTs has been proposed in mammals, as mouse FLRT3 interacts with FGFR1 and FLRTs are expressed in embryonic development at tissue boundaries where FGF signaling is of known importance (Haines et al., 2006). FLRT1 may also promote neurite outgrowth in neurons in cooperation with FGFRs and FGF signaling (Wheldon et al., 2010).

FLRTs have also been proposed to negatively regulate embryonic cell adhesion in *Xenopus* embryos via FGF-independent pathways. FLRT3 interferes with cadherin-mediated adhesion such that increasing FLRT3 levels leads to abnormal cellular dissociation in embryos (Chen et al., 2009). The intracellular C-terminus of FLRT interacts with the small Rho GTPase Rnd1, which is in the embryonic de-adhesion pathway (Chen et al., 2009;

Karaulanov et al., 2009) and is known more generally to regulate cytoskeletal dynamics (Aspenstrom et al., 2004).

These disparate observations hint at FLRTs subserving important and potentially diverse functions in developing organisms, but a coherent picture of FLRT function has not emerged. FLRTs are expressed in the postnatal brain, where the tissue and developmental stage preclude functions in tissue morphogenesis and axon regeneration. The FLRT signaling pathways and molecular interactions described here may be co-opted in neurons, or FLRTs may interact with a different set of molecular partners, for the fulfillment of one or more currently unknown functions in the brain.

1.5: Trans-synaptic organizing complexes and neurological and psychiatric disorders

While the functions of LRR synaptic organizing molecules and their presynaptic receptors *in vivo* are still not well understood and very much under investigation, the prevalence with which mutations in these genes are associated with nervous system disorders suggests they are of critical importance for the proper functioning of neural circuits. Neurexins and their ligands, neuroligins and LRRTMs, have garnered particular interest for relevance to a range of diseases. Specifically, mutations affecting *NRXN1* have been implicated in autism (Feng et al., 2006; Kim et al., 2008; Yan et al., 2008; Zahir et al., 2008) and schizophrenia (Gauthier et al., 2011; Kirov et al.,

2009; Rujescu et al., 2009). If the trans-synaptic interactions of NRXN1 are part of the etiology of these disorders, disruptions of neuroligin and LRRTM genes should also be found in autistic and schizophrenic patients. This seems to be true in some cases, as *NLGN3* and *NLGN4* have been implicated in autism (Jamain et al., 2003; Laumonnier et al., 2004; Yan et al., 2005), while *LRRTM1* has been linked to schizophrenia (Francks et al., 2007; Ludwig et al., 2009) and *LRRTM3* to autism (Sousa et al., 2010). Similarly, single nucleotide polymorphisms (SNPs) in the Netrin-G genes *NTNG1* and *NTNG2* are associated with schizophrenia (Aoki-Suzuki et al., 2005; Fukasawa et al., 2004; Ohtsuki et al., 2008), and Netrin-G mRNA levels may be altered (Aoki-Suzuki et al., 2005; Eastwood and Harrison, 2008). More recently, mutations in the latrophilin gene family member *LPHN3* have been implicated in attention deficit hyperactivity disorder (ADHD) (Arcos-Burgos et al., 2010; Domene et al., 2011; Jain et al., 2011; Ribases et al., 2011).

While the connection between human brain disorders and the cellular functions of synaptic organizing complexes is yet to be made, the confluence may occur at the level of synaptic circuits in the cortex. Altered levels of or structural mutations in synaptic organizing proteins may lead to changes in numbers or properties of synapses broadly or in select cellular and synaptic subpopulations. Synaptic perturbations then would beget disrupted patterns of neuronal activity at the network level and pathological cognitive and behavioral output. Investigation of the roles of synaptic organizing molecules

in synaptic development and function may then aid making the connection between human disorders and underlying cellular pathology.

1.6: Latrophilins and FLRTs are a Receptor-Ligand Pair Involved in Synapse Development

The work reported here identifies FLRTs as novel endogenous ligands for Latrophilins. We used affinity chromatography and mass spectrometry to identify proteins that putatively interact with the extracellular domains of LPHN3 and FLRT3 and detect FLRTs and Latrophilins, respectively (Figures 2.1-2.7). We confirm direct binding between the extracellular domains of the two protein families using heterologous cell-based and cell-free binding assays, and find that they interact with high affinity and in *trans* (Figures 2.8-2.14). We then provide evidence that endogenous Latrophilin interactions, presynaptic LPHN3, and postsynaptic FLRT3 are all involved in regulating glutamatergic synapse number *in vitro* (Figures 3.3-3.6). We also find that postsynaptic FLRT3 is involved in regulating the strength of synaptic input onto and number of dendritic spines on dentate gyrus granule cells in a cell-autonomous manner *in vivo* (Figures 3.8-3.10). Thus we propose that Latrophilins and FLRTs are molecules crucially involved in synapse development as has proven to be the case for NRXNs, the other main class of α-latrotoxin receptors, and their endogenous ligands.

Chapter 2:

Identification of Latrophilins and FLRTs as a Novel Receptor-Ligand Pair

2.1: Introduction

The Latrophilin family consists of 3 isoforms, LPHN1-3, encoded by different genes. *Lphn1* and *Lphn3* expression is largely restricted to the CNS, while *Lphn2* is broadly expressed in many tissues (Ichtchenko et al., 1999; Sugita et al., 1998). Within the brain, *Lphn1* and *Lphn3* are widely expressed across neuronal populations, and neuronal populations co-express both genes (Allen Mouse Brain Atlas). All three LPHNs have a similar domain organization with several conserved motifs (Figure 3.1A). The C-terminal half of the protein is composed of type II GPCR domain with homology to the Secretin receptor family of GPCRs (Ichtchenko et al., 1999; Sugita et al., 1998). The unusually large extracellular N-terminus, termed the N-terminal fragment (NTF), comprises several protein-protein interaction domains typical of adhesive-type extracellular interactions, namely lectin, olfactomedin, and hormone receptor domains (Ichtchenko et al., 1999; Sugita et al., 1998). Interestingly, the GPCR domain and NTF have been shown to exist as non-covalently linked subunits in the mature protein due to constitutive proteolytic processing at a motif termed the G-protein proteolytic site (GPS) (Krasnoperov et al., 2009; Krasnoperov et al., 2002; Silva et al., 2009a; Volynski et al., 2004). The nature of the GPCR-NTF interaction at the plasma membrane remains somewhat nebulous, however, as the two subunits have been alternately reported to behave independently and as a single complex, a duality which has been proposed to be dynamically regulated (Silva et al., 2009a; Volynski et al., 2004).

Though much effort has been expended investigating the mechanisms of α-latrotoxin action (Sudhof, 2001), virtually nothing is known about the endogenous ligand or function of latrophilins in vertebrates. Latrophilins are at or near the presynaptic active zone and the action of α-latrotoxin implicates them as regulators of neurotransmitter release, but the degree to which α-latrotoxin recruits normal latrophilin signaling is unclear. In order to explore the endogenous function of latrophilins, we sought to identify endogenous latrophilin ligands in the brain with the hypothesis that a trans-synaptic interaction between latrophilins and a postsynaptic adhesion-like protein may be of physiological relevance. We used LPHN3 NTF affinity chromatography to purify candidate ligands from rat brains and identified binding proteins by mass spectrometry. Amongst the most abundant putative interactors were FLRT2 and FLRT3, members of the LRR superfamily of transmembrane proteins. We chose to pursue FLRTs as candidate latrophilin ligands due to their homology to known postsynaptic molecules and striking cell-type specific expression patterns. In a complementary affinity chromatography and mass spectrometry experiment with the ectodomain of FLRT3, we found latrophilins to be the most abundant interactors. We then confirmed that LPHN3 and FLRT3 could interact directly via their extracellular domains in a set of *in vitro* protein binding experiments. Together, these experiments identify LPHNs and FLRTs as a novel receptor-ligand pair.

2.2: Results

Identification of FLRTs as Candidate LPHN Ligands

To identify candidate LPHN ligands, we produced recombinant ecto-LPHN3-Fc protein in HEK293 cells by transient transfection and purified the secreted protein from conditioned media (Figure 2.1B). Sample purity was assessed by SDS-PAGE, in which ecto-LPHN3-Fc ran as a single band of the predicted size (~150 kD) (Figure 2.1C). Ecto-LPHN3-Fc protein was then immobilized on Protein A-coupled beads and used to identify putative binding proteins from 3-week-old rat synaptosome extracts by affinity chromatography. As a negative control, we performed multiple parallel purifications using Fc alone as bait. Ecto-LPHN3-Fc bound beads were loaded onto a gravity-flow column, washed, and eluted. The eluate was digested in solution with trypsin and pressure loaded onto the MudPit column and analyzed in-line by electrospray tandem mass spectrometry (LC-MS/MS) (de Wit et al., 2009; Savas et al., 2011; Washburn et al., 2001). Hundreds of unique proteins were detected in the eluate, with multiple isoforms of two families, the ODZ/Teneurins and FLRTs being identified in high abundance (Figure 2.2A). Of the proteins that bound selectively to ecto-LPHN3-Fc, FLRT2 and FLRT3 were amongst the most abundant (Figure 2.2B) and of particular interest due to similarities in domain organization with previously identified postsynaptic organizing molecules (Figure 2.3A) (de Wit et al., 2010; Siddiqui and Craig, 2011; Williams et al., 2010).

To confirm that latrophilins and FLRTs interact as a ligand-receptor pair, we next produced recombinant ecto-FLRT3-Fc (Figure 2.3) and used it for the reverse affinity chromatography and mass spectrometry experiment. In this purification, latrophilins constituted the dominant identified binding protein (Figure 2.4A). High numbers of distinct LPHN1 and LPHN3 peptides were detected, with relatively fewer LPHN2 peptides (Figure 2.4B). We also identified UNC5B in this sample, a previously reported FLRT3 interactor (Karaulanov et al., 2009; Sollner and Wright, 2009; Yamagishi et al., 2011), but at much lower abundance than LPHN3. When total spectra counts from proteins identified in both purifications were compared, LPHN3 and FLRT3 stood out clearly as the proteins most frequently detected in both purifications (with each as bait in one condition and prey in the other) (Figure 2.5), representing a candidate ligand-receptor pair.

To support our mass spectrometry results, we verified the association of FLRT3 with LPHN3 by western blot. We transfected heterologous cells with full-length FLRT3-myc or myc-LRRTM2 as a negative control, collected cell lysate, and used ecto-LPHN3-Fc coupled to beads to precipitate LPHN3-binding proteins in the lysate. We found that FLRT3-myc was precipitated by ecto-LPHN3-Fc (Figure 2.6A), but that myc-LRRTM2 did not co-precipitate with ecto-LPHN3-Fc (Figure 2.6B). In the reverse experiment, LPHN3-GFP co-precipitated with ecto-FLRT3-Fc (Figure 2.6C). We then performed a similar pulldown assay with ecto-FLRT3-Fc on whole rat brain extracts and found that the N-terminal fragment of LPHN3 is highly enriched by ecto-

FLRT3-Fc affinity precipitation (Figure 2.7A). The abundant presynaptic organizing protein and alternate α-Latrotoxin receptor NRXN1, which we did not detect by mass spectrometry in our FLRT3 interaction screen, did not co-precipitate with ecto-FLRT3-Fc (Figure 2.7B). These results confirm our mass spectrometry data, indicating that LPHN3 indeed associates with FLRT3 via its N-terminal fragment (NTF). Moreover, this interaction is specific, as FLRT3 does not capture the presynaptic adhesion molecule NRXN1 (Figure 2.7B) and LPHN3 does not capture the postsynaptic adhesion molecule LRRTM2 (Figure 2.6B). These findings suggest that FLRTs are likely novel endogenous ligands for latrophilins.

FLRT3 Can Directly Interact With LPHN3

To test whether FLRT3 can bind to LPHN3 in a cellular context, we expressed FLRT3-myc in HEK293 cells and applied ecto-LPHN3-Fc or Fc alone to the cells. We observed strong binding of ecto-LPHN3-Fc to cells expressing FLRT3-myc but no binding of the negative control Fc protein (Figure 2.8A). Ecto-LPHN3-Fc did not bind to cells expressing myc-LRRTM2 (Figure 2.9), showing that the LPHN3-FLRT3 interaction is specific. Ecto-LPHN3-Fc also bound strongly to the other FLRT isoforms, FLRT1 and FLRT2 (Figure 2.9), and ecto-LPHN1-Fc bound to all FLRT isoforms as well (Figure 2.10). In complementary experiments, we found that ecto-FLRT3-Fc, but not Fc alone, bound strongly to cells expressing LPHN3-GFP (Figure 2.8). Ecto-FLRT3-Fc also bound the previously identified interactors UNC5A, UNC5B,

and UNC5C (Figure 2.11), consistent with previous reports (Karaulanov et al., 2009; Sollner and Wright, 2009; Yamagishi et al., 2011), but did not bind to NRXN1-expressing cells (Figure 2.12B). Finally, we tested the possibility of homophilic LPHN3 and FLRT3 interactions, and found that these proteins do not show homophilic binding (Figure 2.12A). Thus, we find selective interaction between LPHNs and FLRTs, but promiscuity between isoforms within these protein families.

To eliminate the possibility that an unknown co-receptor present in HEK293 cells might mediate the FLRT-LPHN interaction, we performed a cell-free binding assay using purified proteins. Histidine-tagged FLRT3 and LPHN3-Fc or control Fc proteins were mixed in solution, and the Fc proteins precipitated with bead-coupled Protein A. Binding was then assessed by western blotting for FLRT3-His in the Protein A precipitate. We found that FLRT3-His co-precipitated with ecto-LPHN3-Fc, but not with the control protein NRXN1β(-S4)-Fc or Fc alone (Figure 2.13A). These results confirm a direct interaction between the FLRT3 and LPHN3 ectodomains.

To quantitatively characterize the affinity of the FLRT3-LPHN3 interaction, we employed a surface plasmon resonance (SPR)-based bioassay. SPR is a sensitive and quantitative way of measuring specific ligand-receptor binding in a label-free manner by measuring accumulation of soluble protein along the protein-coated surface of a sensor chip. We immobilized ecto-FLRT3 on a sensor chip, and soluble ecto-LPHN3-Fc was injected in increasing concentrations. Binding of ecto-LPHN3-Fc was

monitored in real time over a series of 6-minute injections followed by wash periods of 10 minutes (Figure 2.13B). Plotting the maximum relative response versus the ecto-LPHN3-Fc concentrations, we calculated the K_D of the LPHN3-FLRT3 interaction to be 14.7 nM (Figure 2.13B), showing a high affinity interaction of FLRT3 with the extracellular domain of LPHN3. Interestingly, the dissociation rate appears to be very slow, as indicated by the slow decay of signal that did not return to baseline during the wash period. The slow dissociated kinetics and high affinity suggest that the binding of LPHN3 to FLRT3 is very stable, with a lifetime of at least tens of minutes.

As a putative trans-synaptic complex, FLRT3 and LPHN3 must be able to interact across sites of cell-cell contact. We tested whether LPHN3 and FLRT3 can interact in *trans* by overexpressing LPHN3-GFP in dissociated hippocampal neurons and co-culturing them with HEK293 cells expressing FLRT3-myc or a control construct. We then fixed and immunostained the cultures and imaged transfected axons where they contacted transfected HEK293 cells. We observed strong clustering of axonal LPHN3-GFP when transfected axons crossed FLRT3-myc-expressing HEK293 cells (Figure 2.14A), but diffuse LPHN3 signal in areas where axons did not contact cells or contacted control HEK293 cells (Figure 2.14B). The accumulation of FLRT3 at sites of contact suggests that FLRT3 is capable of interacting in *trans* with axonal LPHN3 and mediating its recruitment or retention.

2.3: Conclusions

In this line of experiments we identified FLRTs as novel endogenous ligands for latrophilins. Beginning with an unbiased protein binding screen with the NTF of LPHN3, we identified two families of proteins, FLRTs and ODZs/teneurins, as candidate interactors. We chose to pursue the potential interaction with FLRTs since they have homology to LRRTMs, SALMs, and NGLs, known postsynaptic molecules involved in trans-synaptic interactions that affect the development of synapses. A complementary screen for FLRT3 binding partners corroborated the results of the LPHN3 binding screen, as latrophilin proteins were by far the most abundant FLRT3 interactors detected. We then used heterologous cells expressing proteins of interest and soluble recombinant LPHN3 and FLRT3 ectodomain proteins to test binding. We found that all LPHN1 and LPHN3 bind to all 3 FLRT isoforms. These interactions are specific, since FLRT3 does not bind to the alternate α-Latrotoxin receptor neurexin-1 and LPHN3 does not bind to LRRTM2, a postsynaptic regulatory molecule with homology to FLRT3. We also found that FLRT3 and LPHN3 can interact in *trans* at intercellular junctions, as FLRT3 expressed by heterologous cells is able to induce the accumulation of LPHN3 in axons that contact the cells. Both the LPHN3 NTF and GPCR domain are concentrated at these sites of contact, suggesting that either LPHN3 is behaving as a single complex or that FLRT3 binding to the NTF acts indirectly to trap the GPCR domain.

Little is known about the functions of latrophilins or FLRTs, but characterizing their endogenous molecular interactions should aid investigation of their physiological functions. Latrophilins are known to be presynaptic proteins and some evidence using α-Latrotoxin as an exogenous ligand suggests that they may affect vesicle release at presynaptic terminals, but their functions in the absence of exogenous ligands has not been elaborated. FLRTs are single-pass transmembrane proteins of the LRR superfamily about which little is known of their role in the brain. That these two minimally understood proteins interact with one another lead as to the hypothesis that they may participate in a trans-synaptic interaction to regulate synapse development.

2.4: Acknowledgments

The data presented In Chapter 2 of this dissertation has been submitted for publication as part of the following manuscript:

Matthew L. O'Sullivan, Joris de Wit, Jeffrey N. Savas, Stefanie Otto, Davide Comoletti, John R. Yates III, and Anirvan Ghosh. Postsynaptic FLRT proteins are endogenous ligands for the black widow spider venom receptor Latrophilin and regulate excitatory synapse development. *Submitted for publicaton.*

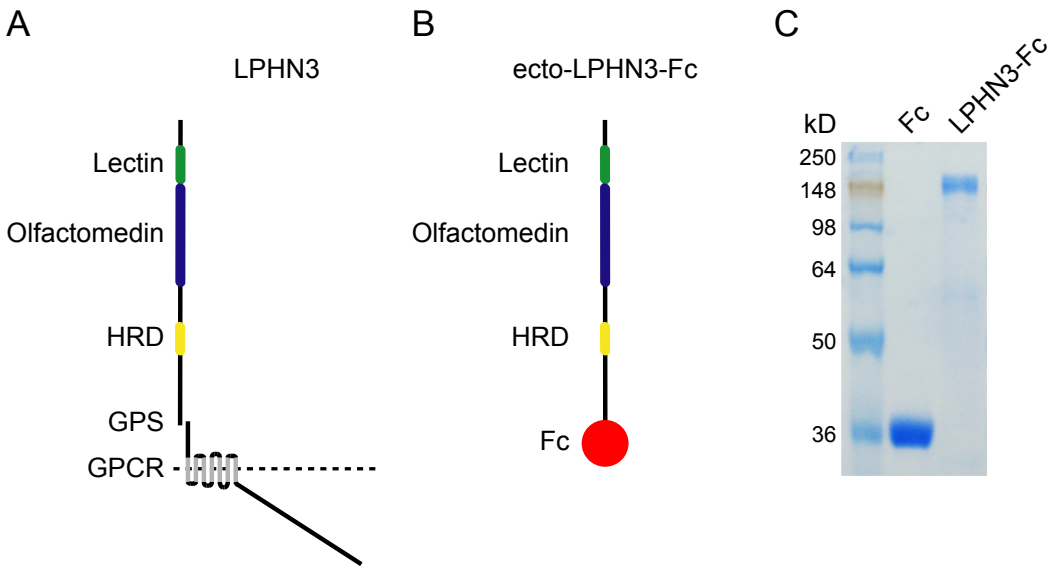

Figure 2.1: Production of recombinant LPHN3 ectodomain protein.
(A) Schematic of latrophilin protein highlighting conserved domains. HRD: Hormone Receptor Domain; GPS: GPCR Proteolytic Site.
(B) Schematic of recombinant ecto-LPHN3-Fc protein, consisting of the extracellular NTF of LPHN3 fused C-terminally to human IgG Fc.
(C) Coomassie stained SDS-PAGE gel showing ecto-LPHN3-Fc purified recombinant protein running as a single band.

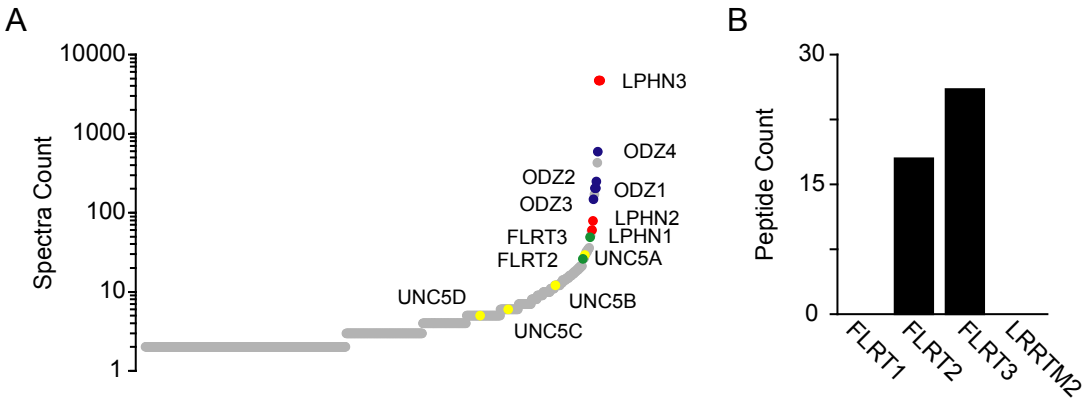

Figure 2.2: LPHN3 affinity chromatography and mass spectrometry identifies FLRTs as candidate ligands.
(A) Distribution of identified protein abundance in ecto-LPHN3-Fc affinity purification. Members of protein families of interest are colored and labeled. Red: LPHNs; Green: FLRTs; Blue: ODZ/Teneurins; Yellow: UNC5s. LPHN3 was identified at high levels due to inclusion of bait protein.
(B) Abundance of selected LRR-family proteins in ecto-LPHN3-Fc affinity purification. High numbers of unique peptides corresponding to FLRT2 and FLRT3 were identified.

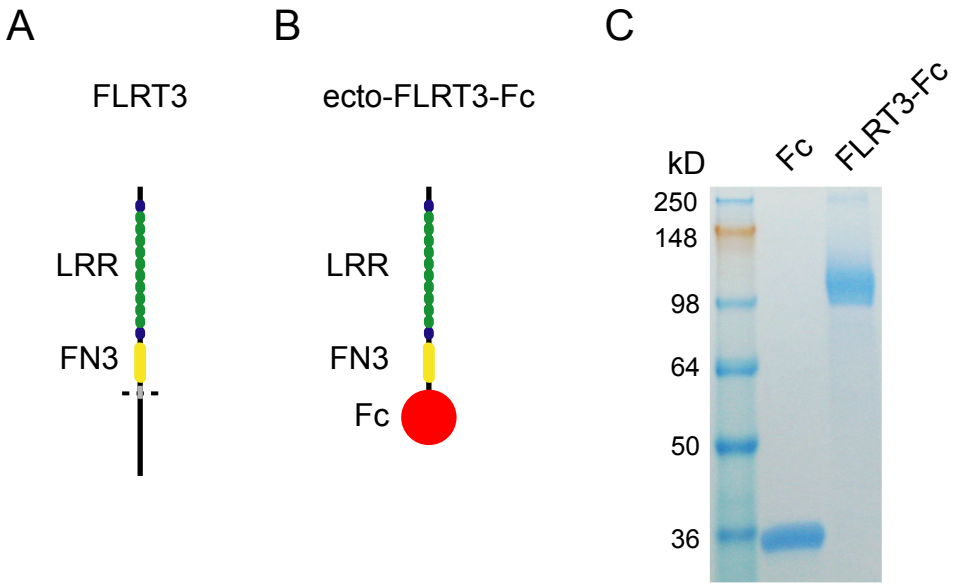

Figure 2.3: Production of recombinant FLRT3 ectodomain protein.
(A) Schematic of FLRT protein highlighting conserved domains. LRR: Leucine Rich Repeat; FN3: Fibronectin Type 3.
(B) Schematic of recombinant ecto-FLRT3-Fc protein, consisting of the extracellular domain of FLRT3 fused C-terminally to human IgG Fc.
(C) Coomassie stained SDS-PAGE gel showing ecto-FLRT3-Fc purified recombinant protein running as a single band.

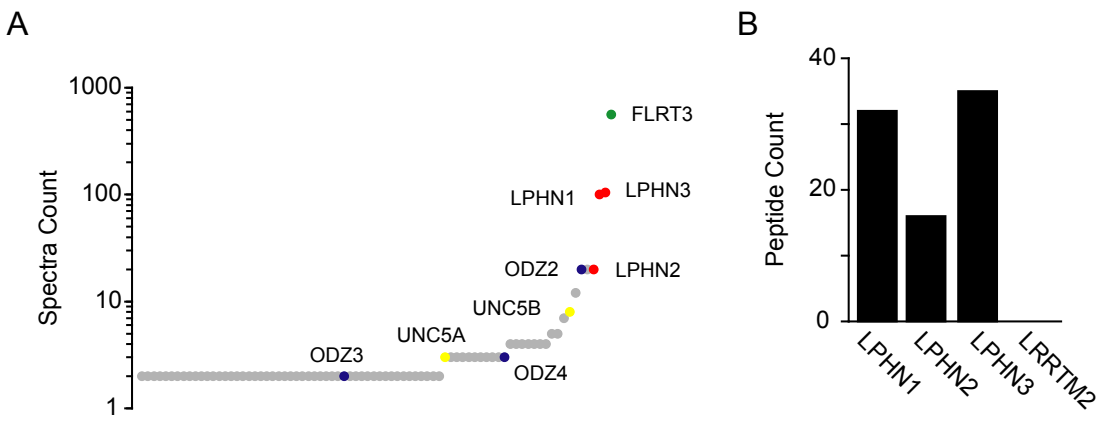

Figure 2.4: FLRT3 affinity chromatography and mass spectrometry identifies latrophilins as candidate receptors.
A) Distribution of identified protein abundance in ecto-FLRT3-Fc affinity purification. Members of protein families of interest are colored and labeled. Red: LPHNs; Green: FLRTs; Blue: ODZ/Teneurins; Yellow: UNC5s. FLRT3 was identified at high levels due to inclusion of bait protein.
(B) Abundance of selected proteins in ecto-LPHN3-Fc affinity purification. High numbers of unique peptides corresponding to all LPHN isoforms were identified.

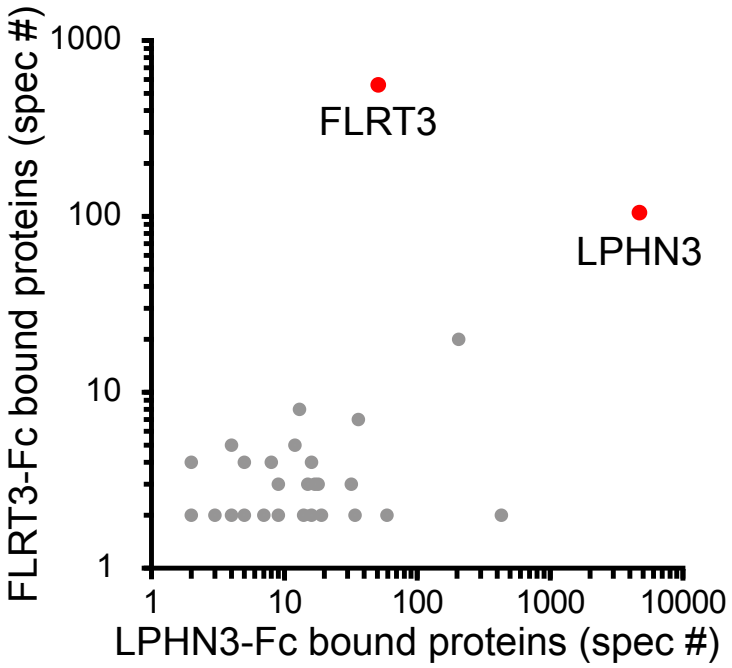

Figure 2.5: ecto-LPHN3-Fc affinity chromatography and mass spectrometry identifies candidate Latrophilin ligands.
Frequency of detection of all peptides for proteins identified in both LPHN3 and FLRT3 affinity purifications. Proteins with high spectra counts in both purifications are in the upper right of the plot. FLRT3 and LPHN3 (red points) were each abundant in both purifications: in one condition due to inclusion as bait, and in the other due to co-purification.

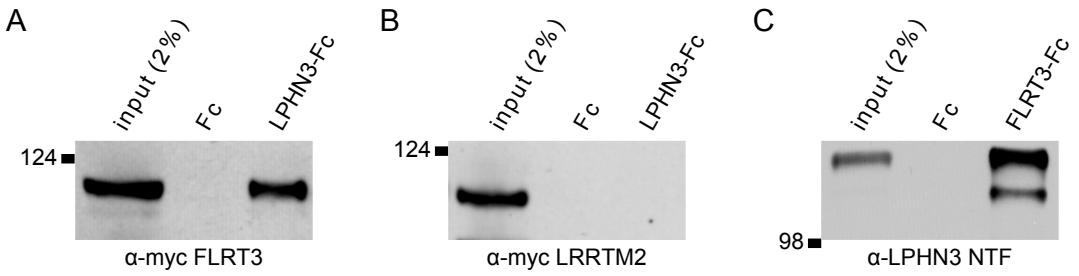

Figure 2.6: Western blot confirmation of FLRT3 affinity purification by ecto-LPHN3-Fc.
(A-C) HEK cells were transfected with FLRT3-myc (A), myc-LRRTM2 (B), or LPHN3-GFP (C) and lysates incubated with ecto-Fc proteins or control Fc-only protein, precipitated with Protein A-coupled beads, and pull-down analyzed by western blot.
(A) Recombinant ecto-LPHN3-Fc precipitates FLRT3-myc from HEK cell lysate.
(B) Recombinant ecto-LPHN3-Fc does not precipitate myc-LRRTM2 from HEK cell lysate.
(C) Recombinant ecto-FLRT3-Fc precipitates LPHN3-GFP NTF from HEK cell lysate.

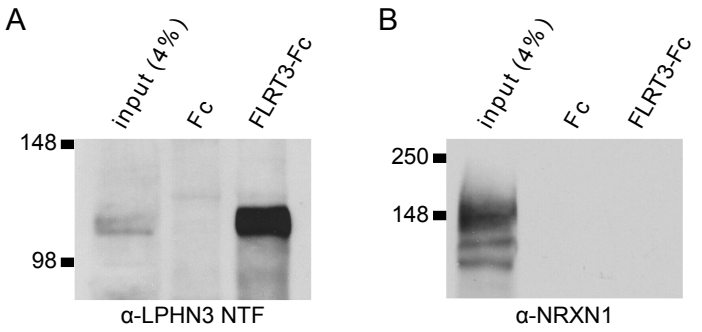

Figure 2.7: Western blot confirmation of LPHN3 affinity purification by ecto-FLRT3-Fc.
(A-B) Whole brain protein samples were incubated with ecto-FLRT3-Fc protein or control Fc-only protein, precipitated with Protein A-coupled beads, and pull-down analyzed by western blot.
(A) Recombinant ecto-FLRT3-Fc precipitates LPHN3 NTF from brain.
(B) Recombinant ecto-FLRT3-Fc does not precipitate NRXN1 from brain.

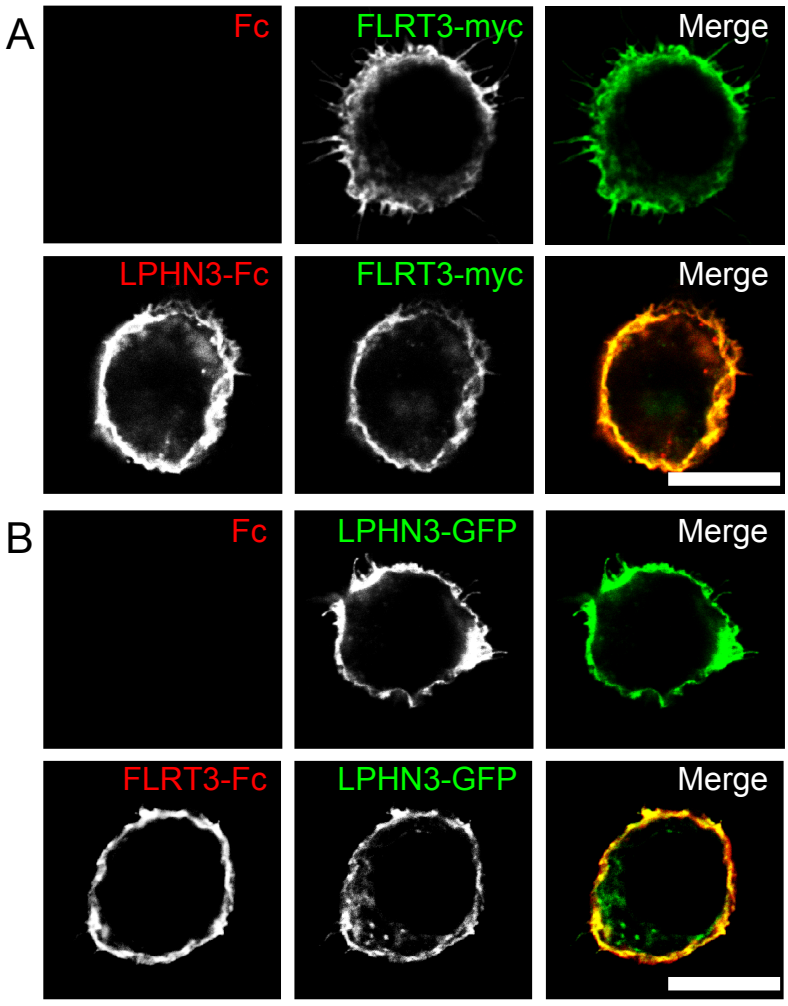

Figure 2.8: Recombinant ecto-LPHN3 and ecto-FLRT3 proteins bind to heterologous cells expressing FLRT3 and LPHN3 respectively.
(A, B) Binding of soluble ecto-LPHN3-Fc (A) and ecto-FLRT3-Fc (B) proteins to HEK cells expressing FLRT3 or LPHN3. Scale bar = 10 μm. Left column: anti-Fc immunofluorescence to detect the indicated control Fc or ecto-Fc protein. Middle column: anti-myc (A) or anti-GFP (B) immunofluorescence showing expression of FLRT3-myc or LPHN3-GFP, respectively, in transfected HEK cells. Right column: overlay of Fc channel and target channel fluorescence. Signal in the anti-Fc channel reflects binding of soluble protein.

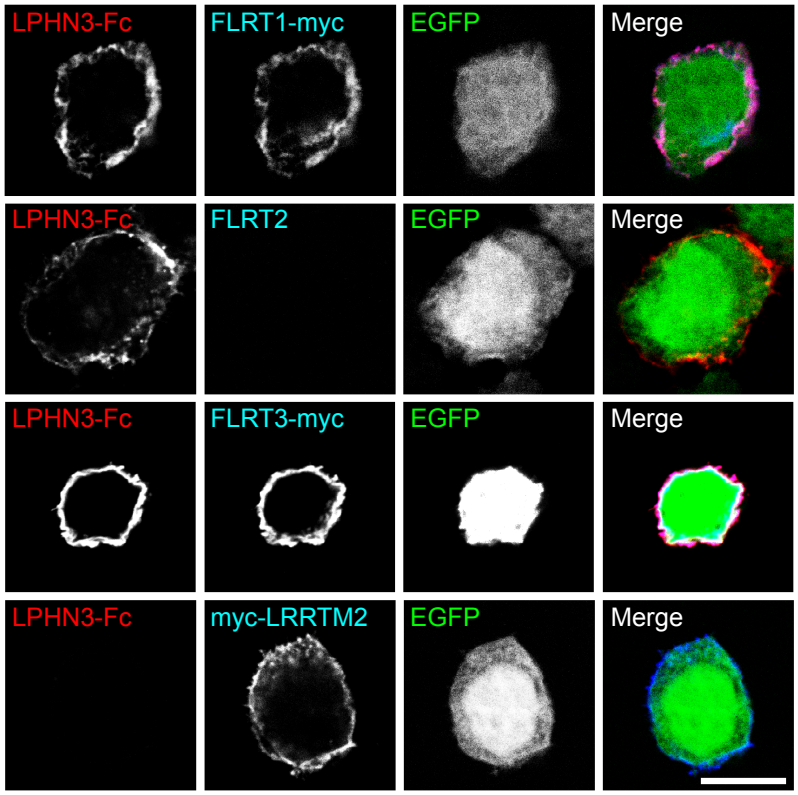

Figure 2.9: Recombinant ecto-LPHN3 binds to heterologous cells expressing FLRT1, FLRT2, or FLRT3.
ecto-LPHN3-Fc binds to FLRT1-myc, FLRT2, and FLRT3-myc, but not myc-LRRTM2. Soluble ecto-Fc proteins were applied to transiently transfected HEK cells expressing candidate interactors, and the cells were fixed and immunostained for Fc to assess binding. Scale bars = 10 μm.

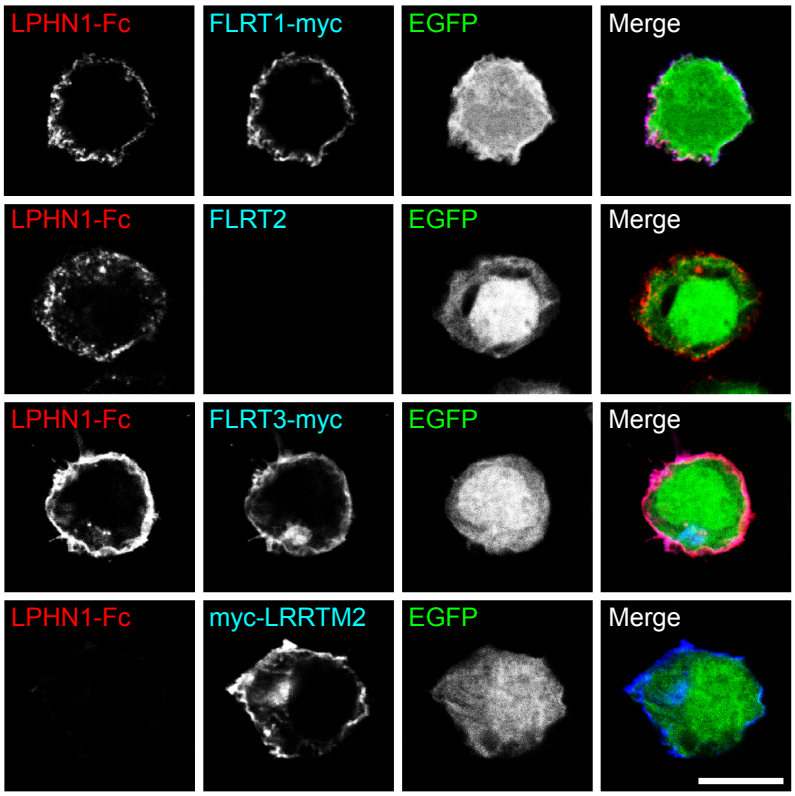

Figure 2.10: Recombinant ecto-LPHN1 binds to heterologous cells expressing FLRT1, FLRT2, or FLRT3.
ecto-LPHN1-Fc binds to FLRT1-myc, FLRT2, and FLRT3-myc, but not myc-LRRTM2. Soluble ecto-Fc proteins were applied to transiently transfected HEK cells expressing candidate interactors, and the cells were fixed and immunostained for Fc to assess binding. Scale bars = 10 μm.

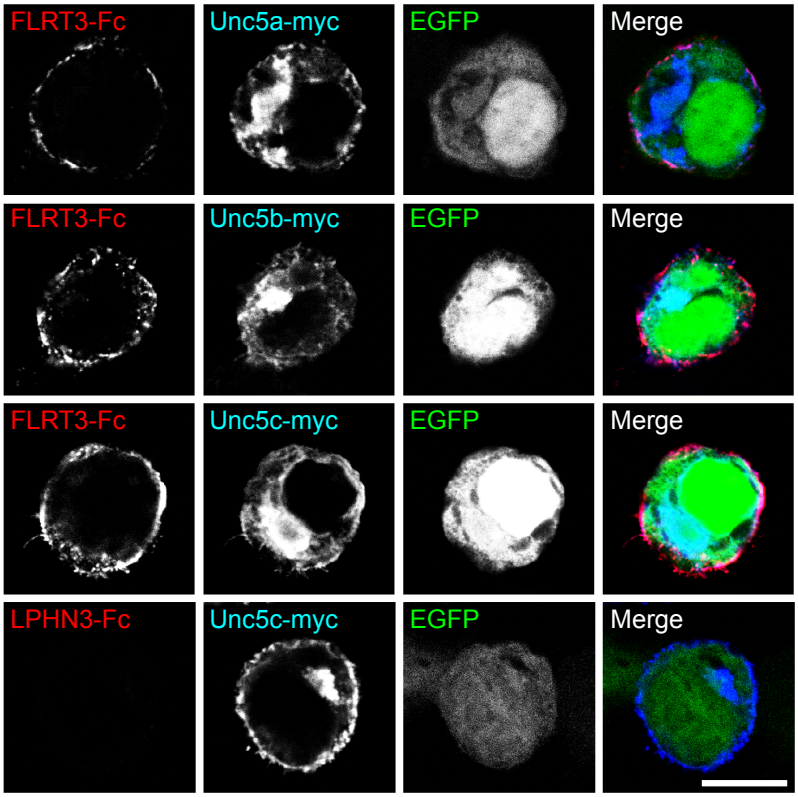

Figure 2.11: Recombinant ecto-FLRT3, but not LPHN3-Fc, binds to heterologous cells expressing Unc5s.
ecto-FLRT3-Fc binds to the previously identified interactors Unc5A-C, while ecto-LPHN3-Fc does not. Soluble ecto-Fc proteins were applied to transiently transfected HEK cells expressing candidate interactors, and the cells were fixed and immunostained for Fc to assess binding. Scale bars = 10 μm.

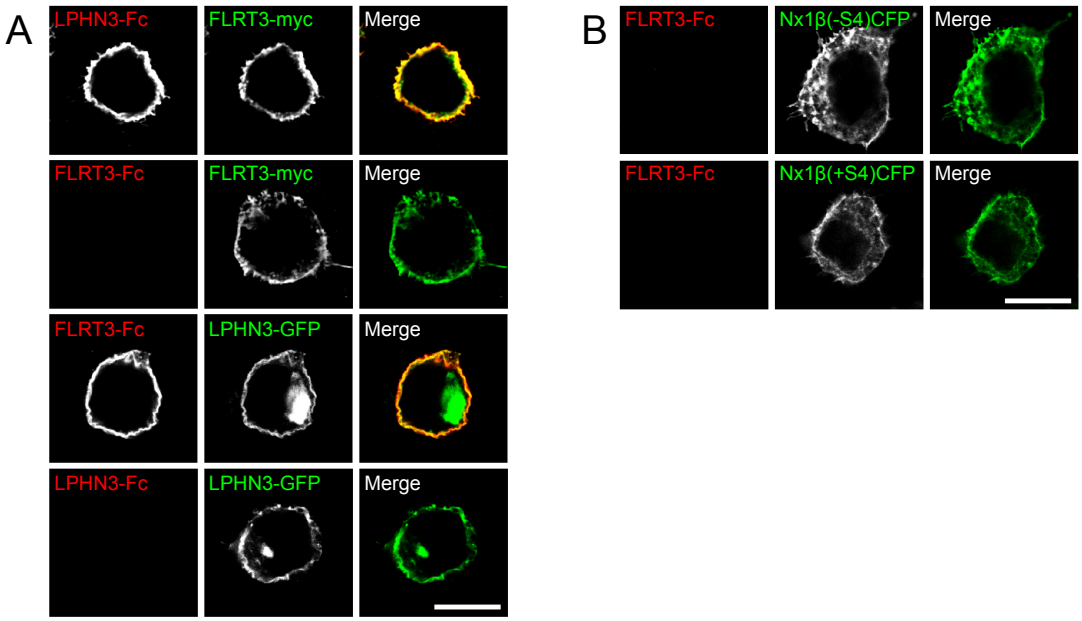

Figure 2.12: LPHN3 and FLRT3 do not display homophilic binding or binding to Neurexin-1.
(A) ecto-LPHN3-Fc does not bind to LPHN3 and ecto-FLRT3-Fc does not bind to FLRT3.
(B) ecto-FLRT3-Fc does not bind to Neurexin 1.
(A-B) Soluble ecto-Fc proteins were applied to transiently transfected HEK cells expressing candidate interactors, and the cells were fixed and immunostained for Fc to assess binding. Scale bars = 10 μm.

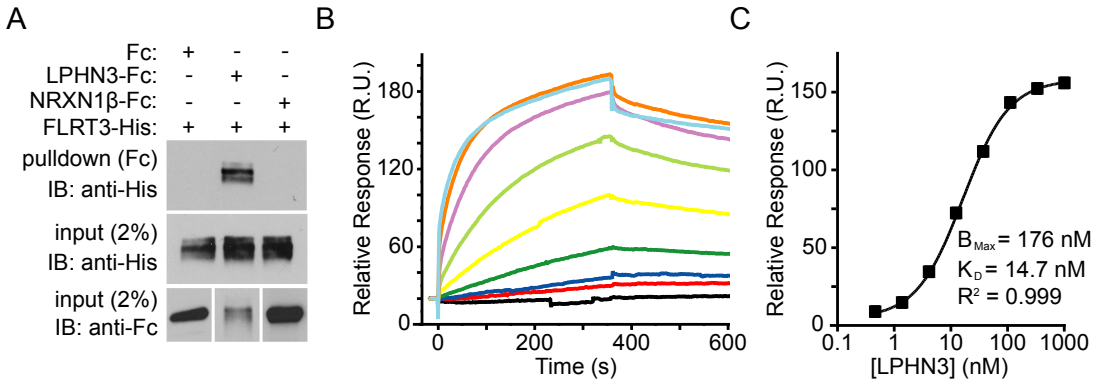

Figure 2.13: Recombinant LPHN3 and FLRT3 ectodomains bind directly in solution with high affinity.
(A) Direct binding of soluble FLRT3 and LPHN3 ectodomain proteins. FLRT3-His was mixed with Fc, LPHN3-Fc, or NRXN1-Fc in solution, precipitated by Protein-A affinity, and detected by western blotting with an anti-His antibody. FLRT3-His can only be detected when precipitated by LPHN3-Fc (top).
(B) Surface Plasmon Resonance (SPR)-based measurement of ecto-LPHN3-Fc binding to immobilized ecto-FLRT3. Increasing concentrations of ecto-LPHN3-Fc were injected in series to the ecto-FLRT3-coated sensor chip. Each colored trace represents a binding curve for a different concentration of ecto-LPHN3-Fc, from 1 μM to 0.45 μM in three-fold dilutions, separated by wash and regeneration steps. Affinity was measured by monitoring SPR response in resonance units (R.U.) during protein application and wash.
(C) Concentration-response function of LPHN3-FLRT3 SPR binding. The K_D of the interaction was calculated to be 14.7 nM.

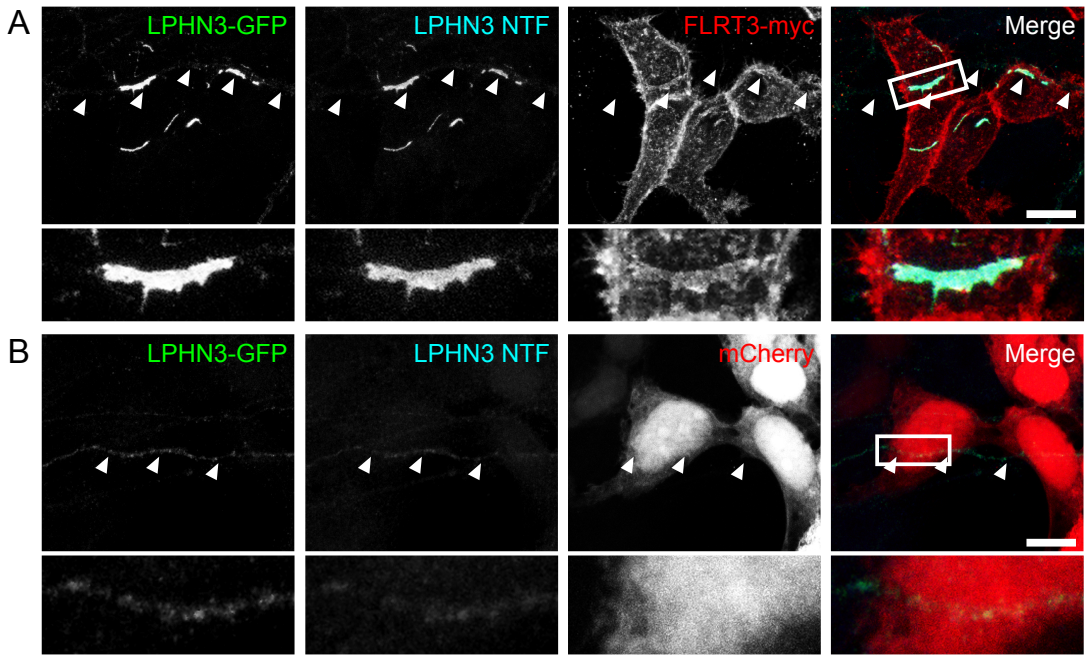

Figure 2.14: LPHN3 and FLRT3 can interact at intercellular junctions in *trans*.
(A, B) Hippocampal neurons transfected with LPHN3-GFP were co-cultured with HEK cells expressing FLRT3-myc (F) or mCherry (G). Immmunostaining for GFP, LPHN3 NTF, and myc or mCherry, at locations where transfected axons (arrowheads) contacted transfected HEK cells shows an accumulation of LPHN3-GFP and LPHN3 NTF in axons crossing FLRT3-myc expressing cells (F). Scale bar = 10 μm.

Chapter 3:

FLRT3 and LPHN3 Positively Regulate Glutamatergic Synapses

3.1: Introduction

Intercellular interactions between axonal and dendritic transmembrane proteins are thought to be crucial for many aspects in the development of neural circuits, from axon guidance to synaptogenesis and synapse maturation (McMahon and Diaz, 2011; Siddiqui and Craig, 2011; Williams et al., 2010). The ability of α-latrotoxin to induce neurotransmitter release by interacting with latrophilin presents the compelling possibility that latrophilins regulate synaptic vesicle cycling under physiological conditions. Latrophilin interacts with $G\alpha_o$ and $G\alpha_q$ but not $G\alpha_i$ (Lelianova et al., 1997; Rahman et al., 1999) and α-latrotoxin induced release by way of latrophilin involves release of calcium from intracellular stores by coupling to the phospholipase-C (PLC) and inositol triphosphate (IP3) pathway (Capogna et al., 2003; Lelianova et al., 1997; Volynski et al., 2004). In addition to latrophilin G-protein signaling, the large NTF could plausibly be involved in presynaptic *cis* interactions, giving latrophilins at least two plausible categories of molecular mechanism by which they could affect synaptic terminals. FLRTs also have identified signaling capabilities, including interacting with FGFRs via its extracellular FN3 domain (Bottcher et al., 2004) and intracellular signalling through the small GTPase Rnd1 (Chen et al., 2009; Karaulanov et al., 2009). Thus both latrophilins and FLRTs have established versatile second messanger signalling capabilites which could affect synapses.

We hypothesized that a trans-synaptic FLRT-latrophilin interaction may regulate the development of glutamatergic synapses. We observe that FLRT3

is expressed in distinct neuronal populations during early postnatal life when synapses are rapidly developing is found at postsynaptic specializations. *In vitro*, loss of LPHN3 or FLRT3 in dentate granule cells leads to a reduction in synapse density, an effect mirrored that is mirrored by disruption of endogenous latrophilin interactions. *In vivo*, loss of FLRT3 in dentate granule cells causes a reduction in dendritic spine density and in the strength of perforant path synaptic input.

3.2: Results

FLRT3 Is a Postsynaptic Protein Expressed by Specific Neuronal Populations

To identify brain regions where FLRT3 is likely to function, we examined *Flrt3* mRNA expression in the developing brain. Analysis of *Flrt3* expression by in situ hybridization on P7 and P14 mouse brain sections revealed that *Flrt3* was highly expressed in specific neuronal populations during the first two postnatal weeks, a time of crucial synaptic development (Figure 3.1). In the hippocampus, the principal cell layers of the dentate gyrus and CA3 showed strong signal, whereas *Flrt3* expression was not detected in CA1.

Since endogenous FLRT3 could not be detected by immunofluorescence with currently available antibodies, we expressed FLRT3-myc in dissociated hippocampal neurons and immunostained for myc and the postsynaptic marker PSD-95 to determine if FLRT3 is targeted to

synaptic sites (Figure 3.2A). FLRT3-myc localizes to dendrites in a highly punctate fashion. We observed striking colocalization between FLRT3-myc and PSD-95, with large FLRT3 puncta closely associated but only partially overlapping with PSD-95 puncta on the dendrites of transfected neurons. This suggests that FLRT3 is selectively trafficked to or retained at postsynaptic sites.

We next employed a subcellular fractionation approach to examine distribution of endogenous FLRT3 across different cellular fractions from rat brain (Figure 3.2B). Consistent with it being a transmembrane protein, we did not detect FLRT3 in cytosolic fractions, but saw progressive enrichment of FLRT3 in more highly purified synaptic fractions. This pattern of enrichment mirrors that seen for the glutamate receptor GluR2 and postsynaptic scaffold PSD-95, and is in contrast to the abundant presynaptic vesicle-associated protein Synaptotagmin 1, which is detected in all fractions. Together these results suggest that FLRT3 is present at or near the glutamatergic postsynaptic specializations of the specific hippocampal principal neurons that express it.

LPHN3 Interactions Regulate Glutamatergic Synapse Density *In Vitro*

After establishing that the latrophilin ligand FLRT3 is expressed in hippocampal neurons and localizes to glutamatergic synapses, we decided to test whether LPHN3 receptor-ligand interactions are of functional importance for synapse development. To this end, we applied excess soluble ecto-

LPHN3-Fc protein to dissociated hippocampal cultures to competitively disrupt endogenous LPHN3 complexes. We analyzed glutamatergic synapses by immunofluorescence with antibodies against the presynaptic marker VGluT1 and the postsynaptic marker PSD-95 after incubation with ecto-LPHN3-Fc or control Fc protein from 9 to 14 days *in vitro* (DIV) (Figure 3.3A). We restricted our analysis to *Flrt3*-expressing dentate granule cells identified by immunoreactivity for Prox1, a transcription factor expressed selectively in dentate granule cells (Allen Mouse Brain Atlas). We found that ecto-LPHN3-Fc treatment reduced the density of VGluT1, PSD-95, and co-localized VGlut1 + PSD-95 puncta on the dendrites of identified granule cells by 17%, 28%, and 32%, respectively (Figure 3.3B). In contrast to synapse number, which was reduced by ecto-LPHN3-Fc treatment, synapse size, as measured by puncta area, was unaffected (Figure 3.3C). Treatment of cultures with ecto-FLRT3-Fc resulted in cell death (data not shown), preventing complementary competition experiments with ecto-FLRT3-Fc. These results suggest that LPHN3 interactions are involved in regulating the number of synapses formed onto granule cells.

LPHN3 Knockdown Reduces mEPSC Frequency *In Vitro*

To examine whether LPHN3 is involved in regulated the number of functional synapses we employed an shRNA-mediated loss-of-function strategy combined with electrophysiology. We designed an shRNA to specifically knock down Lphn3 expression, and verified efficacy of knockdown

in heterologous cells by western blot (Figure 3.4A). To verify specificity of knockdown, we made an shRNA-resistant LPHN3 construct by introducing silent point mutations in the shRNA target sequence. This LPHN3 clone proved to be insensitive to the shRNA, demonstrating that the shRNA was target-sequence specific as well as being highly efficacious (Figure 3.4A). This shRNA was then cloned into a GFP-expressing lentiviral vector, virus produced, and hippocampal cultures infected at 4DIV such that over 90% of neurons in the culture were infected. We then recorded mEPSCs from neurons in cultures infected with shLphn3 or GFP control lentiviruses (Figure 3.4B). shLphn3 reduced the frequency of mEPSCs without affecting mEPSC amplitude (Figure 3.4C), suggesting that loss of LPHN3 affects synapse or synaptic release site number.

Loss of Postsynaptic FLRT3 *In Vitro* Reduces Glutamatergic Synapse Density

If LPHN3 acts on synapses by interacting with FLRT3, reducing levels of postsynaptic FLRT3 should similarly reduce the number of excitatory synapses formed. To examine this possibility, we generated an shRNA to knock down FLRT3. We initially screened shRNAs for efficacy in lysate from transfected HEK293 cells by western blot. After identifying an shRNA (shFlrt3) that strongly reduced levels of FLRT3-myc in HEK293 cells (Figure 3.5A), we generated a FLRT3 mutant with silent point mutations in the shRNA target sequence (FLRT3*) to test the specificity of shFlrt3 knockdown. FLRT3*-myc

proved to be insensitive to shFlrt3, verifying target-sequence specificity of the Flrt3 shRNA. (Figure 3.5A). We then subcloned the shRNA cassette into a GFP-expressing lentiviral vector and produced lentivirus. To test the efficacy and specificity of knockdown of endogenous *Flrt3*, we analyzed mRNA levels of infected dissociated cortical cultures by qPCR. The shFlrt3 lentivirus strongly reduced Flrt3 mRNA levels by 74% without affecting levels for a panel of non-targeted synaptic adhesion molecule transcripts (Figure 3.5B).

Hippocampal neurons were sparsely electroporated with shFlrt3 or control plasmids and immunostained at 14DIV with synaptic markers. When we counted VGluT1, PSD95, and co-localized synapses onto transfected granule cells, we found that Flrt3 knockdown reduced synapse density and synaptic puncta size (Figure 3.5C-E). Co-electroporation with the shRNA resistant FLRT3 expression construct (FLRT3*) rescue these effects.

To see if the reduction in synapse number observed by immunofluorescence with synaptic markers corresponds to a reduction in functional synapses, we recorded mEPSCs from putative granule cells in cultures electroporated with shFLRT3 or control plasmids (Figure 3.6A). We found a large reduction in the frequency of mEPSCs in shFlrt3 electroporated granule cells, as seen in a 198% increase in the mean inter-event interval and a rightward shift in the cumulative distribution of IEIs relative to GFP cells (Figure 3.6B). We also found a small reduction in the amplitude of mEPSCs in shFlrt3 electroporated cells (Figure 3.6C). Thus FLRT3 seems to positively regulate synapses number in granule cells, such that loss of FLRT3 in leads to

a reduction in glutamatergic synapses as measured both by electrophysiology and immunofluorescence.

FLRT3 Is Not Sufficient to Induce Presynaptic Differentiation

Since several postsynaptic transmembrane proteins with effects on synapse number *in vitro* have been shown to be sufficient to induce presynaptic differentiation onto heterologous cells, we decided to test whether FLRT3 possesses this property. We found, however, that axons contacting FLRT3-expressing HEK cells do not display synapsin puncta (Figure 3.7), indicating that FLRT3-mediated adhesion is not sufficient to induce presynaptic differentiation. Thus, while both FLRT3 and the Neurexin ligands LRRTM2 and Neuroligin-1 affect synapse number in neuronal cultures (Chih et al., 2005; de Wit et al., 2009; Ko et al., 2009; Linhoff et al., 2009; Scheiffele et al., 2000), FLRT3 is likely to act through a different kind of mechanism.

FLRT3 Regulates the Strength of Perforant Path Synapses onto Granule Cells *In Vivo*

To test whether endogenous FLRT3 contributes to synaptic function *in vivo*, we stereotaxically injected shFlrt3 or control lentivirus into the hippocampus of postnatal day 5 (P5) rat pups and cut acute slices for electrophysiology between P13 and P16. Infected dentate granule cells were identified by GFP epifluorescence, and simultaneous whole-cell voltage-clamp recordings made from nearby infected and uninfected cells. A single

stimulating electrode placed in the middle of the molecular layer was used to evoke perforant path synaptic inputs. At a holding potential of -60 mV to record AMPAR-mediated EPSCs, we observed that EPSCs onto shFlrt3-infected neurons were strongly reduced in amplitude by 38% relative to simultaneously recorded uninfected control cells (Figure 3.8A). NMDAR-mediated EPSCs, measured 50 ms after the stimulus at a holding potential of +40 mV, were similarly reduced by 33% by FLRT3 knockdown (Figure 3.8B). The reduction in peak synaptic current mediated by these two classes of glutamate receptors was proportional, however, as the ratio of AMPAR EPSC to NMDAR EPSC for each input was not affected by FLRT3 knockdown (Figure 3.8C). These results indicate that loss of FLRT3 leads to an attenuation of evoked glutamatergic transmission at perforant path-granule cell synapses.

The reduction in evoked transmission in cells expressing shFlrt3 could either be due to a reduction in presynaptic release probability or due to a reduction in the number of perforant path-granule cell synapses. To test whether knockdown of postsynaptic FLRT3 affects presynaptic properties, we examined short-term plasticity of synapses onto infected cells using a paired pulse protocol. There was no effect of FLRT3 knockdown on paired pulse ratios of perforant path inputs with 20 Hz stimuli (Figure 3.8D). Granule cells infected with a control, GFP-expressing lentivirus did not differ from uninfected cells by any of these measures (Figure 3.9).

Loss of FLRT3 in Granule Cells Reduces Dendritic Spine Density

To determine whether FLRT3 knockdown compromised the strength of perforant path synaptic input by reducing the strength of single synapses or by reducing the number of synapses, we used *in utero* electroporation to sparsely label and manipulate dentate gyrus granule cells for anatomical analysis. The hippocampi of E15 mouse embryos were electroporated with shFlrt3 or control GFP plasmids, the mice perfused at P14, and brains sectioned and immunostained. GFP-filled granule cell dendrites in the middle molecular layer were imaged on a confocal microscope and dendritic spines counted (Figure 3.10A). shFlrt3 electroporated granule cells showed a highly significant 20% reduction in dendritic protrusion density relative to GFP control cells (Figure 3.10B). The density of spines on the dendrites of electroporated CA1 pyramidal neurons, which do not express *Flrt3,* did not differ between shFlrt3 and control cells (Figure 3.10C,D), ruling out non-specific shRNA effects on spine density. Together, these results indicate that FLRT3 is required *in vivo* to regulate the number of perforant path synapses and the strength of excitatory synaptic drive onto dentate granule cells.

3.3: Conclusions

After identifying FLRTs as latrophilin ligands, we sought to investigate the role of these proteins at synapses. FLRTs are expressed in specific principal neurons in the hippocampus and cortex in adulthood (Allen Mouse Brain Atlas). We found that *Flrt3* is highly expressed in the dentate gyrus and

CA3 regions of the hippocampus during early postnatal development, a period during which synapses are rapidly developing. FLRT3 trafficks to glutamatergic postsynaptic specializations and is enriched in synaptic membranes, indicating that it is a postsynaptic protein. Consistent with our hypothesis that a trans-synaptic interaction between presynaptic latrophilins and postsynaptic FLRTs might regulate synapses, we found that interfering with latrophilin interactions by competition with soluble recombinant LPHN3 ectodomain reduced the density of synapses formed onto granule cells in culture. Further supporting the contention that presynaptic latrophilins positively regulate synapses, we observed a reduction in the frequency of mEPSCs in cultures in which LPHN3 had been knocked down. Concomitantly, postsynaptic loss of FLRT3 leads to a reduction of synapses. *In vivo*, loss of FLRT3 also seems to reduce synapse density, as evidenced by a reduction the strength of evoked synaptic input and a reduction in dendritic spine density. Together, these data indicate that FLRT3 and LPHN3 positively regulate glutamatergic synapse number.

3.4: Acknowledgments

The data presented In Chapter 3 of this dissertation has been submitted for publication as part of the following manuscript:

Matthew L. O'Sullivan, Joris de Wit, Jeffrey N. Savas, Stefanie Otto, Davide Comoletti, John R. Yates III, and Anirvan Ghosh. Postsynaptic FLRT proteins are endogenous ligands for the black widow spider venom receptor Latrophilin and regulate excitatory synapse development. *Submitted for publication.*

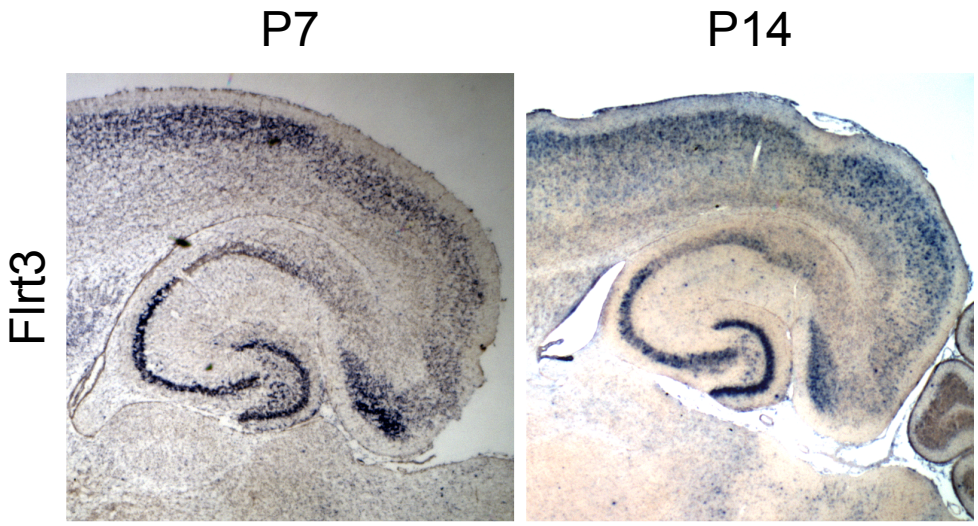

Figure 3.1: *Flrt3* is expressed by select principal neuron populations in early postnatal development.
In situ hybridization with anti-sense *Flrt3* probe in horizontal sections from P7 and P14 mouse brain. High signal can be seen in the DG and CA3 regions of the hippocampus, as well as in L2/3 of neocortex.

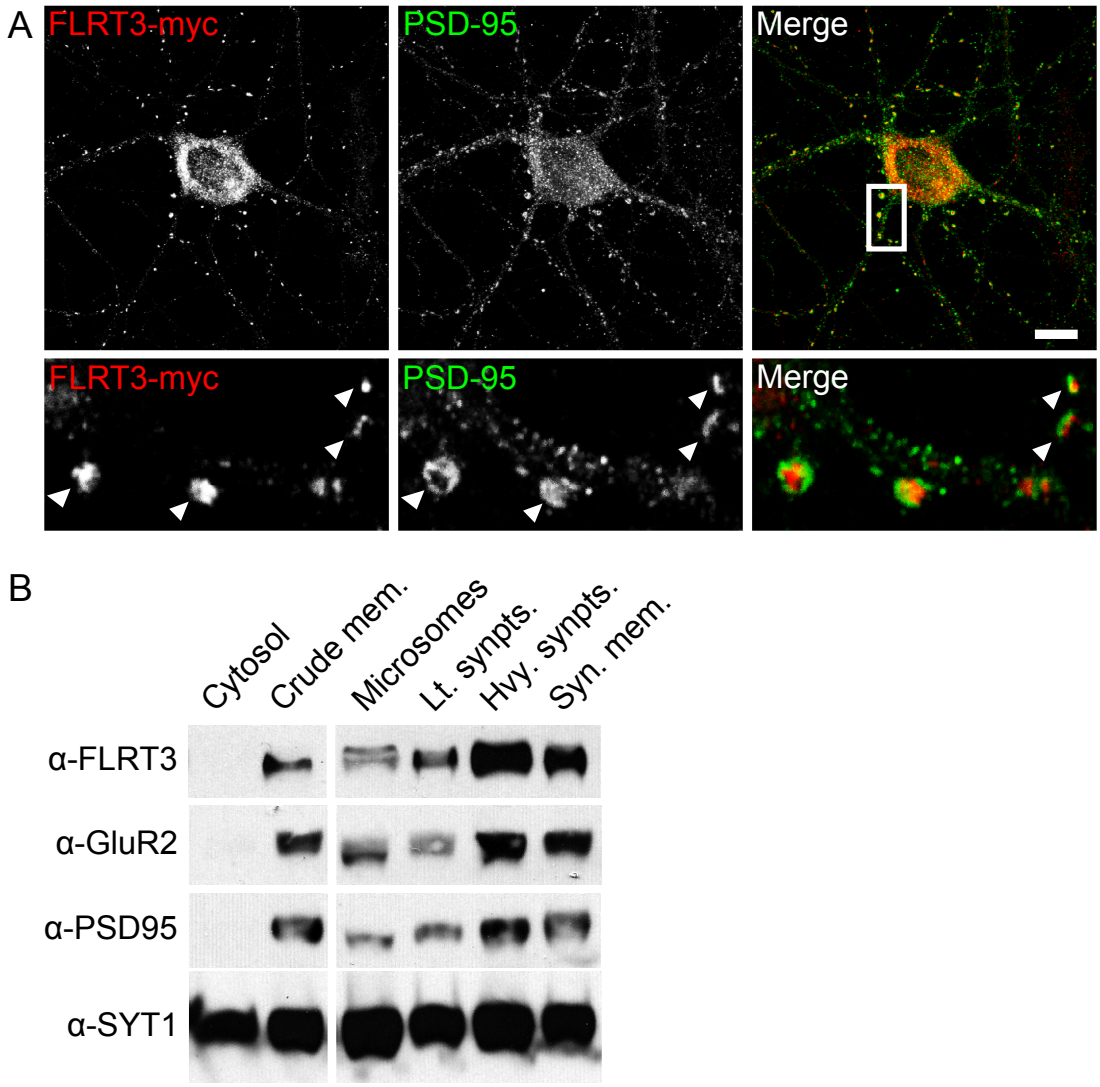

Figure 3.2: FLRT3 is trafficked to postsynaptic sites and is present in synaptic membranes.
(A) Dissociated hippocampal neurons expressing FLRT3-myc and immunostained for myc (red) and the glutamatergic postsynaptic scaffolding protein PSD95 (green). FLRT3-myc localizes to dendrites in the punctate fashion, and colocalizes and partially overlaps with PSD95 (arrowheads). Scale bar = 10 μm.
(B) Western blot for FLRT3 and known synaptic proteins in fractionated rat brain protein samples. Fractions, from left to right, are: cytosol, crude membrane, microsomes, light synaptosomes, heavy synaptosomes, and synaptic membranes. FLRT3 is enriched in more synaptic fractions similar to the pattern seen for the postsynaptic proteins GluR2 and PSD95, and dissimilar to the homogenous levels of the presynaptic protein Synaptotagmin1.

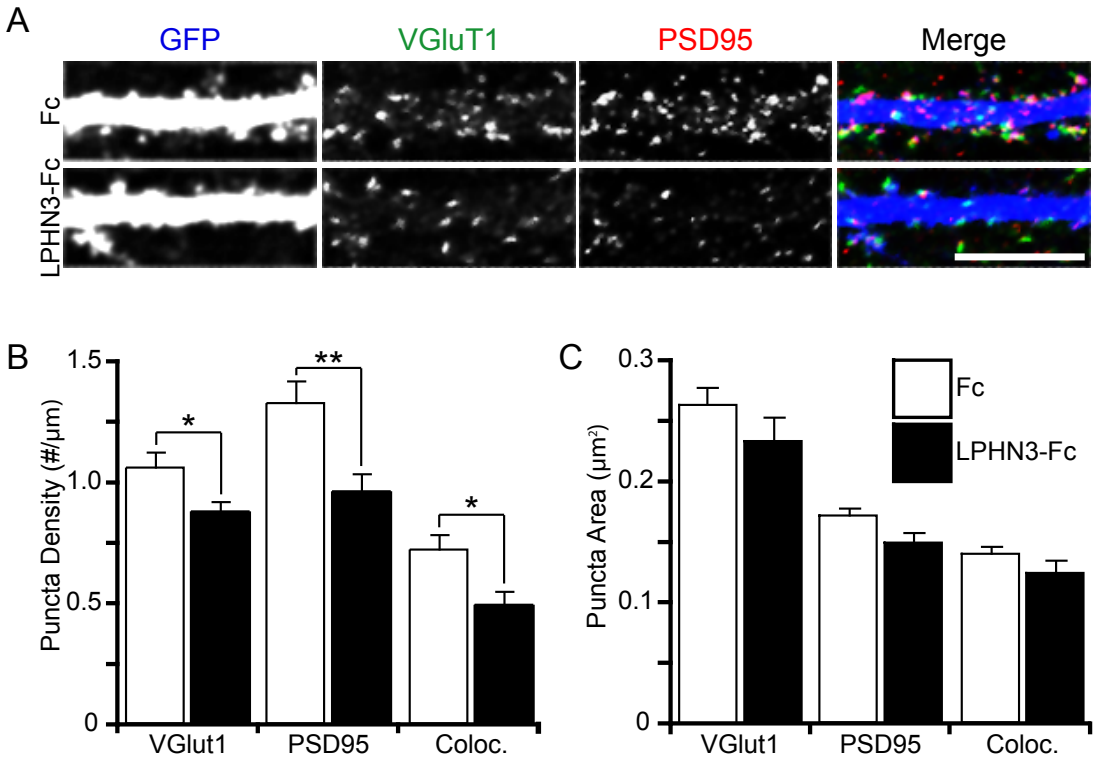

Figure 3.3: Disruption of endogenous LPHN3 interactions with excess soluble ecto-LPHN3-Fc reduces synapse density.
(A) Competition of endogenous LPHN interactions with ecto-LPHN3-Fc reduces synapse density. Hippocampal cultures were fixed and immunostained for VGluT1 (green), PSD95 (red), and GFP (blue) at 14DIV after 6 days of treatment with Fc (left) or LPHN3-Fc (right). Dendrites of granule cells identified by Prox1 immunofluorescence were imaged and puncta on GFP-filled dendrites were analyzed. Scale bar = 10 μm.
(B) Quantification of puncta density. VGluT1 (Fc 1.06 ± 0.07 puncta per μm dendrite, n=17 dendrites; LPHN3-Fc 0.88 ± 0.04, n=14; $p<0.05$), PSD95 (Fc 1.32 ± 0.09, n=17; LPHN3-Fc 0.96 ± 0.07, n=14; $p<0.01$), and colocalized VGlut1 + PSD95 (Fc 0.72 ± 0.06, n=17; LPHN3-Fc 0.49 ± 0.06, n=14; $p=0.01$) puncta were all significantly reduced in density following LPHN3-Fc treatment.
(C) Quantification of puncta area. VGluT1 (Fc 0.263 ± 0.014 μm^2, n=17 dendrites; LPHN3-Fc 0.233 ± 0.020, n=14; n.s.), PSD95 (Fc 0.171 ± 0.007, n=17; LPHN3-Fc 0.148 ± 0.009, n=14; n.s.), and colocalized VGlut1 + PSD95 (Fc 0.139 ± 0.006, n=17; LPHN3-Fc 0.123 ± 0.011, n=14; n.s.) puncta did not significantly differ in size between Fc- and LPHN3-Fc-treated neurons.

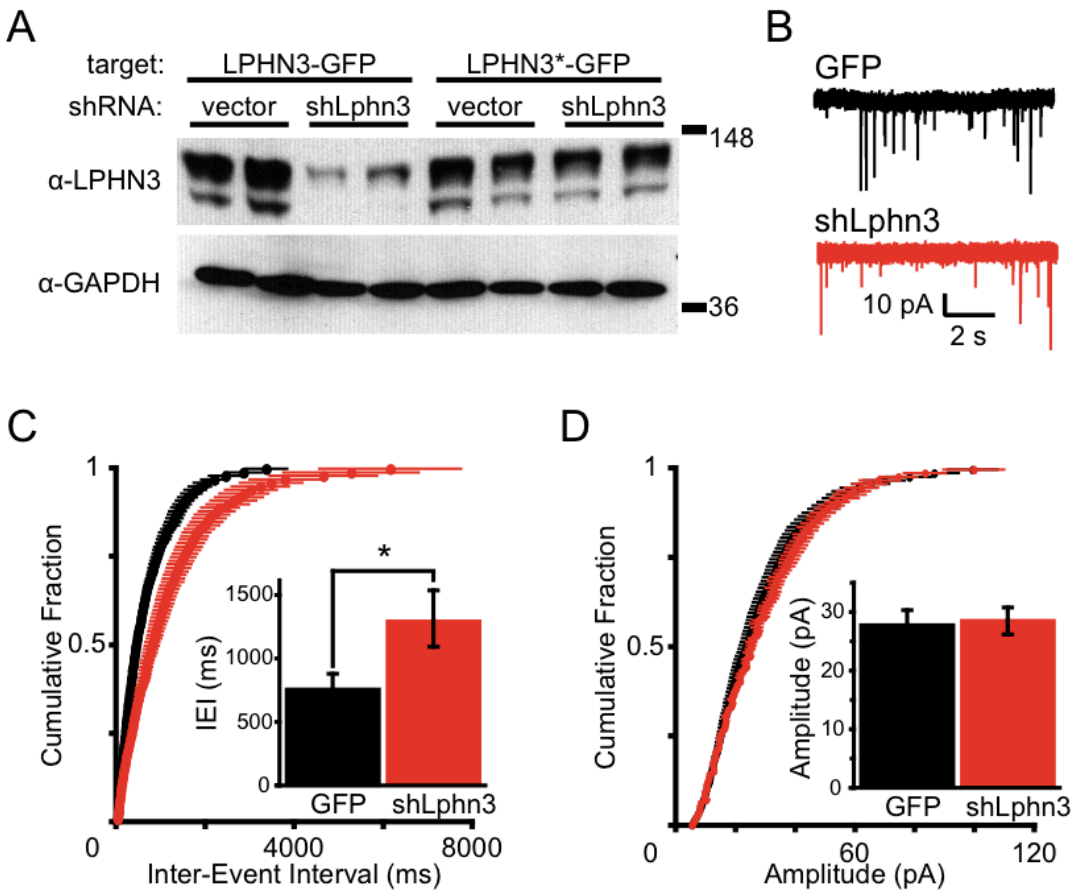

Figure 3.4: Lphn3 knockdown decreases mEPSC frequency without affecting amplitude.
(A) Characterization of LPHN3 shRNA knockdown in heterologous cells. HEK cells were transfected with LPHN3-GFP or an shRNA-resistant LPHN3 construct (LPHN3*-GFP) and Lphn3 shRNA or shRNA vector, lysate collected, and LPHN3-GFP detected by western blot using an anti-LPHN3 NTF antibody. shLphn3 strongly reduces LPHN3-GFP levels but does not affect LPHN3*-GFP levels.
(B) Example mEPSC recordings from 15DIV neurons in hippocampal cultures infected with a GFP control lentivirus (black) or shLphn3 lentivirus (red). >90% of neurons in the culture were infected as evidenced by ubiquitous GFP fluorescence.
(C) Summary of mEPSC frequency plotted as cumulative probability distributions of inter-event intervals (IEIs) for GFP (black) or shLphn3 (red) infected cultures. The rightward shift of the red curve represents a significant shift in the distribution of IEIs for shLphn3 cultures ($p<0.001$) towards longer IEIs. Inset: Quantification of mean mEPSC IEIs. Neurons in shLphn3 infected cultures have longer mean IEIs than neurons in control infected cultures (GFP 745 ± 125 ms, n=19; shLphn3 1254 ± 219 ms, n=17; $p < 0.05$).
(D) Summary of mEPSC amplitude plotted as cumulative probability distributions for GFP (black) or shLphn3 (red) infected cultures. The distribution of mEPSC amplitude did not differ by condition. Inset: Quantification of mean mEPSC amplitude. GFP and shLphn3 infected cultures did not differ in mEPSC amplitude (GFP 27.7 ± 2.6 pA, n=19; shLphn3 28.4 ± 2.3 pA, n=17; n.s.).

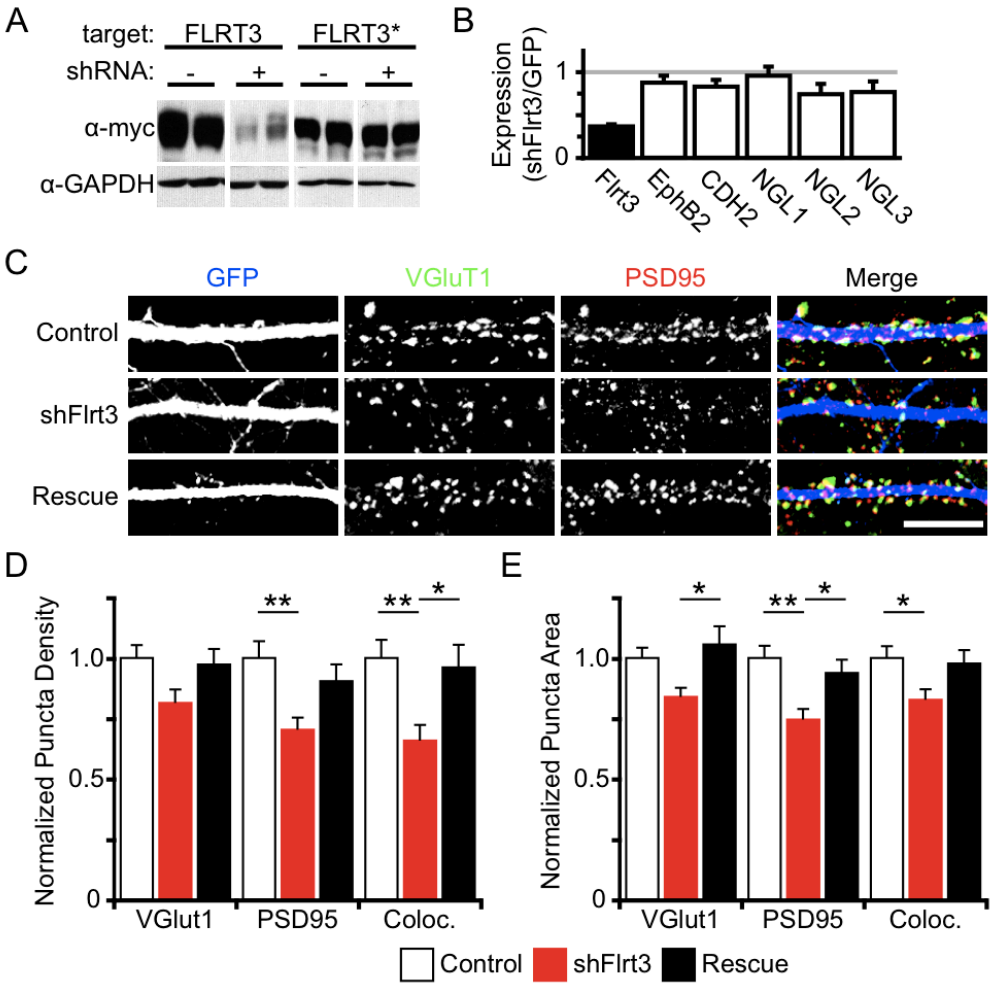

Figure 3.5: Flrt3 knockdown reduces synapse density.
(A) Characterization of FLRT3 shRNA efficacy and specificity in heterologous cells.
(B) Characterization shFlrt3 lentivirus efficacy and specificity against endogenous mRNAs by qPCR from cortical neuron mRNA samples.
(C) FLRT3 knockdown reduces glutamatergic synapse density. Hippocampal cultures were electroporated at 0DIV with plasmids to express GFP, GFP + shFlrt3, or GFP + shFlrt3 + FLRT3*-myc and fixed at 14DIV. Synapses were analyzed by immunostaining for VGluT1 (green), PSD95 (red), and GFP (blue). Scale bar = 10 μm.
(D) Quantification of synaptic puncta density, normalized to GFP control. VGluT1 (Control 1.00 ± 0.05, n=35 cells; shFlrt3 0.81 ± 0.06, n=33; Rescue 0.97 ± 0.06, n=34; n.s.), PSD95 (Control 1.00 ± 0.07; shFlrt3 0.70 ± 0.05; Rescue 0.90 ± 0.07; $p < 0.01$), and colocalized VGlut1 + PSD95 (Control 1.00 ± 0.08; shFlrt3 0.66 ± 0.06; Rescue 0.96 ± 0.09; $p < 0.01$) puncta were analyzed, and PSD95 and colocalized were found to differ by condition.
(E) Quantification of synaptic puncta area, normalized to GFP control. VGluT1 (Control 1.00 ± 0.04; shFlrt3 0.84 ± 0.04; Rescue 1.06 ± 0.08; $p < 0.05$), PSD95 (Control 1.00 ± 0.05; shFlrt3 0.75 ± 0.04; Rescue 0.94 ± 0.05; $p < 0.01$), and colocalized VGlut1 + PSD95 (Control 1.00 ± 0.05; shFlrt3 0.83 ± 0.04; Rescue 0.98 ± 0.06; $p < 0.05$) puncta were analyzed and all were found to differ by condition.

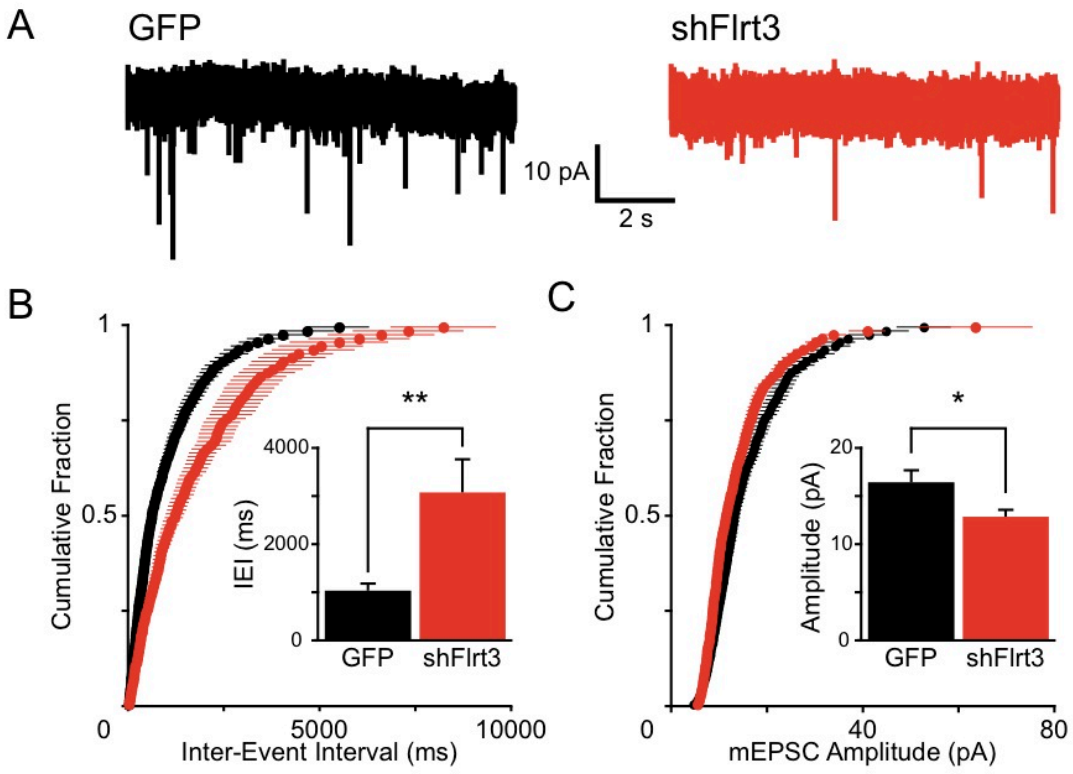

Figure 3.6: Flrt3 knockdown reduces mEPSC frequency and amplitude.
(A) Example mEPSC recordings from 14DIV neurons in hippocampal cultures electroporated with plasmids encoding GFP (black) or GFP plus Flrt3 shRNA. Cultures were sparsely electoporated such that great than 90% of neurons were unmanipulated.
(B) Summary of mEPSC frequency plotted as cumulative probability distributions of inter-event intervals (IEIs) for GFP (black) or shFlrt3 (red) electroporated cells. The rightward shift of the red curve represents a significant shift in the distribution of IEIs for shFlrt3 cells ($p<0.001$) towards longer IEIs. Inset: Quantification of mean mEPSC IEIs. shFlrt3 cells have longer mean IEIs than control GFP electroporated neurons (GFP 1028 ± 147 ms, n=15; shFlrt3 3069 ± 688 ms, n=15; $p < 0.01$).
(D) Summary of mEPSC amplitude plotted as cumulative probability distributions for GFP (black) or shFlrt3 (red) electroporated cells. The distribution of mEPSC amplitude did not significantly differ by condition. Inset: Quantification of mean mEPSC amplitude. shFlrt3 electroporated cells show a small but significant decrease in mean mEPSC amplitude (GFP 16.4 ± 1.2 pA, n=15; shFlrt3 12.8 ± 0.7 pA, n=15; $p < 0.05$).

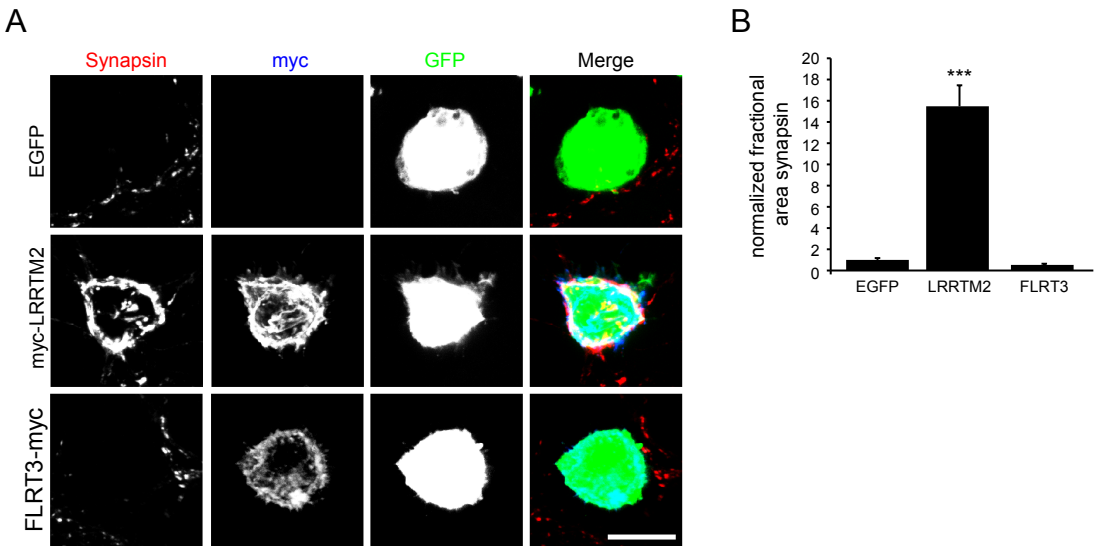

Figure 3.7: Flrt3 is not sufficient to induce presynaptic differentiation.
(A) HEK cells expressing GFP, myc-LRRTM2, or FLRT3-myc were cultured with dissociated hippocampal neurons, then fixed and immunostained. Synapsin immunoreactivity on transfected cells was analyzed as a measure of hemi-synapse induction. Scale bar = 10 μm. (B) Quantification of synapsin staining by transfection condition. By one-way ANOVA, normalized area synapsin staining differed significantly by transfection condition ($F(2,28) = 21.6$, $p < 0.0001$). Post-hoc Tukey tests indicate that LRRTM2 (15.5 ± 0.20, n=11 fields of view) robustly induces presynaptic differentiation over GFP (1.0 ± 0.17, n=10; $p < 0.001$), but that FLRT3 (0.53 ± 0.11, n=10) does not differ from GFP ($p > 0.05$).

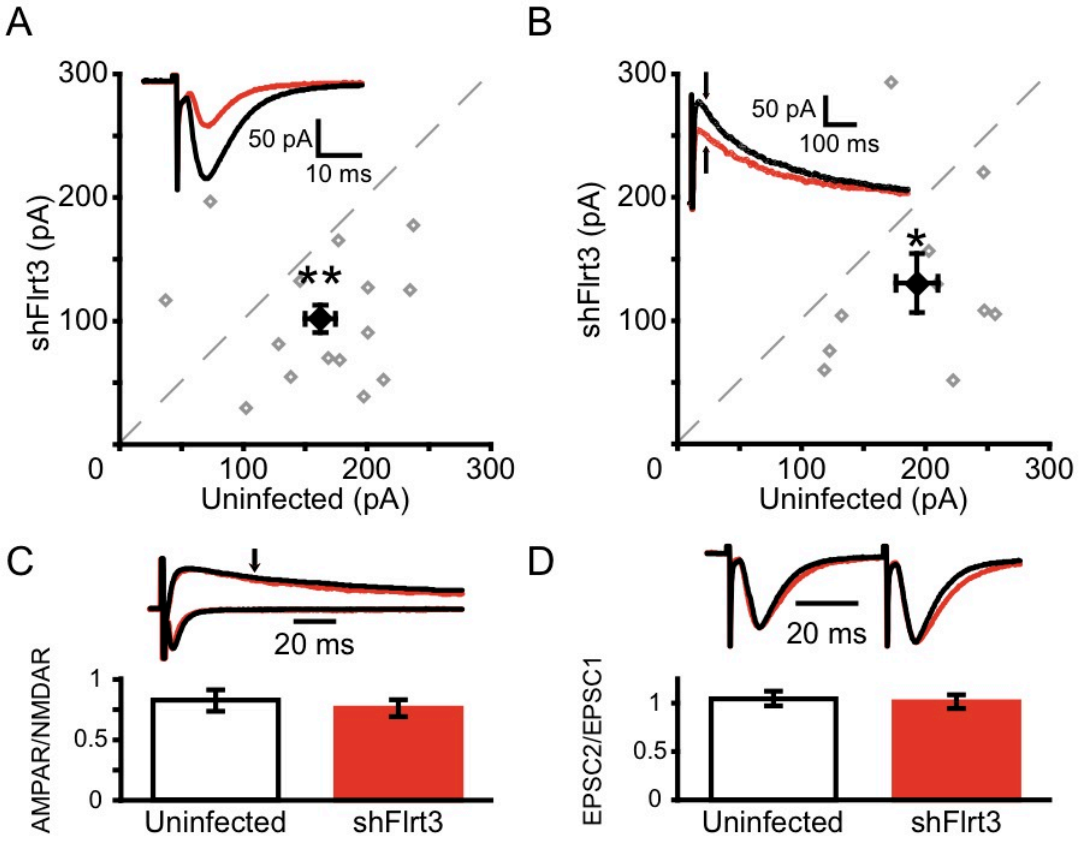

Figure 3.8: *In vivo* knockdown of Flrt3 reduces the strength of perforant path inputs to dentate gyrus granule cells.
P5 rat pups were stereotaxically injected with shFlrt3 lentivirus and acute slices cut at P13-16 for recording.
(A) Simultaneous whole-cell voltage clamp recordings of evoked perforant path EPSCs onto shFlrt3 infected and uninfected dentate gyrus granule cells. shFlrt3 significantly reduces the amplitude of AMPAR-EPSCs (shFlrt3 101.1 ± 13.4 pA, uninfected 162.8 ± 15.0 pA, n=15, $p<0.01$). AMPAR-mediated EPSCs were recorded at -60 mV and evoked with a stimulating electrode placed in the middle molecular layer (MML). Grey symbols represent means from individual experiments and the black symbol represents the group mean ± SEM. Inset: example average evoked AMPAR-EPSCs recorded simultaneously from shFlrt3 infected (red) and uninfected (black) GCs.
(B) shFlrt3 significantly reduces the amplitude of NMDAR-mediated EPSCs (shFlrt3 129.6 ± 23.9 pA, uninfected 193.7 ± 16.9 pA, n= 0, $p<0.05$). NMDAR-EPSCs were measured at +40 mV at a time 50 ms post-stimulus, a point at which the AMPAR-EPSCs as decayed to baseline. Inset: example average evoked NMDAR-EPSCs recorded simultaneously from shFlrt3 infected (red) and uninfected (black) GCs. The NMDAR-EPSC measurement was taken at the time indicated by the arrow.
(C) shFlrt3 does not affect the ratio of AMPAR-EPSCs to NMDAR-EPSCs at single inputs (shFlrt3 0.76 ± 0.07, uninfected 0.83 ± 0.09, n=10, n.s.).
(D) shFlrt3 does not affect the ratio of EPSC amplitudes evoked by pairs of stimuli delivered at 20 Hz (EPSC2/EPSC1) (shFlrt3 1.01 ± 0.07, uninfected 1.04 ± 0.08, n=13, n.s.).

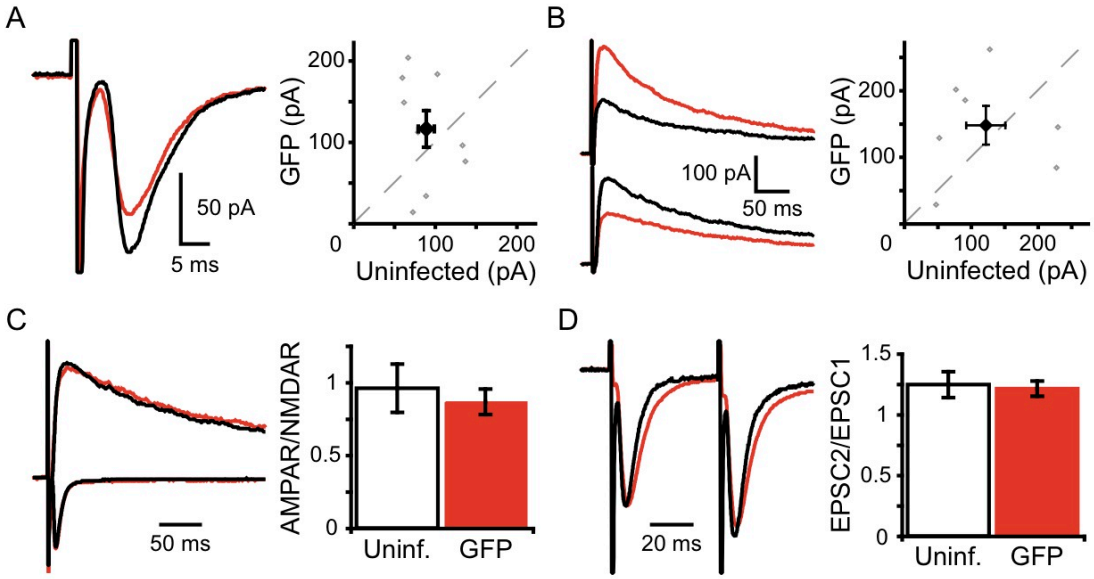

Figure 3.9: Infection with a control lentivirus does not affect perforant path inputs to dentate gyrus granule cells.
P5 rat pups were stereotaxically injected with GFP lentivirus and acute slices cut at P13-16 for recording.
(A) Simultaneous whole-cell voltage clamp recordings of evoked perforant path EPSCs onto GFP infected and uninfected dentate gyrus granule cells. Left: example average evoked AMPAR-EPSCs recorded simultaneously from GFP infected (green) and uninfected (black) GCs. Right: GFP infection does no affect the amplitude of AMPAR-EPSCs (GFP 116.2 ± 22.5 pA, uninfected 89.5 ± 9.8 pA, n=9, n.s.). AMPAR-mediated EPSCs were recorded at -60 mV and evoked with a stimulating electrode placed in the middle molecular layer (MML). Open symbols represent means from individual experiments and the filled symbol represents the group mean ± SEM.
(B) Left: example average evoked NMDAR-EPSCs recorded simultaneously from GFP infected (green) and uninfected (black) GCs. GFP does not affect the amplitude of NMDAR-mediated EPSCs (GFP 147.6 ± 29.2 pA, uninfected 122.3 ± 29.3 pA, n=7, n.s.). NMDAR-EPSCs were measured at +40 mV at a time 50 ms post-stimulus, a point at which the AMPAR-EPSCs as decayed to baseline.
(C) GFP does not affect the ratio of AMPAR-EPSCs to NMDAR-EPSCs at single inputs (GFP 0.87 ± 0.09, uninfected 0.96 ± 0.17, n=7, n.s.).
(D) GFP does not affect the ratio of EPSC amplitudes evoked by pairs of stimuli delivered at 20 Hz (EPSC2/EPSC1) (GFP 1.21 ± 0.06, uninfected 1.25 ± 0.11, n=6, n.s.).

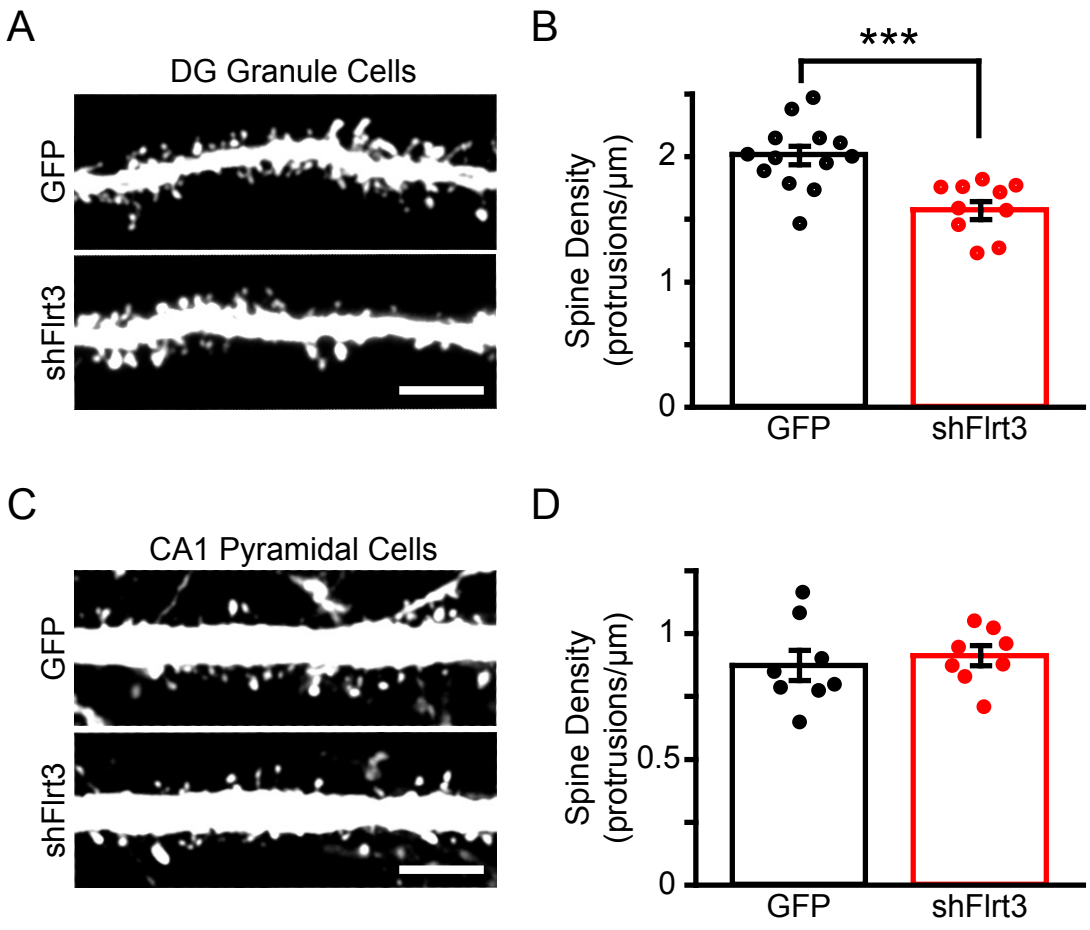

Figure 3.10: *In vivo* knockdown with shFlrt3 reduces the density of dendritic spines on DG granule cells but not CA1 pyramidal cells.
E15 mouse embryos were electroporated *in utero* with plasmids to express GFP or GFP and Flrt3 shRNA
(A) Dendrites of dentate granule cells in the middle molecular layer expressing GFP or GFP and Flrt3 shRNA were imaged in sections from P14 *in utero* electroporated mice. Scale bar = 5 μm.
(B) Quantification of dendritic spine density for control and shFlrt3 electroporated granule cells. Flrt3 shRNA significantly reduces the density of dendritic protrusions relative to controls (GFP 2.01 ± 0.07 protrusions/μm, n=13; shFlrt3 1.60 ± 0.07 protrusions/μm, n=10; $p<0.001$).
(C) Primary apical dendrites in the stratum radiatum of CA1 pyramidal cells, which do not express Flrt3, expressing GFP or GFP and Flrt3 shRNA were imaged in sections from P14 *in utero* electroporated mice. Scale bar = 5 μm.
(D) Quantification of dendritic spine density for control and shFlrt3 electroporated CA1 pyramidal cells. Flrt3 shRNA does not affect the density of dendritic protrusions relative to controls (GFP 0.87 ± 0.06 protrusions/μm, n=8; shFlrt3 0.91 ± 0.04 protrusions/μm, n=8; n.s.).

Chapter 4:

Discussion

The construction of proper synaptic circuits between neurons is a fundamental problem that the nervous system faces during development. The number of cell types and diversity of synapses makes the challenge of establishing proper synaptic connectivity a complicated one. One way this task is handled is by trans-synaptic interaction between pre- and postsynaptic membrane associated proteins to instruct synapse formation or maturation. A growing number of molecules are known to participate in complexes of this kind, typified by presynaptic neurexins and their postsynaptic ligands, the neuroligins and LRRTMs (Siddiqui and Craig, 2011). Several transmembrane proteins with synaptic functions belong to the class of neuronal LRR-containing proteins (Ko and Kim, 2007), of which the functions of many members are still unknown. We have identified a novel trans-synaptic interaction between presynaptic latrophilins and postsynaptic FLRTs, and demonstrated that they have a role in determining the number of glutamatergic synapses in neurons.

4.1: Latrophilins and FLRTs Constitute a Novel Trans-synaptic Receptor-Ligand Interaction

Latrophilins are presynaptic GPCRs initially identified as receptors for the spider venom α-latrotoxin, which induces massive synaptic vesicle exocytosis. These unusual proteins have a large extracellular N-terminal domain (NTF) with several conserved protein-protein interaction motifs and a

seven-transmembrane GPCR domain. These two domains are proteolytically cleaved, and as such are not covalently linked but are associated in the mature protein. We identified FLRTs as novel endogenous latrophilin ligands, with this interaction occurring between the latrophilin NTF and FLRT ectodomain (Figures 2.2, 2.4, and 2.5). All FLRT isoforms bind to both LPHN1 and LPHN3, indicating that binding is possible between all isoforms of both families (Figures 2.8-10). We found that the binding the NTF of LPHN3 with the ectodomain of FLRT3 occurs with high (14.7 nM K_D) affinity and that the interaction has a long lifetime (Figure 2.13). Whether the binding affinities of different pairs of isoforms differ has not been tested yet; it is possible that while all isoforms can interact, that the affinities of certain combinations favor those pairs over others. Additionally, while FLRTs are encoded in single exons and not subject to alternative splicing, latrophilins may be alternatively spliced to generate more than 3 isoforms, providing another level of regulation that could affect ligand binding.

While very little is known about their functions in the brain, both latrophilins and FLRTs have garnered renewed interest. LPHN1 has recently been shown to interact with another neuronal protein that we identified in our mass spectrometry screen (Figure 2.2), ODZ2/teneurin-2 (Silva et al., 2011). The ODZs/teneurins are a 4-gene family of transmembrane proteins that are involved in cell adhesion and axon guidance during development (Tucker and Chiquet-Ehrismann, 2006; Tucker et al., 2007). Teneurin-2 is present postsynaptically and can bind to the NTF of LPHN1 in *trans* (Silva et al.,

2011). Silva et al. show that teneurin-2 selectively precipitate LPHN1 from brain lysate, and not LPHN2 or 3. We, however, found all teneurin isoforms in comparable abundance in our LPHN3 affinity purification (Figure 2.2). This discrepancy in isoform selectivity may be due to technical differences between the experiments; we detected proteins in an unbiased manner by mass spectrometry, while Silva et al. used a western blot approach to detect bound proteins, which then is sensitive to differences in sensitivity and specificity of the antibodies employed. Direct binding experiments between the different LPHNs and teneurins will be required to clarify the relationship between the isoforms. Additionally, whether the presence of teneurins in our FLRT3 ectodomain affinity purification (Figure 2.4) represents direct binding to FLRT3 or indirect binding through latrophilins is not clear. FLRTs and teneurins may bind to the same or different regions of LPHNs. FLRTs and teneurins may compete for mutually exclusive binding to LPHNs like LRRTMs and neuroligins compete for neurexin binding (Ko et al., 2009; Siddiqui et al., 2010) or, alternatively, the large NTF of LPHN may permit a ternary complex involving both FLRTs and teneurins.

FLRTs also have an alternate receptor in the form of Unc5 (Karaulanov et al., 2009; Sollner and Wright, 2009). Were confirmed that FLRT3 can indeed bind to Unc5 (Figure 2.11). Unc5A-D are proteins with axon guidance functions in neural development, serving as receptors for secreted netrins (Moore et al., 2007). It was recently proposed that a soluble, proteolytically cleaved FLRT ectodomains may also act as a repulsive cue for axon guidance

and cell migration through Unc5 receptors, much like netrins (Yamagishi et al., 2011). We, however, have evidence that FLRT3 is a dendritic protein (Figure 3.2 and data not shown) and has the capability to interact with LPHN3 while embedded in the plasma membrane (Figure 2.14) with functions that are cell-autonomous and postsynaptic (Figures 3.5, 3.6, 3.8, and 3.10). Thus it may be that processing of FLRT3 is developmentally regulated such that a cleaved, soluble form acts in axon guidance during embryonic development and uncleaved, transmembrane FLRT3 acts at synapses in the postnatal brain. It seems to be generally true though, that synaptic transmembrane proteins often have multiple specific binding partners, suggesting that their function in a given context may depend in part on the protein with which they interact.

4.2: Latrophilins and FLRTs Contribute to the Control of Glutamatergic Synapse Number

After identifying latrophilins and FLRTs as a receptor-ligand pair, we hypothesized that that they would interact trans-synaptically and affect synaptic development. Latrophilins localize near presynaptic active zones (Silva et al., 2011) and we have shown that FLRT3 is enriched in synaptic membranes and trafficks to postsynaptic sites (Figure 3.2). In dissociated hippocampal cultures, loss of LPHN3, disruption of endogenous latrophilin complexes, and loss of postsynaptic FLRT3 all lead to a reduction in synapse number (Figures 3.3-6). This is mirrored *in vivo*, where a loss of postsynaptic

FLRT3 reduces the strength of afferent innervation and the density of dendritic spines (Figures 3.8, 3.10). The timing and sparsity of our postsynaptic FLRT3 manipulations preclude a non-cell autonomous axon guidance effect as has been proposed for Unc5. Instead, we hypothesize that a trans-synaptic interaction between presynaptic latrophilin and postsynaptic FLRT occurs at synapses at exerts a local influence promoting synapse development (Figure 4.1).

At synapses that exist without FLRT3, we have not observed perturbations in presynaptic function. While FLRT3 is not sufficient to induce presynaptic differentiation (Figure 3.7), we initially thought that FLRT3 might exert a modulatory effect on presynaptic function by signaling retrogradely through latrophilin to affect synaptic vesicle release and cycling, as suggested by the effect α-latrotoxin. Chronic treatment of neuronal cultures with recombinant soluble FLRT3 led to cell death, and acute treatment did not reliably affect mEPSC frequency. *In vivo*, synapses onto FLRT3-deficient cells did not display different short-term plasticity properties under the conditions we employed. We have not yet, however, directly investigated the role of LPHN3 in presynaptic function, and it remains possible that LPHN3 and latrophilin signaling could affect presynaptic properties such as release probability or synaptic vesicle pool sizes.

FLRT3 also does not seem to affect the composition of postsynaptic glutamate receptors, as neither the ratio of synaptic AMPAR current to NMDAR current nor mEPSC amplitude are affected by FLRT3 knockdown *in*

vivo (Figure 2.8). This is in contrast to the effects of the neurexin ligands LRRTM2 and neuroligin-1, which selectively affect synaptic AMPAR and NMDAR levels, respectively, *in vivo* (Appendix 1) (Chubykin et al., 2007; de Wit et al., 2009). Our results therefore suggest that while FLRT3 affects the number of synapses formed onto a postsynaptic neuron, those synapses that still do form in the absence of FLRT3 have grossly normal pre- and postsynaptic properties.

We showed than FLRT3 could *trans*-cellularly induce the accumulation of axonal LPHN3 to sites of contact (Figure 2.14). Both the LPHN3 NTF and GPCR domain localized to sites of FLRT3 contact, raising the intriguing possibility that FLRT3 binding may induce NTF-GPCR re-association in a manner similar to α-latrotoxin binding (Silva et al., 2009a; Volynski et al., 2004). Since α-latrotoxin induces both latrophilin reassembly and G-protein signaling, it has been conjectured that NTF-GPCR interactions may modulate latrophilin G-protein signaling (Capogna et al., 2003; Lelianova et al., 1997; Silva et al., 2009a; Volynski et al., 2004). In this model FLRT would bind trans-synaptically to the latrophilin NTF, binding would engender re-association of the latrophilin NTF and GPCR domains, and this subunit re-association of would modulate G-protein signaling at the synapse. Alternatively, it may be that FLRTs do not act like a typical ligand to induce signaling in their conjugate receptor, but rather serve to localize axonal latrophilins to sites of contact with postsynaptic FLRT-expressing cells where latrophilin signaling is constitutive or regulated by other mechanisms. Latrophilin G-protein signaling could then

exert diverse and unknown influences on axonal and presynaptic processes, including through canonical IP3 and protein kinase C (PKC) pathways, which could increase synapse stabilization or reduce synapse elimination. The large NTF of latrophilin may also interact with other presynaptic proteins in *cis* to facilitate their recruitment to or stabilization at the synapse.

Postsynaptically, FLRTs could affect postsynaptic formation or stabilization by extracellular *cis* interactions or intracellular signaling. The intracellular domain of FLRT3 has been shown to bind to and recruit the small GTPase Rnd1 (Chen et al., 2009; Karaulanov et al., 2009). Rnd1 is present in dendrites and postsynaptic sites and promotes dendritic spine development (Ishikawa et al., 2003); if FLRT3 recruits Rnd1 to developing postsynaptic sites, it may then facilitate the development of the synapse. A potential alternative or complementary postsynaptic signaling pathway may exist via extracellular *cis* interactions through the FN3 or LRR domains. Specifically, the FN3 domain of FLRTs domain has been shown to bind in *cis* to FGFRs (Bottcher et al., 2004; Haines et al., 2006; Wheldon et al., 2010). FGFs and FGFRs positively regulate synapse number, an effect generally attributed to a retrograde, target-derived FGF signal on axonal FGFRs (Li et al., 2002; Terauchi et al., 2010; Umemori et al., 2004). There is also evidence, however, that FGFRs are localized to dendrites of hippocampal neurons (Li et al., 2002), allowing for the possibility of *cis* or potentially *trans* interactions of FLRTs with FGFRs to positively regulate glutamatergic synapses.

We have shown that FLRT3 and LPHN3 contribute to the determination of glutamatergic synaptic density, but the cell biology underlying this function is not clear. Several signaling pathways have been identified in different contexts that could mediate their effects. FLRTs could act as agonists for latrophilins, binding to the NTF, prompting NTF-GPCR re-association, and engendering G-protein signaling. Trans-synaptic binding of FLRTs to latrophilins could also serve to stabilize these proteins at synapses, localizing their signaling to sites of contact. Further investigation will be required to elucidation how this interaction achieves its function.

4.3: Latrophilins May Interact with Different Postsynaptic Ligands at Different Synapses

While *Lphn1-3* are broadly expressed in the brain in overlapping neuronal populations, their ligands show striking cell-type expression patterns In the hippocampus *Flrt2* and *Flrt3* are expressed in non-overlapping populations, with *Flrt3* in the DG and CA3 regions and *Flrt2* in CA1, while the two genes are co-expressed in L2/3 neocortical neurons (Figure 3.1; Allen Mouse Brain Atlas; (Robinson et al., 2004; Tsuji et al., 2004). The teneurins are also expressed in discrete cell populations, with the high expression of *Odz1* in DG and *Odz3* in CA2 and proximal CA1 being particularly notable (Allen Mouse Brain Atlas)(Zhou et al., 2003). We have demonstrated that latrophilins can bind to all FLRT isoforms (Figure 2.9-10) and suggest that

LPHN3 can bind to all teneurin isoforms (Figure 2.2). This suggests that presynaptic latrophilins may interact with different postsynaptic receptors at different synapses depending on the identity of the postsynaptic neuron. It is not known whether the different FLRTs have redundant or separable functions and how cells that express multiple isoforms allocate them to synapses, but the differential expression suggests that these questions may have interesting answers.

4.4: Different Trans-synaptic Complexes May Serve Redundant or Discrete Functions in Guiding Synaptic Development

The number of identified synaptic organizing proteins has increased dramatically in the last 5 years, and more will undoubtedly follow. This raises the question of why there are so many proteins that are not absolutely necessary to make functional synapses but are instead able to directly or indirectly affect the recruitment or function of obligatory synaptic molecules. The variety of their expression patterns and trans-synaptic interactions suggests that different postsynaptic organizing molecules are present at different synapses, with some being more universal than others. For example, neuroligin-1 is expressed ubiquitously in cortex and hippocampus and allocated broadly across the dendritic arbors of pyramidal neurons, suggesting that it is present at the majority of glutamatergic synapses onto principal cells

in the cortex and hippocampus (Ichtchenko et al., 1995; Song et al., 1999). *Flrt* and *Lrrtm* genes, on the other hand, show partially overlapping but cell-type specific expression patterns, such that single cell populations express a subset of all *Flrt* and *Lrrtm* isoforms. NGL1 and NGL2 show a different kind of regulation; they are found in broad and highly overlapping neuronal populations, but the proteins localize to distinct classes of synapses in separate dendritic domains (Kim et al., 2006; Nishimura-Akiyoshi et al., 2007).

The presynaptic receptors for these postsynaptic organizers tend to conform to similar patterns, though perhaps are somewhat more broadly expressed. *Nrxns* are expressed by many neurons, but the different genes do show distinct expression patterns and alternative splicing may add an additional unexplored layer to the regulation of their expression (Ullrich et al., 1995). The Netrin-G genes, *Ntng1* and *Ntng2,* are expressed in select populations corresponding to particular afferent pathways, but, as GPI-anchored proteins that cannot signal intracellularly on their own, require an effector that could be more broadly expressed (Nakashiba et al., 2002; Niimi et al., 2007; Nishimura-Akiyoshi et al., 2007). *Lphns* seem to be almost universally expressed, but may be regulated by alternative splicing (Ichtchenko et al., 1999; Matsushita et al., 1999; Sugita et al., 1998). Together, the expression patterns of pre- and postsynaptic organizing molecules lend themselves to a model in which a specific population of synapses, as defined by the pre- and postsynaptic neurons, has a characteristic complement of organizers that encode its identity.

While the effects of many synaptic organizing complexes on synapses are not yet well demonstrated, a few examples may be drawn upon to illustrate the kinds of consequences for synapses and circuits that they may hold. NL1, presumably interacting trans-synaptically with NRXNs, increases the proportional contribution of NMDARs to postsynaptic glutamatergic synaptic currents (Chubykin et al., 2007), while LRRTM2 boosts the contribution of AMPARs (Appendix 1: (de Wit et al., 2009). We have shown here that FLRT3 affects the number of synapses formed onto postsynaptic neurons without markedly changing the way those synapses behave (Figures 3.5-6, 3.8, and 3.10), an instance of a synaptic organizer regulating rate of connectivity between neurons. Synaptic organizing complexes can also affect presynaptic properties; α-NRXNs are critical regulators of voltage sensitive calcium currents and transmitter release, and postsynaptic NL1 can affect presynaptic release probability retrogradely, presumably through interaction with NRXNs and calcium channels (Futai et al., 2007; Missler et al., 2003; Stan et al., 2010).

Axons from single presynaptic cells also form synapses with different molecular and physiological properties based on the identity of the postsynaptic neuron (Reyes et al., 1998; Scanziani et al., 1998; Shigemoto et al., 1996; Toth et al., 2000), a distinction that requires a postsynaptic retrograde cue to instruct target-cell specific presynaptic differentiation. Synaptic organizers like FLRTs, LRRTMs, and other members of the LRR-containing family that are expressed in specific neuronal subpopulations are

prime candidates for postsynaptic cues to instruct differential presynaptic specialization, though the specific molecules involved have not yet been found.

Mutations or copy number variations in synaptic organizing genes can be found in neurological and psychiatric disorders such as ADHD (Martinez et al., 2011), schizophrenia (Francks et al., 2007; Walsh et al., 2008), and autism (Sudhof, 2008), may then lead to dysfunctions in synaptic circuits. Synapse formation is a robust process and loss of many synaptic proteins can be tolerated without gross pathology, but alternations in synaptic organizing proteins may produce relatively subtle perturbations in synapse that underlie dysfunction in neural circuits and ensuing cognitive and behavioral pathology. Elucidating how the set of organizing molecules expressed by a cell regulate its synaptic connectivity and function may then contribute to a fundamental understanding of how synapses and circuits develop in health and disease.

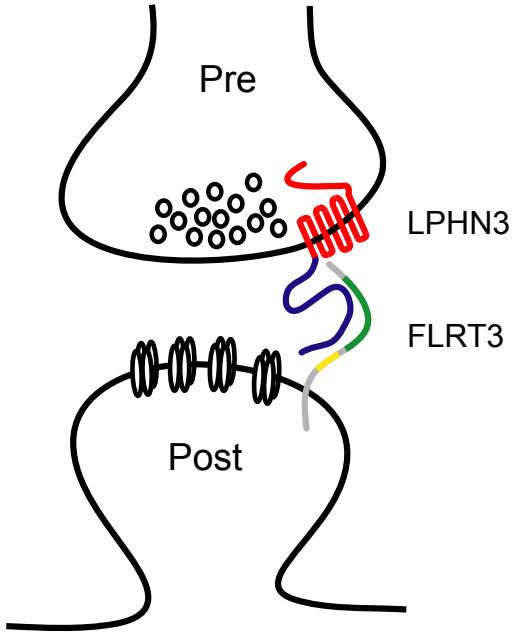

Figure 4.1: Schematic of proposed trans-synaptic LPHN-FLRT organizing complex at a glutamatergic synapse. LPHN3 is found at presynaptic terminals in close proximity to and functionally associated with the active zone. The large extracellular NTF of LPHN3 interacts in *trans* with the extracellular domain of postsynaptic FLRT3 to modulate trans-synaptic signaling and positively regulate synapse development.

Chapter 5:

Methods

Affinity Chromatography

Sixteen P25 rat brains were homogenized in homogenization buffer (50 mM HEPES pH 7.4, 100 mM NaCl, 2 mM $CaCl_2$, 2.5 mM $MgCl_2$ and protease inhibitors) using a Dounce homogenizer. The whole brain homogenate was extracted with 1% Triton X-100 for 2 hrs at 4°C and centrifuged at 100.000 x g for 1 hr at 4°C to pellet insoluble material. Fast-flow Protein A sepharose beads (GE Healthcare; 250 µl slurry) pre-bound in homogenization buffer to 100 µg human Fc, ecto-LPHN3-Fc, or ecto-FLRT3-Fc protein were added to the supernatant and rotated overnight at 4°C. Beads were packed into Poly-Prep chromatography columns (BioRad) and washed with 50 ml of high-salt wash buffer (50 mM HEPES pH 7.4, 300 mM NaCl, 0.1 mM $CaCl_2$, 5% glycerol and protease inhibitors), followed by a wash with 10 ml low-salt wash buffer (50 mM HEPES pH 7.4, 150 mM NaCl, 0.1 mM $CaCl_2$, 5% glycerol and protease inhibitors). Bound proteins were eluted from the beads by incubation with Pierce elution buffer and TCA precipitated overnight. The precipitate was resuspended in 8 M Urea with ProteasMAX (Promega) per the manufacturer's instruction. The samples were subsequently reduced by 20-minute incubation with 5 mM TCEP (*tris*(2 carboxyethyl)phosphine) at room temperature and alkylated in the dark by treatment with 10mM Iodoacetamide for 20 additional minutes. The proteins were digested overnight at 37 degrees with Sequencing Grade Modified Trypsin (Promega) and the reaction was stopped by acidification.

Multidimensional Protein Identification Technology (MudPIT) Mass Spectrometry

The protein digest was pressure-loaded onto a 250 μm i.d. capillary packed with 2.5 cm of 10 μm *Jupiter C18 resin* (Phenomenex) followed by an additional 2.5 cm of 5 μm Partisphere strong cation exchanger (Whatman). The column was washed with buffer containing 95% water, 5% acetonitrile, and 0.1% formic acid. After washing, a 100 μm i.d. capillary with a 5 μm pulled tip packed with 15 cm of 4 μm *Jupiter C18 resin* (Phenomenex, Torrance, CA, USA) was attached to the filter union and the entire split-column (desalting column–filter union–analytical column) was placed inline with an Agilent 1100 quaternary HPLC (Palo Alto, CA) and analyzed using a modified 5-step separation described previously (Washburn et al., 2001). The buffer solutions used were 5% acetonitrile/0.1% formic acid (buffer A), 80% acetonitrile/0.1% formic acid (buffer B), and 500 mM ammonium acetate/5% acetonitrile/0.1% formic acid (buffer C). Step 1 consisted of a 75 min gradient from 0-100% buffer B. Steps 2-5 had a similar profile except 3 min of 100% buffer A, 5 min of X% buffer C, a 10 min gradient from 0-15% buffer B, and a 102 min gradient from 15-45% buffer B. The 5 min buffer C percentages (X) were 10, 40, 60, and 100% respectively for the 5-step analysis. As peptides eluted from the microcapillary column, they were electrosprayed directly into an LTQ mass spectrometer (ThermoFinnigan) with the application of a distal 2.4 kV spray voltage. A cycle of one full-scan mass spectrum (400-1400 m/z) followed by 3 data-dependent MS/MS spectra at a 35% normalized collision energy was

repeated continuously throughout each step of the multidimensional separation. Application of mass spectrometer scan functions and HPLC solvent gradients was controlled by the Xcaliber datasystem.

MS/MS spectra were analyzed using the following software analysis protocol. Poor quality spectra were removed from the dataset using an automated spectral quality assessment algorithm (Bern et al., 2004). MS/MS spectra remaining after filtering were searched with the ProLuCID algorithm against the EBI-IPI_rat_3.30_06-28-2007 concatenated to a decoy database in which the sequence for each entry in the original database was reversed (Peng et al., 2003). All searches were parallelized and performed on a Beowulf computer cluster consisting of 100 1.2 GHz Athlon CPUs (Sadygov et al., 2004). Only peptides with at least 1 tryptic terminus were considered. Searches were performed with cystein carbamidomethylation as a fixed modification. ProLuCID (Eng et al., 1994) results were assembled and filtered using the DTASelect (version 2.0) program (Tabb et al., 2002). DTASelect 2.0 uses a linear discriminant analysis to dynamically set XCorr and DeltaCN thresholds for the entire dataset to achieve a user-specified false positive rate (5% in this analysis). The false positive rates are estimated by matching spectra to the decoy database. Confidence for modifications was estimated from overlapping modified peptides as described previously (MacCoss et al., 2002).

Fc Pull-down Assays

Whole brain extract was prepared as described above. Ten micrograms of human Fc or ecto-FLRT3-Fc was added to 1 ml of extract and rotated overnight at 4°C. Protein A/G agarose beads (Santa Cruz Biotechnology; 50 µl slurry) were added and rotated for 1 hr at 4°C. Beads were washed 3 x in homogenization buffer and 1 x in phosphate buffered saline (PBS), boiled in 50 µl 2x sample buffer and analyzed on Western blot.

For pull-down assays on HEK293T cells, cells were grown in 10 cm dishes in DMEM (Invitrogen) supplemented with 10% FBS (Invitrogen) and penicillin/streptomycin, and transfected with LPHN3-GFP, FLRT3-myc or myc-LRRTM2 expression constructs using Fugene6 (Roche, Basel, Switzerland). Twenty-four hours after transfection, the media was changed to OptiMEM (Invitrogen) for 2 hrs. Cells were lysed in 1 M RIPA buffer (20 mM Tris-HCl pH 7.5, 150 mM NaCl, 5 mM EDTA, 1% Triton-X 100 and protease inhibitors) for 1 hr at 4°C. Lysates were spun at 13.000 rpm for 30 min at 4°C. Three µg of human Fc, ecto-LPHN3-Fc or ecto-FLRT3-Fc was added to 1 ml of supernatant and rotated overnight at 4°C. Protein A/G agarose beads (50 µl slurry) were added and rotated for 1 hr at 4°C. Beads were washed 3 x in RIPA buffer and 1 x in PBS, boiled in 50 µl 2x sample buffer and analyzed by Western blotting.

Cell-based Binding Assays

HEK293T cells were transfected with myc-tagged FLRT or Unc5 constructs; GFP-tagged LPHN3 or CFP-tagged neurexin 1β expression constructs using Fugene6 (Roche). Twenty-four hours after transfection, the cells were incubated with either control Fc, LPHN- or FLRT-Fc proteins (10 μg/ml in DMEM supplemented with 20 mM HEPES pH 7.4) for 1 hour at RT. Following two brief washes with DMEM/20 mM HEPES pH 7.4, cells were fixed and immunostained using goat anti-GFP (Abcam), mouse anti-myc 9E10 (Santa Cruz Biotechnology) and fluorophore conjugated secondary antibodies (Jackson ImmunoResearch or Invitrogen).

Direct Binding Assays

For direct binding of FLRT3 to LPHN3, 5 μg recombinant 6 x His-tagged FLRT3 ectodomain (AAs 29-528) (R&D Systems) was incubated in 1 ml binding buffer (10 mM HEPES pH 7.4, 150 mM NaCl, 2 mM $CaCl_2$, 1 mM $MgCl_2$ and 0.1% Tween-20) with equimolar amounts of control Fc protein (Jackson ImmunoResearch), purified LPHN3-Fc or neurexin 1β1(-S4)-Fc, and rotated end-over-end for 1 hr at RT. Protein A/G agarose beads (100 μl slurry) were added and rotated end-over-end for 1 hr at 4°C. Beads were washed 1 x in binding buffer and 4 x in PBS and boiled in 100 μl 2x sample buffer. Samples were analyzed by Western blot.

Subcellular Fractionation

Performed as described (von Engelhardt et al., 2010). Briefly, rat brains were homogenized in 0.32 M sucrose buffer, pH 7.5, and centrifuged for 10 min at 1,000 g. The supernatant was collected and centrifuged again at 18,000 g for 30 min, giving cytoplasmic (supernatant) and crude membrane (pellet) fractions. The cytoplasmic fraction was then centrifuged at 120,000 g for 2 hrs to pellet the microsome fraction. The crude membrane fraction with loaded on a sucrose density gradient, 0.85/1.2 M, and centrifuged at 120,000 g for 2 hrs. The synaptic membrane fraction was collected from the interface of 0.85 M and 1.2 M sucrose layers.

Surface Plasmon Resonance Binding Assays

Binding experiments were done at 25°C in 10 mM HEPES buffer, pH 7.4, containing 150 mM NaCl, 2 mM $CaCl_2$ and 0.005% (v/v) surfactant P20, on a BIAcore 3000 instrument (GE Healthcare). Ecto-FLRT3 protein (100 Resonance units) with the Fc tag proteolytically removed was immobilized on the surface of a C1 chip using amine-coupling chemistry according to the manufacturer's instructions. LPHN3-Fc was injected for 360 s at concentrations ranging from 1000 nM to 0.45 nM in three fold dilutions. Spontaneous dissociation was monitored for seven minutes and complete regeneration of the surface was achieved with 30 s injections of 100 mM Na Acetate pH2.0. Signal obtained from an empty flow cell was systematically subtracted from those obtained with the FLRT3 cells to obtain the specific

binding response. The K_D and B_{Max} were obtained by nonlinear regression using the one-site binding model in GraphPad Prism (GraphPad Software).

Neuronal Cultures

Hippocampal neurons were cultured from P0 Long-Evans rats (Charles River) and plated on poly-D-lysine (Millipore), and laminin (Invitrogen) coated chamber slides (Nalge Nunc International). Neurons were maintained in Neurobasal-A medium (Invitrogen) supplemented with B27, glucose, glutamax, penicillin/streptomycin (Invitrogen) and 25 μM β-mercaptoethanol. Neurons were electroporated at time of plating using a Bio-Rad Gene Pulser Xcell (Bio-Rad Laboratories).

Cortical neurons were cultured from E18 Long-Evans rat embryos and plated on poly-D-lysine and laminin coated 12-well tissue culture plates. Neurons were maintained in Neurobasal medium supplemented with B27, glucose, glutamax, penicillin/streptomycin, and FBS. Cultures were infected at 4DIV with lentivirus such that the preponderance (≥90%) of neurons was infected.

Immunocytochemistry

Neurons were fixed in 4% paraformaldehyde, 4% sucrose in PBS, washed in PBS and blocked in 3% bovine serum albumin (BSA), 0.2% Triton X-100 in PBS. Primary antibodies were: goat anti-GFP (Abcam), mouse anti-PSD-95 (Thermo Scientific/Affinity BioReagents), mouse anti-Prox1, guinea

pig anti-VGlut1, rabbit anti-synapsin (all from Millipore, Billerica, MA, USA), mouse anti-myc 9E10 (Santa Cruz Biotechnology). Fluorophore-conjugated secondary antibodies were from Jackson ImmunoResearch or Invitrogen. Quantification of synapse density was performed as described (de Wit et al., 2009) in a blinded manner.

Antibodies used for Western blotting were: sheep anti-LPHN3 (R&D Systems), mouse anti-neurexin 1 (BD Transduction Laboratories), mouse anti-myc 9E10 (Santa Cruz Biotechnology), mouse anti-FLRT3 (R&D Systems), mouse anti-GluR2 (Millipore), mouse anti-PSD-95 (Thermo Scientific/Affinity BioReagents) and mouse anti-synaptotagmin 1 (clone 604.1, Synaptic Systems), rabbit anti-6x-his (Thermo Scientific). HRP-conjugated secondary antibodies were from Jackson ImmunoResearch.

Mixed-culture Assay

Mixed-culture assays were performed as described (Biederer and Scheiffele, 2007). Briefly, HEK293T cells were transfected with myc-tagged FLRT3 or LRRTM2 constructs and EGFP using Fugene6 (Roche), trypsinized and co-cultured with hippocampal neurons (6-7 DIV) for 24 hours and immunostained for synapsin, myc, and GFP. To test whether LPHN3 and FLRT3 can interact in *trans*, hippocampal neurons were electroporated with LPHN3-GFP and co-cultured with FLRT3-myc expressing 293T cells and immunostained with GFP, LPHN3 and myc antibodies.

In Situ Hybridization

Digoxigenin-labeled cRNA probes were generated using a protocol adapted from the protocol available at the Allen Brain Atlas. Template for the reverse transcription reaction was synthesized by PCR using the following primer sequences: forward; ACAAGCCTGAAACGCCTG, SP6-tagged reverse; GCGATTTAGGTGACACTATAGAGGGGCAGTTTGGGTCTC. In situ hybridizations were then performed as previously described (Pasterkamp et al., 1999) on 20 µm horizontal P7 and P14 C57Bl/6 mouse brain cryosections.

Lentivirus Production

Second generation VSV.G pseudotyped lentiviruses were produced either as follows or by the Salk Institute Viral Vector Core. For lentivirus production, 293T cells were transfected with control or shFlrt3 containing FUGW vector plasmids and helper plasmids MDL, RSV-REV and VSVG using Lipofectamine 2000 (Invitrogen). Supernatant was collected 48 hrs after transfection, spun at 2000 rpm to remove debris and filtered through a 0.22 µm filter (Millipore). Viral particles were polluted using two centrifugation steps at 19500 rpm for 2 hrs each. The final pellet was resuspended in 100 µL PBS and stored at -80°C in 10 µL aliquots.

Quantitative Real-Time PCR

At 12DIV, mRNA was isolated from cortical cultures using Trizol (Invitrogen) and cDNA was synthesized using iScript cDNA synthesis kit

(BioRad). Quantitative PCR was performed in an Applied Biosystems PRISM 7900HT Fast Real-Time PCR system with SYBR green PCR master mix. For analysis of cDNA levels, primers were designed around exon/intron boundaries using NCBI Primer Blast. PCR was run using the following cycling conditions: 95°C/10 min, 95°C/15 s and 57°C/1 min for 40 cycles. The relative abundance of each cDNA was determined by using a standard curve generated from 10-fold serial dilutions of cDNA from rat hippocampal neurons that were infected with control lentivirus. These values were normalized to GAPDH cDNA levels. Primers used were as follows; Flrt3 forward TTGTGTGCACTGG ATGCCGCG, reverse ACTGAGCACCTCCAGGAAGACGAG; GAPDH forward GGGGGCTCTCT GCTCCTCCC, reverse CAGGCGTCCGATACGGCCAA; CDH2 forward AGGATCGTGGGTGCA GGGCT, reverse CTGCTTGGCCTGGCGCTCTT; EphB2 forward AGAAGCTGGTACGAATGGGAGAAGT, reverse CCCTGCGAATAAGGCCACTTCGG; NGL1 forward CGTTGCCTATTTACTGCATAGAGAC, reverse GTTAAACCTAGGACCTATCATTATCTGC; NGL2 forward ACTGTGCCAAAAGGTTGAGAGGCA, reverse TGCACATGTACAAAGAAACAGCCCC; NGL3 forward GCTACCTGAACTTGCAAGAGAAC, reverse GAGTTCCAGTGTGTTGAGACTG.

In Utero Electroporation

Hippocampi of 15 day-old (E15) embryos of timed pregnant CD1 mice (Charles River) were unilaterally electroporated with control or shFlrt3 FUGW plasmid. Briefly, the dam was anesthetized with isoflurane and the uterus exposed. A solution of DNA and 0.01% Fast Green dye was injected into the embryonic lateral ventricle with a beveled glass micropipette. The embryo's head was positioned between the paddles of pair of platinum tweezer-type electrodes (BTX) with the cathode medial to the filled ventricle, and a 1 Hz train of 50 ms, 36 V pulses delivered by a CUY21 electroporator (BEX). After electroporation, the uterus was replaced, the incision sutured closed, and the dam allowed to give birth normally.

Dendritic Spine Imaging and Analysis

At P14, electroporated mice were transcardially perfused with 4% PFA in PBS, brains removed and post-fixed overnight in the same solution, and 150 μm coronal sections cut on a vibratome. Sections in which dentate gyrus granule neurons visibly expressed GFP were then immunostained with a goat polyclonal anti-GFP primary antibody (1:1000 dilution; Abcam) and an Alexa 488-conjugated donkey anti-goat secondary antibody (1:1000; Invitrogen). The dendrites of suprapyramidal blade dentate granule cells in the middle molecular layer or primary apical dendrites of CA1 pyramidal neurons were imaged on an Olympus FV300 confocal microscope. Dendritic protrusions

were counted in Z-stacks in ImageJ and the length of dendritic segments measured with the Simple Neurite Tracer plug-in.

Neonatal Stereotaxic Virus Injection

P5-6 Long Evans rat pups were anesthetized with isoflurane and mounted on a mouse stereotaxic apparatus. A longitudinal incision was cut in the scalp and the skull exposed. Small craniotomies (~2 mm diameter) were made at sites of injection with a drill with burr bit and the dura punctured with a hypodermic needle. 0.5-1 μL of lentivirus was delivered through a 33 G removable needle attached to Hamilton syringe mounted on the stereotax. Bilateral dentate gyrus injections were made using the following coordinates: 0.09 cm posterior, 0.20 cm lateral of bregma, 0.21-0.22 cm ventral to the dura.

Electrophysiology

Acute parasagittal slice from P13-16 virus-injected rats were cut on a vibratome. Rats were deeply anesthetized with isoflurane and rapidly decapitated. 300-400 μM thick slices were cut in a sucrose-substituted artificial cerebrospinal fluid (ACSF) that consisted of (in mM): 83 NaCl, 2.5 KCl, 1 NaH_2PO_4, 26.2 $NaHCO_3$, 22 glucose, 72 sucrose, 0.5 $CaCl_2$, 3.3 $MgSO_4$. Slices were allowed to recover at 32°C for 1 hr, and then maintained at room temperature in the same sucrose ACSF.

For evoked EPSC recordings, slices from P13-16 animals were transferred one at a time to the recording chamber and perfused at 1-2 mL/min

with an ACSF that consisted of (in mM): 119 NaCl, 2.5 KCl, 1 NaH_2PO_4, 26 $NaHCO_3$, 4 $CaCl_2$, 4 $MgSO_4$, 11 glucose, and 0.1 picrotoxin. Elevated divalent cation concentrations were used to reduce the likelihood of recruiting disynaptic excitation through the hilar associational circuit. Dentate granule cells (GCs) of the suprapyramidal blade were visualized by infrared differential interference and GFP epifluorescence microscopy (Olympus BX51WI). Whole-cell voltage clamp recordings were made simultaneously from infected and nearby (<50 μm) uninfected GCs under visual guidance with 3-6 MΩ pipettes pulled on a horizontal micropipette puller (Sutter P-97) and filled with an internal solution that contained (in mM): 130 Cs-methanesulfonate, 5 NaCl, 10 EGTA, 10 HEPES, 10 phosphocreatine, and 2 Mg-ATP, pH 7.3 with CsOH, 280-290 mOsm. Synaptic responses were evoked every 15 s with glass pipettes placed in the middle and/or outer third of the molecular layer. AMPAR-mediated EPSCs were recorded at a holding potential of -60 mV and amplitude taken as the average 1 ms around the peak; compound AMPAR- and NMDAR-mediated EPSCs were recorded at +40 mV and with the amplitude 50 ms after the stimulus taken as the amplitude of the NMDAR-mediated EPSC. AMPA/NMDA ratios were calculated from these values. Stimulus intensity was adjusted such that the AMPAR EPSC recorded in the uninfected cell was around 100 pA in peak amplitude and EPSC amplitudes were stable over time. Pairs of 20 Hz stimuli were delivered to measure paired-pulse ratios (PPRs), calculated as EPSC2/EPSC1. Averages of 10 or more consecutive sweeps were analyzed.

Whole-cell voltage clamp recordings were gained 10-20 x, low-pass filtered at 2 kHz, and digitized at 10 kHz (Molecular Devices DigiData 1440A and Multiclamp 700B). Series resistance (R_s) and input resistance (R_{in}) were monitored in all voltage clamp experiments by measuring the capacitative transient and steady state deflection in response to a -5 mV test pulse, respectively. Neither R_s (shFlrt3 21.6 ± 1.0 MΩ; uninfected 20.8 ± 0.8 MΩ) nor R_{in} (shFlrt3 1692 ± 334 MΩ; uninfected 1466 ± 226 MΩ) differed significantly by condition. Experiments in which R_s exceeded 10% of R_{in}, varied by more than 20% over the experiment, or differed by more than 20% between simultaneously recorded cells were excluded.

Plasmids

Full-length cDNAs encoding mouse Flrt1, Flrt2, Flrt3, and Lphn3 (accession numbers BC070403, BC096471, BC052043, and BC088989, respectively) and a partial Lphn1 cDNA (BC085138) were purchased from Thermo Scientific/Open Biosystems. Flrt cDNAs were c-terminally epitope tagged with myc (GAACAAAAACTTATTTCTGAAGAAGATCTG) by PCR and subcloned into the pEF-BOS expression vector. The Lphn3 cDNA with the stop codon removed was subcloned into the pEGFP-N1 expression vector (Clontech) in frame with eGFP to produce a c-terminally GFP-tagged Lphn3.

shRNA constructs were designed and ligated into pSuper.retro.neo+GFP (OligoEngine) according to the vendor's directions. shRNA targeting the following sequence of Flrt3 (conserved between mouse

and rat), respectively, was generated: CTCGGCTGTTAGCATAGAA. shRNA targeting the following sequences of Lphn3 (conserved between mouse and rat) was generated: CCAGATGCCTATAAGATTA. After testing in heterologous cells, the H1 promoter-driven shRNA cassettes were cut out of pSuper with HindIII and StuI and blunt ligated into the PacI site of the lentiviral plasmid pFUGW (Lois et al., 2002). Clones in which the H1-shRNA cassette was in the same orientation as the GFP cassette were selected.

Introducing silent mutations into the targeted sequences using PCR generated shRNA-resistant Flrt3 and Lphn3 cDNAs. Flrt3* contained the modified sequence aCGcAAtCAtCTcAGtACg, and Lphn3* contained the modified sequence CcgGAcGCtTAcAAaATcA.

Ectodomain-Fc fusion constructs were generated by PCR amplifying the predicted extracellular domains of Flrt3, Lphn3, and Lphn1, minus the signal peptide (predicated using SignalP 3.0), and subcloning the product into p3Cpro between and in frame with the Caspr2 signal peptide and human Fc. The myc-tagged human LRRTM2 expression construct was described previously (de Wit et al., 2009). CFP-tagged neurexin 1β expression constructs were a gift from Dr. A.M. Craig (University of British Columbia, Vancouver, Canada).

Protein Production

Ecto-Fc recombinant proteins were produced by transient transfection of HEK293T cells with FuGene 6 (Roche) or PEI (Polysciences). Six to eight

hours after transfection, media was changed to OptiMEM (Invitrogen) and harvested 4-5 days later. Conditioned media was centrifuged, sterile filtered and run over a fast-flow Protein A sepharose (GE Healthcare) column. After extensive washing with wash buffer (50 mM HEPES pH 7.4, 300 mM NaCl), the column was eluted with Pierce elution buffer. Eluted fractions containing proteins were pooled and dialyzed against PBS using a Slide-a-Lyzer (Pierce) and concentrated using an Amicon Ultra centrifugal unit (Millipore). The integrity and purity of the purified ecto-Fc proteins was confirmed with SDS-PAGE and Coomassie staining.

Appendix 1:

LRRTM2 Regulates Perforant Path Synapses onto Granule Cells *In Vivo*

The LRRTM subfamily of synaptic organizing proteins consists of 4 genes, *Lrrtm1-4*, encoding homologous single pass transmembrane proteins with 10 extracellular LRR motifs and an C-terminus PDZ-binding domain on most isoforms (Lauren et al., 2003). We and others initially found that LRRTMs have a role at synapses by observing their sufficiency to induce presynaptic differentiation when transfected into HEK cells in the heterologous cell-neuron co-culture paradigm (de Wit et al., 2009; Linhoff et al., 2009). We also found that LRRTMs are ligands for presynaptic neurexins, demonstrating that neurexins interact with multiple classes of postsynaptic proteins (de Wit et al., 2009; Ko et al., 2009). The level of LRRTM2 regulates the density of glutamatergic but not GABAergic synapses onto hippocampal neurons in culture, such that LRRTM2 knockdown by shRNA reduces synapse density and LRRTM2 overexpression increases synapse density (de Wit et al., 2009).

To examine the role of LRRTM2 in synaptic function *in vivo*, I generated and stereotaxically injected lentiviruses expressing shLRRTM2 and GFP or a control GFP lentivirus into the dentate gyrus of P5–P6 rat pups. Hippocampal slices were cut between P13 and P16, and simultaneous recordings made from uninfected and nearby infected dentate granule cells. A stimulating electrode placed in the outer half of the molecular layer was used to stimulate perforant path (PP) inputs onto granule cells (Figure A1.1A-B). No differences in cellular measures of integrity such as input resistance were found between treatment conditions (data not shown). Simultaneous recordings showed that knockdown of LRRTM2 in granule cells revealed a 58% reduction in the

strength of AMPAR-mediated EPSCs compared to neighboring uninfected cells (Figure A1.1C). In addition to AMPAR-mediated EPSCs, the strength of NMDAR-mediated PP inputs onto sh-LRRTM2-expressing granule cells was also significantly reduced by 54% (Figure A1.1D), indicating that endogenous LRRTM2 contributes significantly to excitatory synaptic transmission *in vivo*. LRRTM2 knockdown caused a reduction in the ratio of AMPAR-mediated synaptic current to that carried by NMDARs (Figure A1.1E). LRRTM2 knockdown did not affect paired-pulse ratios (PPRs), a measure of presynaptic release probability, of the same inputs (Figure A1.1F). Infection with a control virus did not affect synaptic function by any of these measures (Figure A1.2). Together, these results demonstrate that loss of LRRTM2 function *in vivo* leads to a reduction in the glutamatergic transmission.

Since other LRRTMs also induce synapses in the co-culture assay, we wanted to investigate their roles at synapses. In identified granule cells in dissociated hippocampal cultures, shRNA knockdown of LRRTM4 decreased and LRRTM4 overexpression increased glutamatergic synapse density, but neither manipulation affected GABAergic synapse density (Joris de Wit, unpublished observations). This corresponds to changes in the number of functional synapses, as I found that shRNA knockdown of LRRTM4 in putative granule cells reduces mEPSC frequency by 47% and has no effect on mEPSC amplitude (Figure A1.3). mIPSC frequency and amplitude were not affected, confirming the specific role of LRRTM4 at glutamatergic synapses (Figure A1.4).

LRRTMs, like FLRTs, are postsynaptic transmembrane proteins involved in synapse development. They interact with structurally unrelated presynaptic receptors, NRXNs and LPHNs, that both also serve as receptors for α-latrotoxin. Loss of either LRRTM2 or FLRT3 from dentate gyrus granule cells impairs the strength of perforant path afferent synaptic input (Figures 3.8 and A1.1), but due to different underlying cellular changes. LRRTM2 seems to act at least in part by controlling recruitment of AMPARs to synapses *in vivo* (Figure A1.1 and (de Wit et al., 2009), while FLRT3 acts primarily by regulating the number of synapses formed onto the postsynaptic neuron (Figures 3.8 and 3.10). *In vitro*, FLRT3, LRRTM2, and LRRTM4 all seem to promote synapse number (Figures 3.5, 3.6, and A.1.3, (de Wit et al., 2009), and Joris de Wit, unpublished observations). Since LRRTM2 is capable of inducing presynaptic differentiation through NRXNs (de Wit et al., 2009) and FLRT3 does not have this property (Figure 3.7), different mechanisms are likely to underlie their effects on synapse density. How FLRTs, LRRTMs, and other postsynaptic organizing molecules interact to coordinate synapse development remains to be seen.

Acknowledgements

The work presented in this Appendix has been published in the following paper:

de Wit, J., Sylwestrak, E., O'Sullivan, M.L., Otto, S., Tiglio, K., Savas, J.N., Yates, J.R. 3rd, Comoletti, D., Taylor, P., and Ghosh, A. (2009). LRRTM2 interacts with Neurexin1 and regulates excitatory synapse function. *Neuron 64(6)*, 799-806.

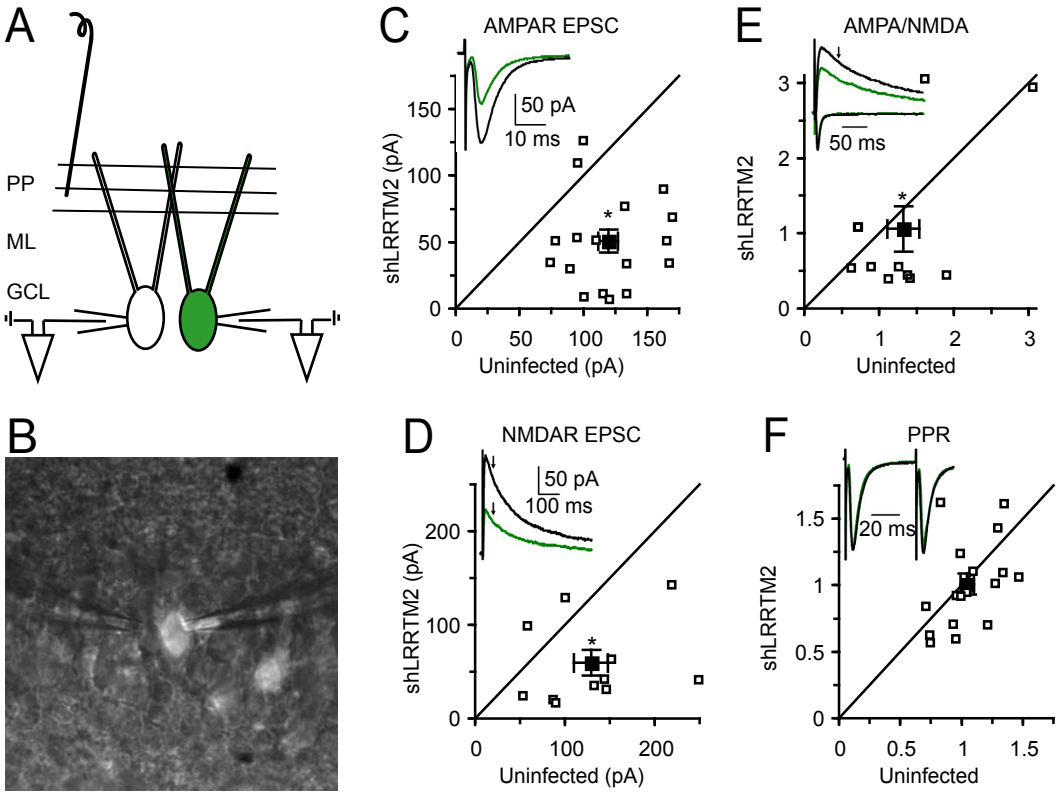

Figure A1.1: Postsynaptic LRRTM2 positively regulates synaptic transmission *in vivo*.
(A) Schematic of experimental configuration. Rats were stereotaxically injected with lentivirus at P5 and acute slices cut between P13 and P16. Whole cell recordings were made from nearby infected and uninfected granule cells in the granule cell layer (GCL) identified by DIC and GFP epifluorescence. Perforant path (PP) inputs were stimulated with an electrode in the outer half of the molecular layer (ML).
(B) Overlaid GFP epifluorescence and DIC images of a simultaneous recording.
(C) LRRTM2 shRNA causes a large reduction in AMPAR-mediated EPSCs (Uninfected 119.5 ± 7.7: shLRRTM2 50.7 ± 8.5: n = 17 pairs, $p < 0.0001$). For all scatter plots open symbols represent means from individual experiments and the filled symbol represents the group mean ± S.E.M. Inset: Example average evoked PP AMPAR EPSCs recorded simultaneously from shLRRTM2 infected (green) and uninfected (black) GCs at a holding potential of -60 mV.
(D) LRRTM2 shRNA causes a large reduction in NMPAR-mediated EPSCs (Uninfected 129.0 ± 18.7: shLRRTM2 59.7 ± 13.5: n = 11 pairs, $p = 0.005$). Inset: Example average evoked PP compound AMPAR- and NMDAR-mediated EPSCs record at a holding potential of +40 mV. Arrows indicate the time point 50 ms after the stimulus at which the NMDAR-mediated amplitude was measured.
(E) LRRTM2 shRNA causes a slight reduction in AMPA/NMDA (Uninfected 1.32 ± 0.21: shLRRTM2 1.06 ± 0.30: n = 11 pairs, $p = 0.04$). Inset: Example average overlaid AMPAR and NMDAR EPSCs with traces scaled to the peak of the AMPAR EPSC.
(F) LRRTM2 shRNA does not affect the paired pulse ratio (PPR) of PP inputs onto GCs (Uninfected 1.05 ± 0.06: shLRRTM2 1.01 ± 0.08: n = 17, $p = 0.54$). Inset: Example average PP EPSCs from a simultaneous recording. Stimuli were delivered at 20 Hz. Traces are scaled to the peak of the first EPSC.

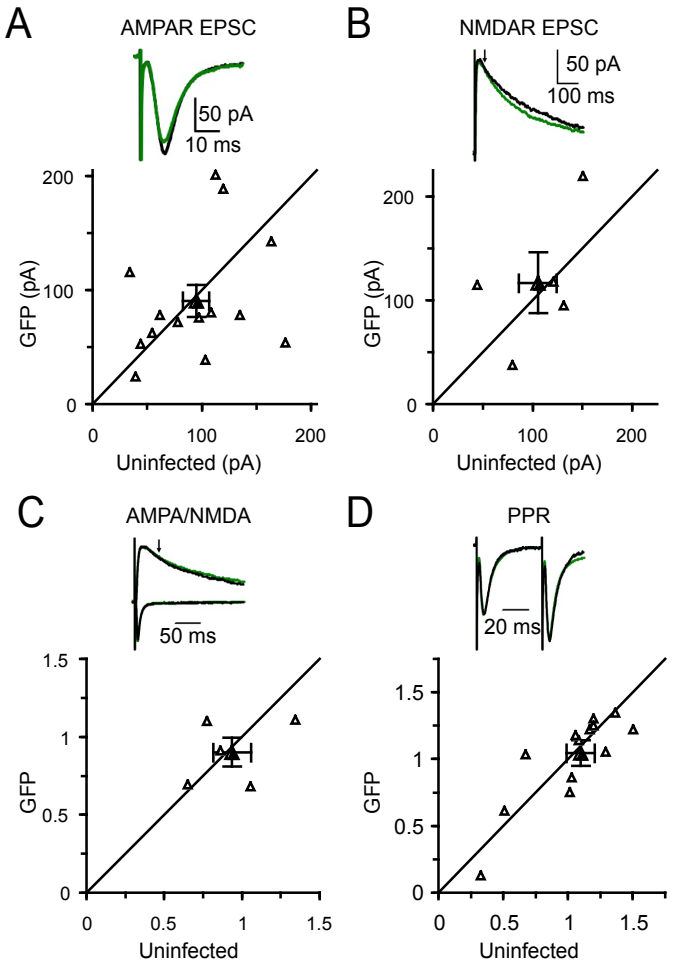

Figure A1.2: Lentivirus infection and GFP expression *in vivo* do not affect synaptic transmission.
(A) GFP infected and uninfected cells receive PP AMPAR EPSCs of similar strengths (Uninfected 94.7 ± 12.1: GFP 90.4 ± 14.2: n = 14 pairs, p = 0.73). For all scatter plots open symbols represent mean amplitudes from individual pairs and the filled symbol represents the group mean ± S.E.M. Inset: Example average evoked PP AMPAR EPSCs recorded simultaneously from GFP infected (green) and uninfected (black) GCs at a holding potential of -60 mV.
(B) GFP infected and uninfected cells receive PP NMDAR EPSCs of similar strengths (Uninfected 105.3 ± 19.1: GFP 116.7 ± 29.4: n = 5 pairs, p = 0.84). Inset: Example average evoked PP compound AMPAR- and NMDAR-mediated EPSCs record at a holding potential of +40 mV. Arrows indicate the time point 50 ms after the stimulus at which the NMDAR-mediated amplitude was measured.
(C) GFP infected and uninfected cells have similar AMPA/NMDA (Control 0.94 ± 0.12: GFP 0.90 ± 0.09: n = 5 pairs, p > 0.99). Inset: Example average overlaid AMPAR and NMDAR EPSCs with traces scaled to the peak of the AMPAR EPSC.
(D) GFP infection does not affect the paired pulse ratio (PPR) of PP inputs onto GCs (Control 1.05 ± 0.06: shLRRTM2 1.01 ± 0.08: n = 17, p = 0.54). Inset: Example average PP EPSCs from a simultaneous recording. Stimuli were delivered at 20 Hz. Traces are scaled to the peak of the first EPSC.

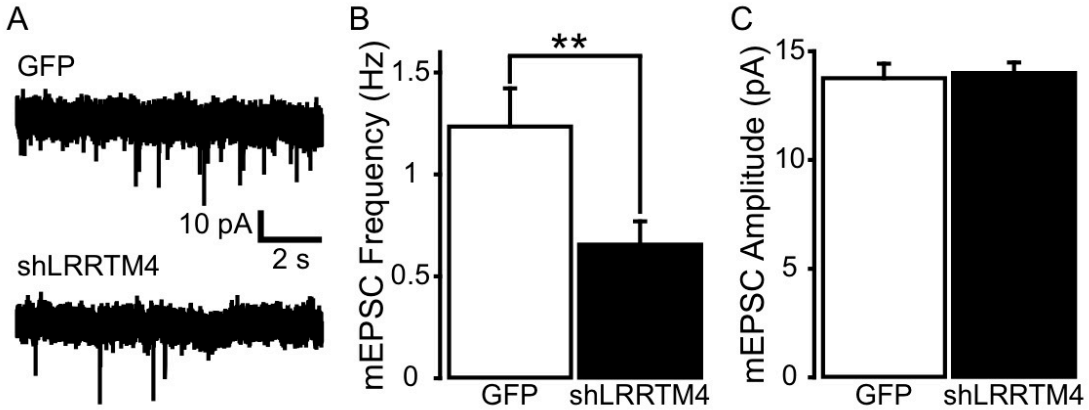

Figure A1.3: Knockdown of LRRTM4 in DG granule cells reduces mEPSC frequency without affecting amplitude in hippocampal cultures.
(A) Representative mEPSC recordings (V_{hold} -80 mV) from a GFP control transfected (top) and an shLRRTM4 transfected (bottom) neuron.
(B) Mean mEPSC frequency is reduced by LRRTM4 knockdown (GFP 1.23 ± 0.19 Hz; shLRRTM4 0.65 ± 0.11 Hz; p = 0.0082).
(C) Mean mEPSC amplitude is not affected by LRRTM4 knockdown (GFP 13.73 ± 0.66 pA; shLRRTM4 13.98 ± 0.48 Hz; p = 0.76).

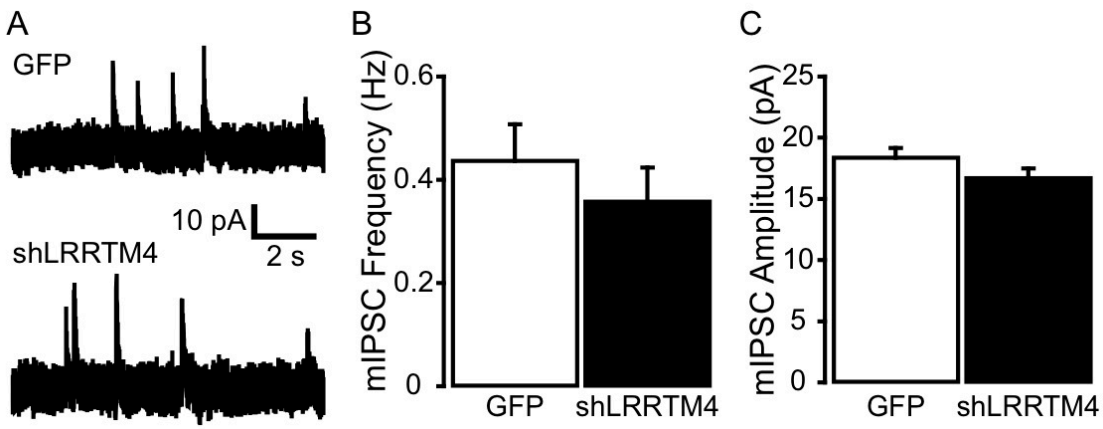

Figure A1.4: Knockdown of LRRTM4 in DG granule cells does not affect mIPSC frequency or amplitude.
(A) Representative mIPSC recordings (V_{hold} 0 mV) from a GFP control transfected (top) and an shLRRTM4 transfected (bottom) neuron.
(B) Mean mIPSC frequency is not affected by LRRTM4 knockdown (GFP 0.44 ± 0.07 Hz; shLRRTM4 0.36 ± 0.07 Hz; n.s.).
(C) Mean mIPSC amplitude is not affected by LRRTM4 knockdown (GFP 18.32 ± 0.78 pA; shLRRTM4 16.63 ± 0.81 Hz; n.s.).

REFERENCES

Allen Mouse Brain Atlas [Internet]. Seattle (WA): Allen Institute for Brain Science. ©2009. Available from: http://mouse.brain-map.org.

Aoki-Suzuki, M., Yamada, K., Meerabux, J., Iwayama-Shigeno, Y., Ohba, H., Iwamoto, K., Takao, H., Toyota, T., Suto, Y., Nakatani, N.*, et al.* (2005). A family-based association study and gene expression analyses of netrin-G1 and -G2 genes in schizophrenia. Biol Psychiatry *57*, 382-393.

Arcos-Burgos, M., Jain, M., Acosta, M.T., Shively, S., Stanescu, H., Wallis, D., Domene, S., Velez, J.I., Karkera, J.D., Balog, J.*, et al.* (2010). A common variant of the latrophilin 3 gene, LPHN3, confers susceptibility to ADHD and predicts effectiveness of stimulant medication. Mol Psychiatry *15*, 1053-1066.

Aspenstrom, P., Fransson, A., and Saras, J. (2004). Rho GTPases have diverse effects on the organization of the actin filament system. Biochem J *377*, 327-337.

Bella, J., Hindle, K.L., McEwan, P.A., and Lovell, S.C. (2008). The leucine-rich repeat structure. Cell Mol Life Sci *65*, 2307-2333.

Bern, M., Goldberg, D., McDonald, W.H., and Yates, J.R., 3rd (2004). Automatic quality assessment of peptide tandem mass spectra. Bioinformatics *20 Suppl 1*, i49-54.

Biederer, T., and Scheiffele, P. (2007). Mixed-culture assays for analyzing neuronal synapse formation. Nat Protoc *2*, 670-676.

Bittner, M.A. (2000). Alpha-latrotoxin and its receptors CIRL (latrophilin) and neurexin 1 alpha mediate effects on secretion through multiple mechanisms. Biochimie *82*, 447-452.

Bittner, M.A., Krasnoperov, V.G., Stuenkel, E.L., Petrenko, A.G., and Holz, R.W. (1998). A Ca2+-independent receptor for alpha-latrotoxin, CIRL, mediates effects on secretion via multiple mechanisms. J Neurosci *18*, 2914-2922.

Bolliger, M.F., Frei, K., Winterhalter, K.H., and Gloor, S.M. (2001). Identification of a novel neuroligin in humans which binds to PSD-95 and has a widespread expression. Biochem J *356*, 581-588.

Bolliger, M.F., Pei, J., Maxeiner, S., Boucard, A.A., Grishin, N.V., and Sudhof, T.C. (2008). Unusually rapid evolution of Neuroligin-4 in mice. Proc Natl Acad Sci U S A *105*, 6421-6426.

Bottcher, R.T., Pollet, N., Delius, H., and Niehrs, C. (2004). The transmembrane protein XFLRT3 forms a complex with FGF receptors and promotes FGF signalling. Nat Cell Biol *6*, 38-44.

Boucard, A.A., Chubykin, A.A., Comoletti, D., Taylor, P., and Sudhof, T.C. (2005). A splice code for trans-synaptic cell adhesion mediated by binding of neuroligin 1 to alpha- and beta-neurexins. Neuron *48*, 229-236.

Capogna, M., Volynski, K.E., Emptage, N.J., and Ushkaryov, Y.A. (2003). The alpha-latrotoxin mutant LTXN4C enhances spontaneous and evoked transmitter release in CA3 pyramidal neurons. J Neurosci *23*, 4044-4053.

Chen, X., Koh, E., Yoder, M., and Gumbiner, B.M. (2009). A protocadherin-cadherin-FLRT3 complex controls cell adhesion and morphogenesis. PLoS One *4*, e8411.

Chen, Y., Aulia, S., Li, L., and Tang, B.L. (2006). AMIGO and friends: an emerging family of brain-enriched, neuronal growth modulating, type I transmembrane proteins with leucine-rich repeats (LRR) and cell adhesion molecule motifs. Brain Res Rev *51*, 265-274.

Chih, B., Engelman, H., and Scheiffele, P. (2005). Control of excitatory and inhibitory synapse formation by neuroligins. Science *307*, 1324-1328.

Chubykin, A.A., Atasoy, D., Etherton, M.R., Brose, N., Kavalali, E.T., Gibson, J.R., and Sudhof, T.C. (2007). Activity-dependent validation of excitatory versus inhibitory synapses by neuroligin-1 versus neuroligin-2. Neuron *54*, 919-931.

Davletov, B.A., Meunier, F.A., Ashton, A.C., Matsushita, H., Hirst, W.D., Lelianova, V.G., Wilkin, G.P., Dolly, J.O., and Ushkaryov, Y.A. (1998). Vesicle exocytosis stimulated by alpha-latrotoxin is mediated by latrophilin and requires both external and stored Ca2+. EMBO J *17*, 3909-3920.

de Wit, J., Hong, W., Luo, L., and Ghosh, A. (2010). Role of Leucine-Rich Repeat Proteins in the Development and Function of Neural Circuits. Annu Rev Cell Dev Biol.

de Wit, J., Sylwestrak, E., O'Sullivan, M.L., Otto, S., Tiglio, K., Savas, J.N., Yates, J.R., 3rd, Comoletti, D., Taylor, P., and Ghosh, A. (2009). LRRTM2 interacts with Neurexin1 and regulates excitatory synapse formation. Neuron *64*, 799-806.

Deak, F., Liu, X., Khvotchev, M., Li, G., Kavalali, E.T., Sugita, S., and Sudhof, T.C. (2009). Alpha-latrotoxin stimulates a novel pathway of Ca2+-dependent

synaptic exocytosis independent of the classical synaptic fusion machinery. J Neurosci *29*, 8639-8648.

Dean, C., Scholl, F.G., Choih, J., DeMaria, S., Berger, J., Isacoff, E., and Scheiffele, P. (2003). Neurexin mediates the assembly of presynaptic terminals. Nat Neurosci *6*, 708-716.

Dolan, J., Walshe, K., Alsbury, S., Hokamp, K., O'Keeffe, S., Okafuji, T., Miller, S.F., Tear, G., and Mitchell, K.J. (2007). The extracellular leucine-rich repeat superfamily; a comparative survey and analysis of evolutionary relationships and expression patterns. BMC Genomics *8*, 320.

Domene, S., Stanescu, H., Wallis, D., Tinloy, B., Pineda, D.E., Kleta, R., Arcos-Burgos, M., Roessler, E., and Muenke, M. (2011). Screening of human LPHN3 for variants with a potential impact on ADHD susceptibility. Am J Med Genet B Neuropsychiatr Genet *156B*, 11-18.

Eastwood, S.L., and Harrison, P.J. (2008). Decreased mRNA expression of netrin-G1 and netrin-G2 in the temporal lobe in schizophrenia and bipolar disorder. Neuropsychopharmacology *33*, 933-945.

Egea, J., Erlacher, C., Montanez, E., Burtscher, I., Yamagishi, S., Hess, M., Hampel, F., Sanchez, R., Rodriguez-Manzaneque, M.T., Bosl, M.R.*, et al.* (2008). Genetic ablation of FLRT3 reveals a novel morphogenetic function for the anterior visceral endoderm in suppressing mesoderm differentiation. Genes Dev *22*, 3349-3362.

Eng, J., McCormack, A., and Yates, J. (1994). An Approach to Correlate Tandem Mass Spectral Data of Peptides with Amino Acid Sequences in a Protein Database. J Am Soc Mass Spectrom *5*, 976-989.

Feng, J., Schroer, R., Yan, J., Song, W., Yang, C., Bockholt, A., Cook, E.H., Jr., Skinner, C., Schwartz, C.E., and Sommer, S.S. (2006). High frequency of neurexin 1beta signal peptide structural variants in patients with autism. Neurosci Lett *409*, 10-13.

Francks, C., Maegawa, S., Lauren, J., Abrahams, B.S., Velayos-Baeza, A., Medland, S.E., Colella, S., Groszer, M., McAuley, E.Z., Caffrey, T.M.*, et al.* (2007). LRRTM1 on chromosome 2p12 is a maternally suppressed gene that is associated paternally with handedness and schizophrenia. Mol Psychiatry *12*, 1129-1139, 1057.

Fu, Z., Washbourne, P., Ortinski, P., and Vicini, S. (2003). Functional excitatory synapses in HEK293 cells expressing neuroligin and glutamate receptors. J Neurophysiol *90*, 3950-3957.

Fukasawa, M., Aoki, M., Yamada, K., Iwayama-Shigeno, Y., Takao, H., Meerabux, J., Toyota, T., Nishikawa, T., and Yoshikawa, T. (2004). Case-control association study of human netrin G1 gene in Japanese schizophrenia. J Med Dent Sci *51*, 121-128.

Futai, K., Kim, M.J., Hashikawa, T., Scheiffele, P., Sheng, M., and Hayashi, Y. (2007). Retrograde modulation of presynaptic release probability through signaling mediated by PSD-95-neuroligin. Nat Neurosci *10*, 186-195.

Gauthier, J., Siddiqui, T.J., Huashan, P., Yokomaku, D., Hamdan, F.F., Champagne, N., Lapointe, M., Spiegelman, D., Noreau, A., Lafreniere, R.G*., et al.* (2011). Truncating mutations in NRXN2 and NRXN1 in autism spectrum disorders and schizophrenia. Hum Genet.

Geppert, M., Khvotchev, M., Krasnoperov, V., Goda, Y., Missler, M., Hammer, R.E., Ichtchenko, K., Petrenko, A.G., and Sudhof, T.C. (1998). Neurexin I alpha is a major alpha-latrotoxin receptor that cooperates in alpha-latrotoxin action. J Biol Chem *273*, 1705-1710.

Haines, B.P., Wheldon, L.M., Summerbell, D., Heath, J.K., and Rigby, P.W. (2006). Regulated expression of FLRT genes implies a functional role in the regulation of FGF signalling during mouse development. Dev Biol *297*, 14-25.

Hata, Y., Butz, S., and Sudhof, T.C. (1996). CASK: a novel dlg/PSD95 homolog with an N-terminal calmodulin-dependent protein kinase domain identified by interaction with neurexins. J Neurosci *16*, 2488-2494.

Hata, Y., Davletov, B., Petrenko, A.G., Jahn, R., and Sudhof, T.C. (1993). Interaction of synaptotagmin with the cytoplasmic domains of neurexins. Neuron *10*, 307-315.

Ichtchenko, K., Bittner, M.A., Krasnoperov, V., Little, A.R., Chepurny, O., Holz, R.W., and Petrenko, A.G. (1999). A novel ubiquitously expressed alpha-latrotoxin receptor is a member of the CIRL family of G-protein-coupled receptors. J Biol Chem *274*, 5491-5498.

Ichtchenko, K., Hata, Y., Nguyen, T., Ullrich, B., Missler, M., Moomaw, C., and Sudhof, T.C. (1995). Neuroligin 1: a splice site-specific ligand for beta-neurexins. Cell *81*, 435-443.

Ichtchenko, K., Khvotchev, M., Kiyatkin, N., Simpson, L., Sugita, S., and Sudhof, T.C. (1998). alpha-latrotoxin action probed with recombinant toxin: receptors recruit alpha-latrotoxin but do not transduce an exocytotic signal. EMBO J *17*, 6188-6199.

Ichtchenko, K., Nguyen, T., and Sudhof, T.C. (1996). Structures, alternative splicing, and neurexin binding of multiple neuroligins. J Biol Chem *271*, 2676-2682.

Irie, M., Hata, Y., Takeuchi, M., Ichtchenko, K., Toyoda, A., Hirao, K., Takai, Y., Rosahl, T.W., and Sudhof, T.C. (1997). Binding of neuroligins to PSD-95. Science *277*, 1511-1515.

Ishikawa, Y., Katoh, H., and Negishi, M. (2003). A role of Rnd1 GTPase in dendritic spine formation in hippocampal neurons. J Neurosci *23*, 11065-11072.

Jain, M., Velez, J.I., Acosta, M.T., Palacio, L.G., Balog, J., Roessler, E., Pineda, D., Londono, A.C., Palacio, J.D., Arbelaez, A*., et al.* (2011). A cooperative interaction between LPHN3 and 11q doubles the risk for ADHD. Mol Psychiatry *[Epub ahead of print]*.

Jamain, S., Quach, H., Betancur, C., Rastam, M., Colineaux, C., Gillberg, I.C., Soderstrom, H., Giros, B., Leboyer, M., Gillberg, C*., et al.* (2003). Mutations of the X-linked genes encoding neuroligins NLGN3 and NLGN4 are associated with autism. Nat Genet *34*, 27-29.

Karaulanov, E., Bottcher, R.T., Stannek, P., Wu, W., Rau, M., Ogata, S., Cho, K.W., and Niehrs, C. (2009). Unc5B interacts with FLRT3 and Rnd1 to modulate cell adhesion in Xenopus embryos. PLoS One *4*, e5742.

Kim, H.G., Kishikawa, S., Higgins, A.W., Seong, I.S., Donovan, D.J., Shen, Y., Lally, E., Weiss, L.A., Najm, J., Kutsche, K*., et al.* (2008). Disruption of neurexin 1 associated with autism spectrum disorder. Am J Hum Genet *82*, 199-207.

Kim, S., Burette, A., Chung, H.S., Kwon, S.K., Woo, J., Lee, H.W., Kim, K., Kim, H., Weinberg, R.J., and Kim, E. (2006). NGL family PSD-95-interacting adhesion molecules regulate excitatory synapse formation. Nat Neurosci *9*, 1294-1301.

Kirov, G., Rujescu, D., Ingason, A., Collier, D.A., O'Donovan, M.C., and Owen, M.J. (2009). Neurexin 1 (NRXN1) deletions in schizophrenia. Schizophr Bull *35*, 851-854.

Ko, J., Fuccillo, M.V., Malenka, R.C., and Sudhof, T.C. (2009). LRRTM2 functions as a neurexin ligand in promoting excitatory synapse formation. Neuron *64*, 791-798.

Ko, J., and Kim, E. (2007). Leucine-rich repeat proteins of synapses. J Neurosci Res *85*, 2824-2832.

Ko, J., Kim, S., Chung, H.S., Kim, K., Han, K., Kim, H., Jun, H., Kaang, B.K., and Kim, E. (2006). SALM synaptic cell adhesion-like molecules regulate the differentiation of excitatory synapses. Neuron *50*, 233-245.

Kobe, B., and Deisenhofer, J. (1994). The leucine-rich repeat: a versatile binding motif. Trends Biochem Sci *19*, 415-421.

Kobe, B., and Kajava, A.V. (2001). The leucine-rich repeat as a protein recognition motif. Curr Opin Struct Biol *11*, 725-732.

Krasnoperov, V., Deyev, I.E., Serova, O.V., Xu, C., Lu, Y., Buryanovsky, L., Gabibov, A.G., Neubert, T.A., and Petrenko, A.G. (2009). Dissociation of the subunits of the calcium-independent receptor of alpha-latrotoxin as a result of two-step proteolysis. Biochemistry *48*, 3230-3238.

Krasnoperov, V., Lu, Y., Buryanovsky, L., Neubert, T.A., Ichtchenko, K., and Petrenko, A.G. (2002). Post-translational proteolytic processing of the calcium-independent receptor of alpha-latrotoxin (CIRL), a natural chimera of the cell adhesion protein and the G protein-coupled receptor. Role of the G protein-coupled receptor proteolysis site (GPS) motif. J Biol Chem *277*, 46518-46526.

Krasnoperov, V.G., Bittner, M.A., Beavis, R., Kuang, Y., Salnikow, K.V., Chepurny, O.G., Little, A.R., Plotnikov, A.N., Wu, D., Holz, R.W.*, et al.* (1997). alpha-Latrotoxin stimulates exocytosis by the interaction with a neuronal G-protein-coupled receptor. Neuron *18*, 925-937.

Kwon, S.K., Woo, J., Kim, S.Y., Kim, H., and Kim, E. (2010). Trans-synaptic adhesions between netrin-G ligand-3 (NGL-3) and receptor tyrosine phosphatases LAR, protein-tyrosine phosphatase delta (PTPdelta), and PTPsigma via specific domains regulate excitatory synapse formation. J Biol Chem *285*, 13966-13978.

Lacy, S.E., Bonnemann, C.G., Buzney, E.A., and Kunkel, L.M. (1999). Identification of FLRT1, FLRT2, and FLRT3: a novel family of transmembrane leucine-rich repeat proteins. Genomics *62*, 417-426.

Laumonnier, F., Bonnet-Brilhault, F., Gomot, M., Blanc, R., David, A., Moizard, M.P., Raynaud, M., Ronce, N., Lemonnier, E., Calvas, P.*, et al.* (2004). X-linked mental retardation and autism are associated with a mutation in the NLGN4 gene, a member of the neuroligin family. Am J Hum Genet *74*, 552-557.

Lauren, J., Airaksinen, M.S., Saarma, M., and Timmusk, T. (2003). A novel gene family encoding leucine-rich repeat transmembrane proteins differentially expressed in the nervous system. Genomics *81*, 411-421.

Lelianova, V.G., Davletov, B.A., Sterling, A., Rahman, M.A., Grishin, E.V., Totty, N.F., and Ushkaryov, Y.A. (1997). Alpha-latrotoxin receptor, latrophilin, is a novel member of the secretin family of G protein-coupled receptors. J Biol Chem *272*, 21504-21508.

Li, A.J., Suzuki, S., Suzuki, M., Mizukoshi, E., and Imamura, T. (2002). Fibroblast growth factor-2 increases functional excitatory synapses on hippocampal neurons. Eur J Neurosci *16*, 1313-1324.

Lin, J.C., Ho, W.H., Gurney, A., and Rosenthal, A. (2003). The netrin-G1 ligand NGL-1 promotes the outgrowth of thalamocortical axons. Nat Neurosci *6*, 1270-1276.

Linhoff, M.W., Lauren, J., Cassidy, R.M., Dobie, F.A., Takahashi, H., Nygaard, H.B., Airaksinen, M.S., Strittmatter, S.M., and Craig, A.M. (2009). An unbiased expression screen for synaptogenic proteins identifies the LRRTM protein family as synaptic organizers. Neuron *61*, 734-749.

Lois, C., Hong, E.J., Pease, S., Brown, E.J., and Baltimore, D. (2002). Germline transmission and tissue-specific expression of transgenes delivered by lentiviral vectors. Science *295*, 868-872.

Ludwig, K.U., Mattheisen, M., Muhleisen, T.W., Roeske, D., Schmal, C., Breuer, R., Schulte-Korne, G., Muller-Myhsok, B., Nothen, M.M., Hoffmann, P.*, et al.* (2009). Supporting evidence for LRRTM1 imprinting effects in schizophrenia. Mol Psychiatry *14*, 743-745.

MacCoss, M.J., Wu, C.C., and Yates, J.R., 3rd (2002). Probability-based validation of protein identifications using a modified SEQUEST algorithm. Anal Chem *74*, 5593-5599.

Mah, W., Ko, J., Nam, J., Han, K., Chung, W.S., and Kim, E. (2010). Selected SALM (synaptic adhesion-like molecule) family proteins regulate synapse formation. J Neurosci *30*, 5559-5568.

Maretto, S., Muller, P.S., Aricescu, A.R., Cho, K.W., Bikoff, E.K., and Robertson, E.J. (2008). Ventral closure, headfold fusion and definitive endoderm migration defects in mouse embryos lacking the fibronectin leucine-rich transmembrane protein FLRT3. Dev Biol *318*, 184-193.

Martinez, A.F., Muenke, M., and Arcos-Burgos, M. (2011). From the black widow spider to human behavior: Latrophilins, a relatively unknown class of G protein-coupled receptors, are implicated in psychiatric disorders. Am J Med Genet B Neuropsychiatr Genet *156B*, 1-10.

Matsushita, H., Lelianova, V.G., and Ushkaryov, Y.A. (1999). The latrophilin family: multiply spliced G protein-coupled receptors with differential tissue distribution. FEBS Lett *443*, 348-352.

McMahon, S.A., and Diaz, E. (2011). Mechanisms of excitatory synapse maturation by trans-synaptic organizing complexes. Curr Opin Neurobiol.

Missler, M., Zhang, W., Rohlmann, A., Kattenstroth, G., Hammer, R.E., Gottmann, K., and Sudhof, T.C. (2003). Alpha-neurexins couple Ca2+ channels to synaptic vesicle exocytosis. Nature *423*, 939-948.

Moore, S.W., Tessier-Lavigne, M., and Kennedy, T.E. (2007). Netrins and their receptors. Adv Exp Med Biol *621*, 17-31.

Muller, P.S., Schulz, R., Maretto, S., Costello, I., Srinivas, S., Bikoff, E., and Robertson, E. (2011). The fibronectin leucine-rich repeat transmembrane protein Flrt2 is required in the epicardium to promote heart morphogenesis. Development *138*, 1297-1308.

Nakashiba, T., Nishimura, S., Ikeda, T., and Itohara, S. (2002). Complementary expression and neurite outgrowth activity of netrin-G subfamily members. Mech Dev *111*, 47-60.

Nam, J., Mah, W., and Kim, E. (2011). The SALM/Lrfn family of leucine-rich repeat-containing cell adhesion molecules. Semin Cell Dev Biol.

Niimi, K., Nishimura-Akiyoshi, S., Nakashiba, T., and Itohara, S. (2007). Monoclonal antibodies discriminating netrin-G1 and netrin-G2 neuronal pathways. J Neuroimmunol *192*, 99-104.

Nishimura-Akiyoshi, S., Niimi, K., Nakashiba, T., and Itohara, S. (2007). Axonal netrin-Gs transneuronally determine lamina-specific subdendritic segments. Proc Natl Acad Sci U S A *104*, 14801-14806.

Ohtsuki, T., Horiuchi, Y., Koga, M., Ishiguro, H., Inada, T., Iwata, N., Ozaki, N., Ujike, H., Watanabe, Y., Someya, T.*, et al.* (2008). Association of polymorphisms in the haplotype block spanning the alternatively spliced exons of the NTNG1 gene at 1p13.3 with schizophrenia in Japanese populations. Neurosci Lett *435*, 194-197.

Olivera, B.M., Miljanich, G.P., Ramachandran, J., and Adams, M.E. (1994). Calcium channel diversity and neurotransmitter release: the omega-conotoxins and omega-agatoxins. Annu Rev Biochem *63*, 823-867.

Pasterkamp, R.J., Giger, R.J., Ruitenberg, M.J., Holtmaat, A.J., De Wit, J., De Winter, F., and Verhaagen, J. (1999). Expression of the gene encoding the chemorepellent semaphorin III is induced in the fibroblast component of neural

scar tissue formed following injuries of adult but not neonatal CNS. Mol Cell Neurosci *13*, 143-166.

Peng, J., Elias, J.E., Thoreen, C.C., Licklider, L.J., and Gygi, S.P. (2003). Evaluation of multidimensional chromatography coupled with tandem mass spectrometry (LC/LC-MS/MS) for large-scale protein analysis: the yeast proteome. J Proteome Res *2*, 43-50.

Rahman, M.A., Ashton, A.C., Meunier, F.A., Davletov, B.A., Dolly, J.O., and Ushkaryov, Y.A. (1999). Norepinephrine exocytosis stimulated by alpha-latrotoxin requires both external and stored Ca2+ and is mediated by latrophilin, G proteins and phospholipase C. Philos Trans R Soc Lond B Biol Sci *354*, 379-386.

Reyes, A., Lujan, R., Rozov, A., Burnashev, N., Somogyi, P., and Sakmann, B. (1998). Target-cell-specific facilitation and depression in neocortical circuits. Nat Neurosci *1*, 279-285.

Ribases, M., Ramos-Quiroga, J.A., Sanchez-Mora, C., Bosch, R., Richarte, V., Palomar, G., Gastaminza, X., Bielsa, A., Arcos-Burgos, M., Muenke, M.*, et al.* (2011). Contribution of LPHN3 to the genetic susceptibility to ADHD in adulthood: a replication study. Genes Brain Behav *10*, 149-157.

Robinson, M., Parsons Perez, M.C., Tebar, L., Palmer, J., Patel, A., Marks, D., Sheasby, A., De Felipe, C., Coffin, R., Livesey, F.J.*, et al.* (2004). FLRT3 is expressed in sensory neurons after peripheral nerve injury and regulates neurite outgrowth. Mol Cell Neurosci *27*, 202-214.

Rujescu, D., Ingason, A., Cichon, S., Pietilainen, O.P., Barnes, M.R., Toulopoulou, T., Picchioni, M., Vassos, E., Ettinger, U., Bramon, E.*, et al.* (2009). Disruption of the neurexin 1 gene is associated with schizophrenia. Hum Mol Genet *18*, 988-996.

Sadygov, R.G., Liu, H., and Yates, J.R. (2004). Statistical models for protein validation using tandem mass spectral data and protein amino acid sequence databases. Anal Chem *76*, 1664-1671.

Savas, J.N., Stein, B.D., Wu, C.C., and Yates, J.R., 3rd (2011). Mass spectrometry accelerates membrane protein analysis. Trends Biochem Sci *[Epub ahead of print]*.

Scanziani, M., Gahwiler, B.H., and Charpak, S. (1998). Target cell-specific modulation of transmitter release at terminals from a single axon. Proc Natl Acad Sci U S A *95*, 12004-12009.

Scheer, H., Madeddu, L., Dozio, N., Gatti, G., Vicentini, L.M., and Meldolesi, J. (1984). Alpha latrotoxin of black widow spider venom: an interesting neurotoxin and a tool for investigating the process of neurotransmitter release. J Physiol (Paris) *79*, 216-221.

Scheiffele, P., Fan, J., Choih, J., Fetter, R., and Serafini, T. (2000). Neuroligin expressed in nonneuronal cells triggers presynaptic development in contacting axons. Cell *101*, 657-669.

Seabold, G.K., Wang, P.Y., Chang, K., Wang, C.Y., Wang, Y.X., Petralia, R.S., and Wenthold, R.J. (2008). The SALM family of adhesion-like molecules forms heteromeric and homomeric complexes. J Biol Chem *283*, 8395-8405.

Shigemoto, R., Kulik, A., Roberts, J.D., Ohishi, H., Nusser, Z., Kaneko, T., and Somogyi, P. (1996). Target-cell-specific concentration of a metabotropic glutamate receptor in the presynaptic active zone. Nature *381*, 523-525.

Siddiqui, T.J., and Craig, A.M. (2011). Synaptic organizing complexes. Curr Opin Neurobiol *21*, 132-143.

Siddiqui, T.J., Pancaroglu, R., Kang, Y., Rooyakkers, A., and Craig, A.M. (2010). LRRTMs and neuroligins bind neurexins with a differential code to cooperate in glutamate synapse development. J Neurosci *30*, 7495-7506.

Silva, J.P., Lelianova, V., Hopkins, C., Volynski, K.E., and Ushkaryov, Y. (2009a). Functional cross-interaction of the fragments produced by the cleavage of distinct adhesion G-protein-coupled receptors. J Biol Chem *284*, 6495-6506.

Silva, J.P., Lelianova, V.G., Ermolyuk, Y.S., Vysokov, N., Hitchen, P.G., Berninghausen, O., Rahman, M.A., Zangrandi, A., Fidalgo, S., Tonevitsky, A.G.*, et al.* (2011). Latrophilin 1 and its endogenous ligand Lasso/teneurin-2 form a high-affinity transsynaptic receptor pair with signaling capabilities. Proc Natl Acad Sci U S A *108*, 12113-12118.

Silva, J.P., Suckling, J., and Ushkaryov, Y. (2009b). Penelope's web: using alpha-latrotoxin to untangle the mysteries of exocytosis. J Neurochem *111*, 275-290.

Sollner, C., and Wright, G.J. (2009). A cell surface interaction network of neural leucine-rich repeat receptors. Genome Biol *10*, R99.

Song, J.Y., Ichtchenko, K., Sudhof, T.C., and Brose, N. (1999). Neuroligin 1 is a postsynaptic cell-adhesion molecule of excitatory synapses. Proc Natl Acad Sci U S A *96*, 1100-1105.

Sousa, I., Clark, T.G., Holt, R., Pagnamenta, A.T., Mulder, E.J., Minderaa, R.B., Bailey, A.J., Battaglia, A., Klauck, S.M., Poustka, F.*, et al.* (2010). Polymorphisms in leucine-rich repeat genes are associated with autism spectrum disorder susceptibility in populations of European ancestry. Mol Autism *1*, 7.

Stacey, M., Lin, H.H., Gordon, S., and McKnight, A.J. (2000). LNB-TM7, a group of seven-transmembrane proteins related to family-B G-protein-coupled receptors. Trends Biochem Sci *25*, 284-289.

Stan, A., Pielarski, K.N., Brigadski, T., Wittenmayer, N., Fedorchenko, O., Gohla, A., Lessmann, V., Dresbach, T., and Gottmann, K. (2010). Essential cooperation of N-cadherin and neuroligin-1 in the transsynaptic control of vesicle accumulation. Proc Natl Acad Sci U S A *107*, 11116-11121.

Sudhof, T.C. (2001). alpha-Latrotoxin and its receptors: neurexins and CIRL/latrophilins. Annu Rev Neurosci *24*, 933-962.

Sudhof, T.C. (2008). Neuroligins and neurexins link synaptic function to cognitive disease. Nature *455*, 903-911.

Sugita, S., Ichtchenko, K., Khvotchev, M., and Sudhof, T.C. (1998). alpha-Latrotoxin receptor CIRL/latrophilin 1 (CL1) defines an unusual family of ubiquitous G-protein-linked receptors. G-protein coupling not required for triggering exocytosis. J Biol Chem *273*, 32715-32724.

Sugita, S., Khvochtev, M., and Sudhof, T.C. (1999). Neurexins are functional alpha-latrotoxin receptors. Neuron *22*, 489-496.

Tabb, D.L., McDonald, W.H., and Yates, J.R., 3rd (2002). DTASelect and Contrast: tools for assembling and comparing protein identifications from shotgun proteomics. J Proteome Res *1*, 21-26.

Terauchi, A., Johnson-Venkatesh, E.M., Toth, A.B., Javed, D., Sutton, M.A., and Umemori, H. (2010). Distinct FGFs promote differentiation of excitatory and inhibitory synapses. Nature *465*, 783-787.

Tobaben, S., Sudhof, T.C., and Stahl, B. (2002). Genetic analysis of alpha-latrotoxin receptors reveals functional interdependence of CIRL/latrophilin 1 and neurexin 1 alpha. J Biol Chem *277*, 6359-6365.

Toth, K., Suares, G., Lawrence, J.J., Philips-Tansey, E., and McBain, C.J. (2000). Differential mechanisms of transmission at three types of mossy fiber synapse. J Neurosci *20*, 8279-8289.

Tsuji, L., Yamashita, T., Kubo, T., Madura, T., Tanaka, H., Hosokawa, K., and Tohyama, M. (2004). FLRT3, a cell surface molecule containing LRR repeats

and a FNIII domain, promotes neurite outgrowth. Biochem Biophys Res Commun *313*, 1086-1091.

Tucker, R.P., and Chiquet-Ehrismann, R. (2006). Teneurins: a conserved family of transmembrane proteins involved in intercellular signaling during development. Dev Biol *290*, 237-245.

Tucker, R.P., Kenzelmann, D., Trzebiatowska, A., and Chiquet-Ehrismann, R. (2007). Teneurins: transmembrane proteins with fundamental roles in development. Int J Biochem Cell Biol *39*, 292-297.

Ullrich, B., Ushkaryov, Y.A., and Sudhof, T.C. (1995). Cartography of neurexins: more than 1000 isoforms generated by alternative splicing and expressed in distinct subsets of neurons. Neuron *14*, 497-507.

Umemori, H., Linhoff, M.W., Ornitz, D.M., and Sanes, J.R. (2004). FGF22 and its close relatives are presynaptic organizing molecules in the mammalian brain. Cell *118*, 257-270.

Ushkaryov, Y.A., Petrenko, A.G., Geppert, M., and Sudhof, T.C. (1992). Neurexins: synaptic cell surface proteins related to the alpha-latrotoxin receptor and laminin. Science *257*, 50-56.

Ushkaryov, Y.A., Rohou, A., and Sugita, S. (2008). alpha-Latrotoxin and its receptors. Handb Exp Pharmacol, 171-206.

Van Renterghem, C., Iborra, C., Martin-Moutot, N., Lelianova, V., Ushkaryov, Y., and Seagar, M. (2000). alpha-latrotoxin forms calcium-permeable membrane pores via interactions with latrophilin or neurexin. Eur J Neurosci *12*, 3953-3962.

Varoqueaux, F., Aramuni, G., Rawson, R.L., Mohrmann, R., Missler, M., Gottmann, K., Zhang, W., Sudhof, T.C., and Brose, N. (2006). Neuroligins determine synapse maturation and function. Neuron *51*, 741-754.

Volynski, K.E., Meunier, F.A., Lelianova, V.G., Dudina, E.E., Volkova, T.M., Rahman, M.A., Manser, C., Grishin, E.V., Dolly, J.O., Ashley, R.H.*, et al.* (2000). Latrophilin, neurexin, and their signaling-deficient mutants facilitate alpha -latrotoxin insertion into membranes but are not involved in pore formation. J Biol Chem *275*, 41175-41183.

Volynski, K.E., Silva, J.P., Lelianova, V.G., Atiqur Rahman, M., Hopkins, C., and Ushkaryov, Y.A. (2004). Latrophilin fragments behave as independent proteins that associate and signal on binding of LTX(N4C). EMBO J *23*, 4423-4433.

von Engelhardt, J., Mack, V., Sprengel, R., Kavenstock, N., Li, K.W., Stern-Bach, Y., Smit, A.B., Seeburg, P.H., and Monyer, H. (2010). CKAMP44: a brain-specific protein attenuating short-term synaptic plasticity in the dentate gyrus. Science *327*, 1518-1522.

Walsh, T., McClellan, J.M., McCarthy, S.E., Addington, A.M., Pierce, S.B., Cooper, G.M., Nord, A.S., Kusenda, M., Malhotra, D., Bhandari, A.*, et al.* (2008). Rare structural variants disrupt multiple genes in neurodevelopmental pathways in schizophrenia. Science *320*, 539-543.

Wang, C.Y., Chang, K., Petralia, R.S., Wang, Y.X., Seabold, G.K., and Wenthold, R.J. (2006). A novel family of adhesion-like molecules that interacts with the NMDA receptor. J Neurosci *26*, 2174-2183.

Washburn, M.P., Wolters, D., and Yates, J.R., 3rd (2001). Large-scale analysis of the yeast proteome by multidimensional protein identification technology. Nat Biotechnol *19*, 242-247.

Wheldon, L.M., Haines, B.P., Rajappa, R., Mason, I., Rigby, P.W., and Heath, J.K. (2010). Critical role of FLRT1 phosphorylation in the interdependent regulation of FLRT1 function and FGF receptor signalling. PLoS One *5*, e10264.

Williams, M.E., de Wit, J., and Ghosh, A. (2010). Molecular mechanisms of synaptic specificity in developing neural circuits. Neuron *68*, 9-18.

Woo, J., Kwon, S.K., Choi, S., Kim, S., Lee, J.R., Dunah, A.W., Sheng, M., and Kim, E. (2009a). Trans-synaptic adhesion between NGL-3 and LAR regulates the formation of excitatory synapses. Nat Neurosci *12*, 428-437.

Woo, J., Kwon, S.K., and Kim, E. (2009b). The NGL family of leucine-rich repeat-containing synaptic adhesion molecules. Mol Cell Neurosci *42*, 1-10.

Yamagishi, S., Hampel, F., Hata, K., Del Toro, D., Schwark, M., Kvachnina, E., Bastmeyer, M., Yamashita, T., Tarabykin, V., Klein, R.*, et al.* (2011). FLRT2 and FLRT3 act as repulsive guidance cues for Unc5-positive neurons. EMBO J *[Epub ahead of print]*.

Yan, J., Noltner, K., Feng, J., Li, W., Schroer, R., Skinner, C., Zeng, W., Schwartz, C.E., and Sommer, S.S. (2008). Neurexin 1alpha structural variants associated with autism. Neurosci Lett *438*, 368-370.

Yan, J., Oliveira, G., Coutinho, A., Yang, C., Feng, J., Katz, C., Sram, J., Bockholt, A., Jones, I.R., Craddock, N.*, et al.* (2005). Analysis of the neuroligin 3 and 4 genes in autism and other neuropsychiatric patients. Mol Psychiatry *10*, 329-332.

Zahir, F.R., Baross, A., Delaney, A.D., Eydoux, P., Fernandes, N.D., Pugh, T., Marra, M.A., and Friedman, J.M. (2008). A patient with vertebral, cognitive and behavioural abnormalities and a de novo deletion of NRXN1alpha. J Med Genet *45*, 239-243.

Zhou, X.H., Brandau, O., Feng, K., Oohashi, T., Ninomiya, Y., Rauch, U., and Fassler, R. (2003). The murine Ten-m/Odz genes show distinct but overlapping expression patterns during development and in adult brain. Gene Expr Patterns *3*, 397-405.